Master's thesis in chemical and process engineering

SYNTHESIS AND SCREENING OF TiO$_2$-BASED PHOTOCATALYSTS FOR AIR PURIFICATION

Supervisors: Prof. Paolo Canu, Prof. Klass Engvall

Co-supervisors: Francesco Montecchio, Prof. Roberto Lanza

Author: DAMIANO TRENTO

"To my father,
a special person of my life"

Acknowledgements

I would first like to thank Professor Klas Engvall for giving me the opportunity to work in his research group at the department of Chemical Technology of KTH and Professor Paolo Canu for the support in this project.

I would like to extend my sincere gratitude to my supervisor and friend Francesco Montecchio for the continuous support, for his patience and motivation. His guidance helped me in all the time of research and writing of this thesis. I could not have imagined having a better advisor and mentor.

A special thanks is for Roberto Lanza, who were also involved in this research project, for his passionate participation and input but mostly for his super-training at the beginning and all the explanations during the entire period of this experience.

To Jack Delin and his colleagues at Centriair for always keeping the market point of view on the research project. For the constant focus on applications and realistic cases in on-going research keeps the motivation on top.

To all the people I met in Stockholm, from the colleagues to friends I met even if I cannot mention all of you.

To my special colleagues of Padova and all the other friends that have supported me in this difficult years.

Finally, I must express my very profound gratitude to my entire family and, in particular, to my mother and my sister for providing me with unfailing support throughout my years of study and through the process of researching and writing this thesis. This accomplishment would not have been possible without them. Vi voglio bene.

Damiano Trento

Abstract

Many industrial processes involve complex steps of transformation matter, habitually in presence of solvents, which emit a considerable amount of VOCs that are very often toxic at very low concentration. In the past years came out an attractive system for removing these pollutants based on the photocatalytic technology.

The investigation is focused on understanding, improving and classify different photocatalysts to find a replacement of a common used P25, a commercial sample leader in this field.

The first part of this work is dedicated apprehending the different strategies to improve the titanium dioxide used as a semiconductor. Some solutions are selected after a deep investigation into the literature; five photocatalysts are produced with two different methods (Sol gel and Mesoporous) and two dopants (with cerium and silica) that are potentially the best solutions to improve the activity.

There isn't a standard methodology on how to test the activity the different samples, this problem is overcome with the introduction of the relative activity that removes the dependences of the systems.

The synthetized powders are immobilized on a ceramic support to avoid issues inside the reactor with a dip coating techniques.

A sublayer is also introduced to prevent the critical problem of the attachment on the support; it is a film to interpose between the support and the photocatalytic layer that confers also improvements for the aging and the charge imbalance that are other important issues of this technology.

The samples are finally tested together with some establish commercial catalysts in an optimized system for the screening of photocatalysts with a designed reactor to detect only the differences among the different catalysts.

the efficacy the relative activity is verified as an efficient way to compare different systems otherwise impossible to correlate.

The test's results reveal a substantial improvement in the products samples made with the sol-gel technique and all the commercial solutions; P90 is the best sample tested, it has an improvement of more than 100% compared to the product currently used.

Riassunto

Una gran quantità di processi industriali coinvolgono abitualmente l'uso di solventi e sono caratterizzati da emissioni, a volte considerevoli, di inquinanti organici in atmostera che spesso sono molto tossici anche a basse concentrazioni. Di recente è stata valutata l'idea di rimuovere tali inquinanti usando la fotocatalisi.

Questa indagine è centrata sulla comprensione, il miglioramento e classificazione di una valida alternativa al comune P25, un prodotto industriale leader del settore e tutt'ora utilizzato.

La prima parte di questo lavoro è stata dedicata alla comprensione delle differenti tecnologie volte al miglioramento del diossido di carbonio usato come semiconduttore. Diverse soluzioni sono state quindi selezionate dopo una profonda ricerca in letteratura e infine cinque siversi fotocatalizzatori sono stati prodotti attraverso due diverse tipologie di sintesi (sol gel e mesoporosa) e due dopanti (cerio e silica) che sono potenzialmente le migliori soluzioni per il miglioramento dell'attività.

La mancanza di una metodologia standard per testare differenti campioni è stata superata dall'introduzione dell'attività relativa che rimuove la dipendenza dei sistemi valutando la solo il potere di ossidazione del catalizzatore.

La polvere di diossido di titanio prodotta è stata successivamente immobilizzata su un supporto ceramico per evitare problemi all'interno del reattore tramite dip coating.

Per prevenire il critico problema dell'attaccamento al supporto, è stato introdotto un sublayer; si tratta di un film da interporre tra la superficie ceramica e lo strato attivo di campione e conferisce miglioramenti anche per problemi come la disattivazione del catalizzatore e per l'immobilizzazione delle cariche.

I campioni sono stati infine testati in un impianto appositamente costruito dotato di un reattore progettato allo scopo di valutare le sole differenze tra i diversi catalizzatori.

É stata verificata l'efficacia dell'attività relativa come un metodo efficace per comparare diversi sistemi altrimenti impossibili da correlare.

I risultati dei test rivelano un sostanziale miglioramento dell'attività del campione prodotto con la tecnica sol gel e delle soluzioni commerciali, tra di essi infatti risiede il miglior campione testato con un miglioramento maggiore del 100% rispetto al prodotto attualmente utilizzato.

Table of contents

Chapter 1

Introduction

In this chapter there is an overall description of the technology and the theoretical basis used in this work.

1.1 Volatile organic compounds (VOCs)

Volatile organic compounds (VOCs), according to the European directive, include all the compounds that have a vapor pressure of 0.01 kPa or more at atmospheric pressure; they contain at least the element carbon and one or more of hydrogen, halogens, oxygen, sulphur, phosphorus, silicon, or nitrogen, with the exception of carbon oxides and inorganic carbonates and bicarbonates (methane, ethane, CO, CO_2, organometallic compounds and organic acids are excluded)[1].

These compounds are among the most common pollutants emitted by the chemical process industries and because of the environment and human risk they have received great attention. VOCs can be toxic at very low concentrations(Fenger 1999) and another problem is derived by the food industry since a mixture of different VOCs may have a very pungent odor (Montecchio et al. 2016). For example, in a frying industries the regulation is stricter in the last few years because of the increasing of the number of complains to the local authorities (Montecchio et al. 2016).

There are many different available technics for controlling this problem, as it is schematized in figure 1.1, we can summarize them in two different strategies (Khan and Kr. Ghoshal 2000):

- Process and equipment modification
- Installation of a purification system

The first group is the most preferred alternative because the emissions are reduced changing the process variables or the raw material.

The other strategy includes all the known methodology for recovering or destroying the pollutants. Recovering systems work transferring hazardous compounds from the process stream to a liquid solvent (ammine scrubbing) or to a solid adsorbed material (active carbon or zeolites) but the issue remains because it is required a purification downline of the secondary stream that usually it is not easy, inexpensive or environmentally-friendly.

_____

The last category is the destruction of the VOC and the system act oxidizing the organic compounds (thermal oxidation, catalytic or biocatalytic system). This is a definitive way to remove them but other issues may affect these technologies:

- The thermal oxidation works at high temperature and there is a huge consumption of fossil fuel
- The biocatalytic patch is very sensible to impurities and selective in extraneous compounds that could be present in the system and where a little change in the working standard conditions can make the system ineffective or even worse the bio organisms may be destroyed (Khan and Kr. Ghoshal 2000).
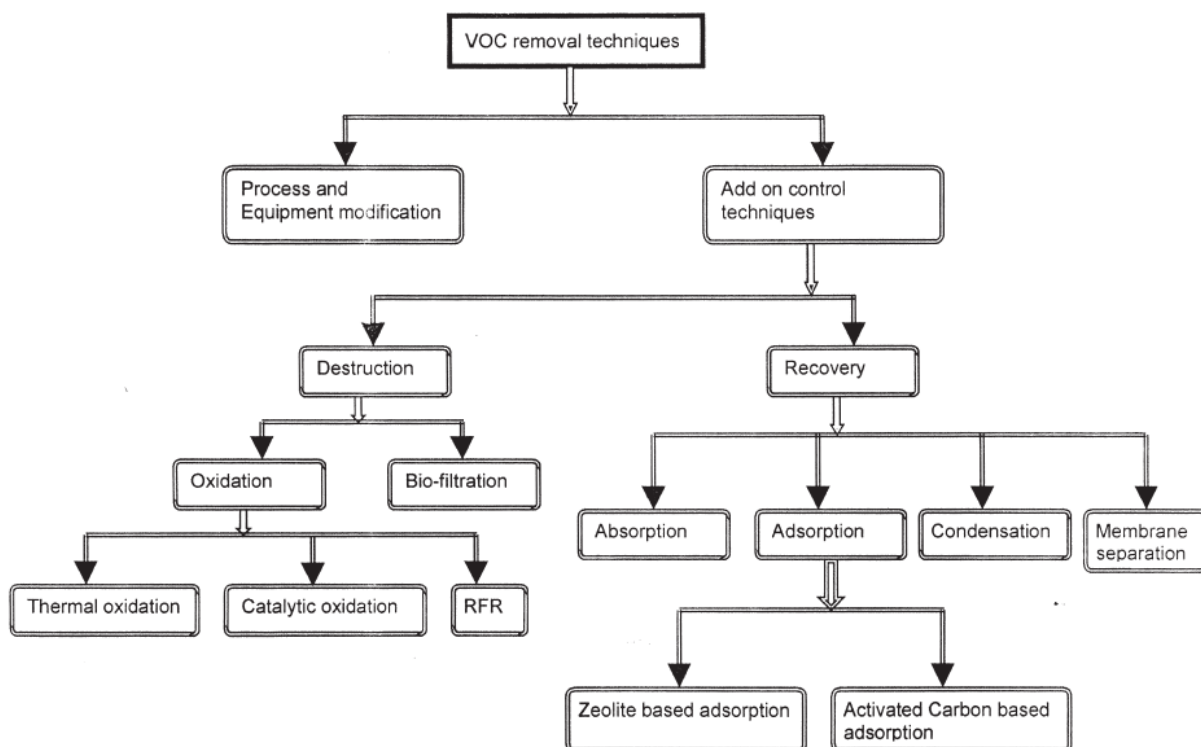
Figure 1.1. Classification of VOC control techniques. (Khan and Kr. Ghoshal 2000)

In addition to these standard methodologies, a new way to oxidize and remove the VOCs came up in the early years and it is called photocatalysis (Fujishima, Rao, and Tryk 2000).

1.2 Photochemistry

Sometimes photochemical reactions are valuable because they proceed differently than thermal reactions: the activation energy is provided by light instead of heat so they do not require heat energy to promote the reaction (Prashant V. Kamat 1993).
Light is an electromagnetic radiation and it has a certain quantity of energy related on its wavelength (Planck's equation) and this energy could be adsorbed by specific molecules to cause a chemical reaction.

_____

1.2.1 UV light

Ultraviolet light (UV) is part of the light spectrum with a wavelength from 10nm to 400nm and it can cause chemical reaction due to his quite high energy.

There are three general ways to use this technology for removing the VOCs, usually called advanced oxidation process (AOP). The mechanism began with the generations of hydroxyl radicals, in the second stage these radicals attacks and breakdown the organic molecules and finally there is compete mineralisation of the organic compounds.

The differences between the different AOP methodologies are how the radical are formed. They can be divided in three groups (Stocking et al. 2011):

- UV/H_2O_2
- UV/OZONE
- Photocatalytic oxidation of TiO_2

Without going deeply into details, in this work is investigated only the last one: the mineralization of the VOC with a photocatalyst.

1.2.2 Photocatalytic technology

The basic idea of this technology is using a semiconductor excited by UV light, the formed electron-holes are capable to generate radicals without the introduction of other elements into the system (for example hydrogen peroxide is used in other AOP) or without troublesome generation of critical species like ozone or other toxic oxidant.

A semiconductor is an element with an intermediate electronic structure between insulator and resistance: it has a small energy gap that allows electrons to be transferred from one band to the other. When an electron has enough energy to pass from the valence band to the conductive band (excitation) it leaves a hole that has the effect of a positive charge (Khan and Kr. Ghoshal 2000).

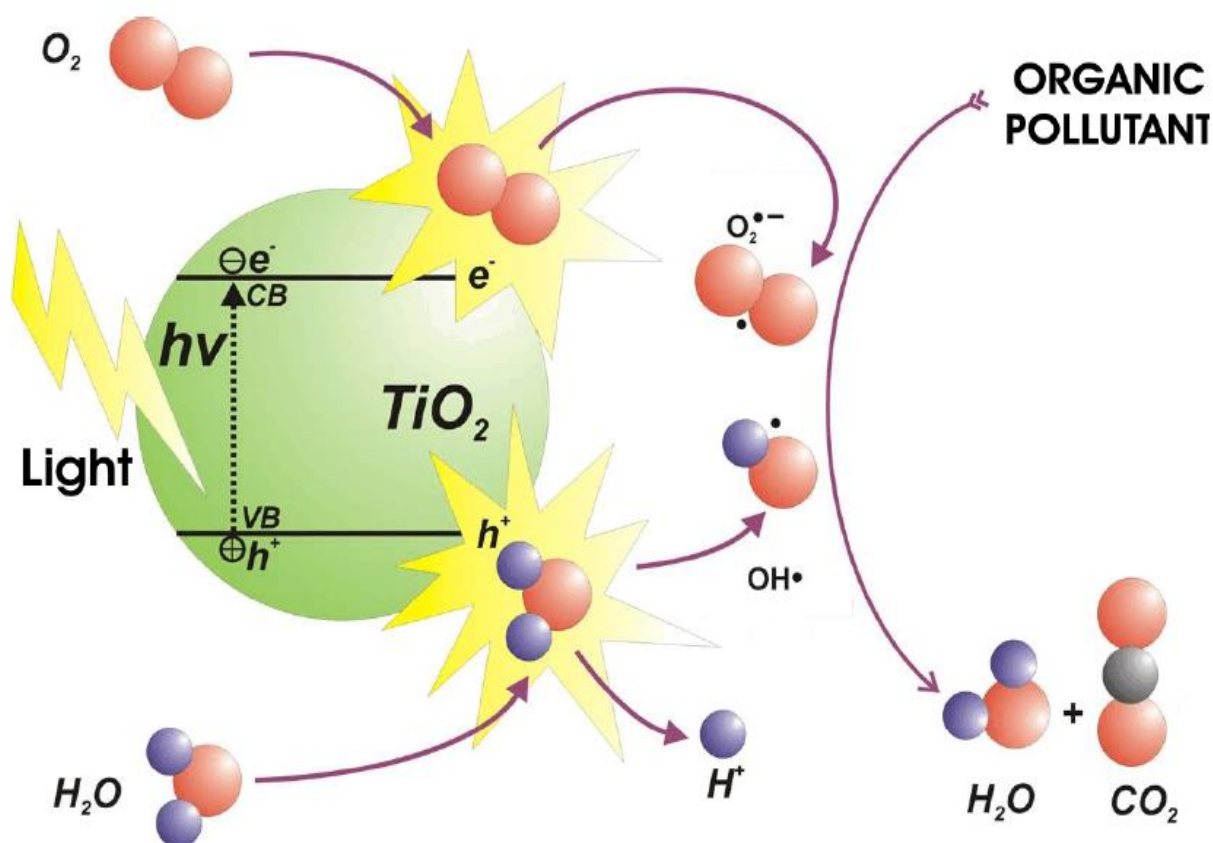In the figure 1.2 there is the complete mechanism of the process.

_____

Figure 1.2. Schematic of semiconductor excitation by band gap illumination leading to the creation of "electrons" in the conduction band and "holes" in the valance band. (Ibhadon and Fitzpatrick 2013)

The process starts with the irradiation of the semiconductor by light; the photons of the light are absorbed by the surface and due to its semiconductor's characteristics the material creates a charge carries inside the crystals (Nursam, Wang, and Caruso 2015). In order to excite the catalyst, the radiation needs to be of the appropriate wavelength: with energy higher than the band gap of the semiconductor (Nursam, Wang, and Caruso 2015). At this point, he first pathway is the recombination of the electrons with the holes because of crystal imperfections, such as defects or presence of impurities and this is a reason why is very important to avoid contaminant in the matrix of the catalysts during the synthesis of the photocatalyst (Ibhadon and Fitzpatrick 2013). The other option of the charge separations, that is suitable to our process, is the reduction of an electron-acceptor by the electrons in the valence band and the oxidation of an electron-donor that gives an to refill the hole (Ibhadon and Fitzpatrick 2013).

 The two formed species create hydroxyl radicals if combined with water, they are very strong oxidant and reactive species that are able to disrupt a wide range of different organic compounds (Hoffmann et al. 1995).

_____

There are several different materials with characteristics of electron–hole pair generation and the figure 1.3 shows some examples of the most famous compounds with their characteristic band gap.
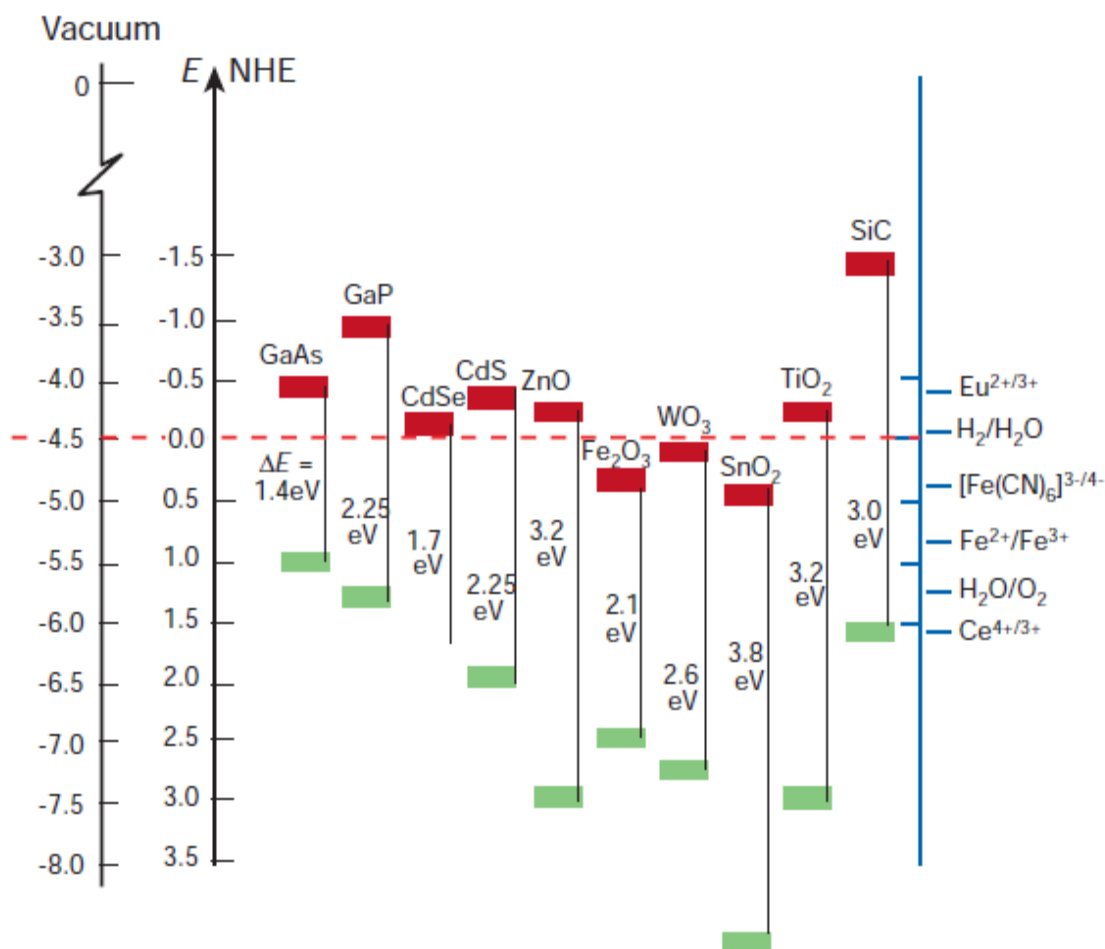
Figure 1.3. Energy level diagram indicating conduction (red) and valence (green) band edge positions for various semiconductors in contact with an aqueous electrolyte at pH = 1. (Gauthier et al. 2006)

In order to use the generated electrons and their vacancies in our system, the bandgap edge-positions is of fundamental importance: the lower-edge position (LUMO) is the reduction strength of the photoexited electrons and it must be lower than the required for reducing the oxygen. The upper-edge position (HOMO) is the potential oxidation energy of the hole and it must be higher than the required of the water splitting reaction (Nursam, Wang, and Caruso 2015).

_____

1.3 Titanium dioxide

Titanium dioxide is one of the materials with enough power to create hydroxyl radicals (see figure 1.3); beside this it has a very high stability both chemical and biological, it is inexpensive, very abundant and is has tailorable electronic and morphology proprieties (Nursam, Wang, and Caruso 2015) that make the TiO_2 the most practical and used semiconductor as photocatalyst (Hoffmann et al. 1995).

The research over Titanium dioxide is a very active field of investigations due to its characteristics and numerous applications (Ibhadon and Fitzpatrick 2013); the importance and variety of the applications of this compound, especially in the form of nanomaterials, varies from common products, such as sunscreens, to advanced devices, such as photovoltaic cells or as a photocatalytic degradation of pollutants (Mills and Lee 2002). It has spurred enormous interest and substantial advances in the fabrication, characterization, and fundamental understanding of TiO_2 nanomaterials in the past decades (Chen and Selloni 2014).

It can occur in three main different crystalline structures: rutile, anatase or brookite but the last one is difficult to prepare (Wold 1993) beyond the fact that is uncommon, unstable and hence that do not make a material with a future in any discussion of photocatalyst materials (Ibhadon and Fitzpatrick 2013). Rutile is the most common phase of titanium dioxide in nature, it has a band gap of 3 eV; anatase shows a considerably higher activity than rutile with a band gap of 3.2eV but it is metastable and it is irreversibly converted to rutile at 600-800°C so its production has to consider this particular. The photocatalyst gets activated when it receives photons with enough energy and, in particular, the titanium dioxide needs a wavelength of the irradiated light less than 400 nm (Nursam, Wang, and Caruso 2015).

1.3.1 Physical modifications

Physical characteristics are fundamental aspects because they are directly related to the activity of the catalyst (Puddu et al. 2010). Surface area is the first parameter to consider because the reaction takes place by absorbing chemicals on the interphase and for this reason it is required a very high specific surface area in order to maximize the active sites that can be irradiated by the UV light (Kumar and Devi 2011).

Another important parameter is the crystal size, the charge separations take place into the crystals and their size affect the activity of the catalyst. The perfect dimension is a trade-off: a small size ensures more sites for the reaction because in the same amount of material there are more crystals and bigger surface are. A big size of crystals is also desired to avoid the light scattering and to have more light absorption; another important factor is related to the recombinations of charges, they occur in the discontinuities between the crystals because of the defects so this is usually minimized with bigger size of the crystal: that means a longer, so

_____

a better crystallization of the material that contains less structural defects (Jackson 1988). The perfect solution is found between 10 nm and 40 nm (Almquist and Biswas 2002).

The size and the quantity of the pores also influence the performances of the titanium dioxide; a different dimensions change how chemicals diffuse into them so a good catalyst need big pores and high grade of porosity (the empty space in a material); the relation however is not linear because also the shape or the tortuosity of the pore are important, also the surface area is correlated to these parameters (Busuioc et al. 2006).

These characteristics about the physical characteristics of the titanium dioxide are tuned controlling the synthesis.

Titanium dioxide is relatively easy to obtain so there are many different methodologies to produce it: sol gel, micelle, hydrothermal, solvothermal, chemical vapour deposition, physical vapour deposition, electrodeposition, sonochemical, microwave, mesoporous just to cite the most common techniques for obtaining nanoparticles (Chen and Mao 2007). The first decision is to discard the deposition methods because they are not suitable in large scale production: these technologies create a dense film of titanium; they are also high-priced if correlated to all the other methodologies reported before (Richard et al. 2011). Sol gel and mesoporous are the only methods investigated in this work because of their characteristics to be inexpensive, they do not require high temperature in this process, are relatively fast to produce, simply to reproduce and very flexible; lastly they are interesting and adapt for the production of photocatalysts because all the parameters in the synthesis can be easily changed to optimize and adapt the material to obtain the desired properties(Chen and Mao 2007).

Sol gel is largely investigated to produce nanoparticles of all types of ceramics, there are more than ten-thousand papers regarding the production of titanium dioxide just in 2015[2] and this variety derives from the extremely high flexibility of the process where all the parameters and reagents can be changed to influence the final product.

A typical procedure of a sol gel is shown in figure 1.4 and consists in the use of a precursor in a solvent and a possible dopant, then hydrolysed in water. The solution, or a suspension is dried and finally calcined to create the titanium dioxide.

_____
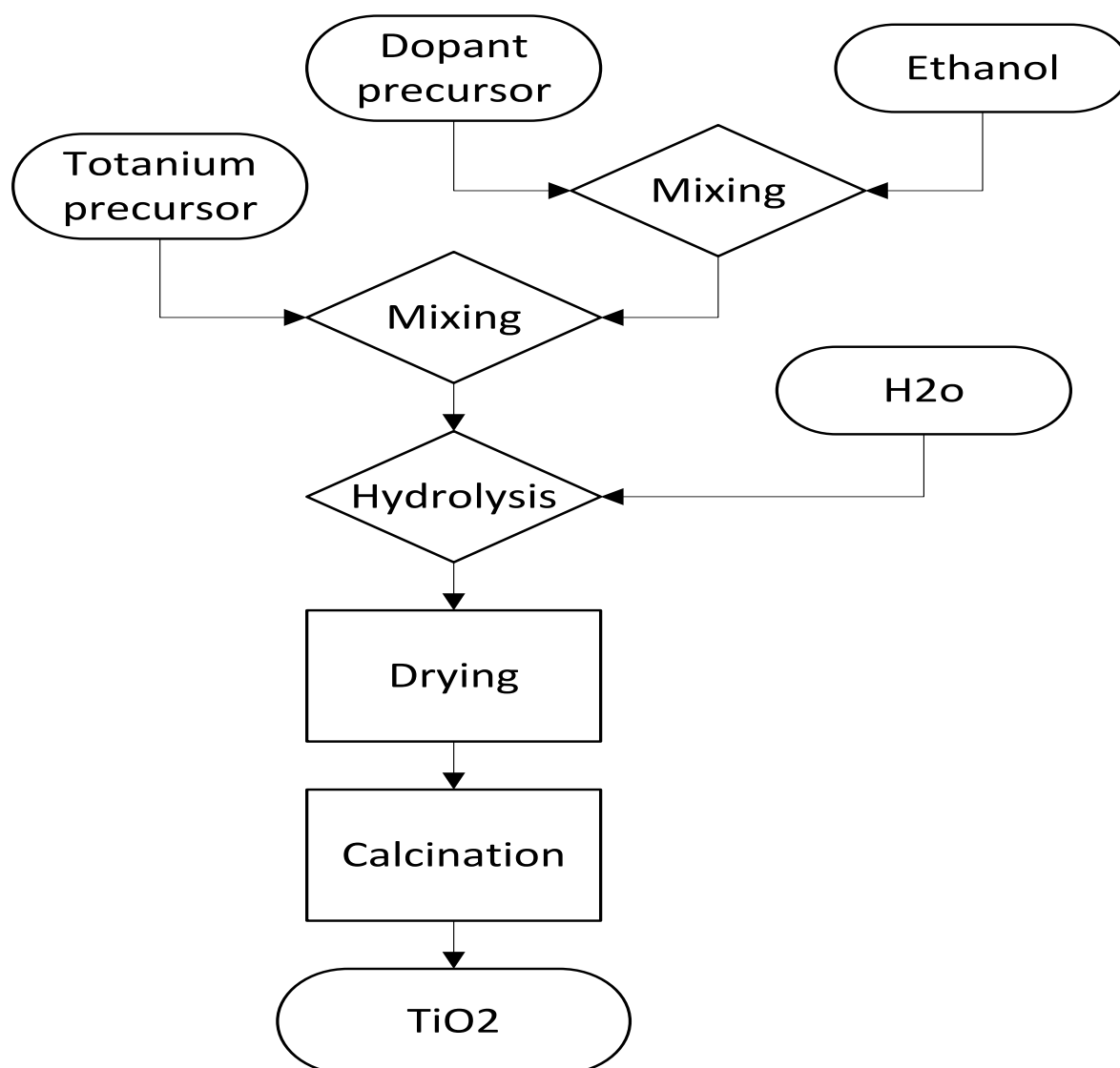
Figure 1.4. General procedure of the sol gel methodology.

Mesoporous TiO_2 is a technique that is well described in a famous paper of Yang (Yang et al. 1998), the basic idea consists to add a block copolymer (structuring agent) for conferring a very regular structure and the subsequent evaporation of this polymeric chain leaves the holes into this structure called worm-like channels. It is a development of a classical sol gel because it confers a higher surface area with large, regular and straight pores. A simple scheme of the process is shown in figure 1.5.

Figure 1.5. Scheme presenting the most representative steps of the mesoporous synthesis method. (Machado et al. 2015)

1.3.2 Doping

Titanium dioxide can be altered by doping its structure; the procedure changes the electronic properties of the material; the doping introduces impurities into the structure of a semiconductor to create physical and electronical distortions and this phenomenon is used to improve the catalyst activities (Chen and Mao 2007).
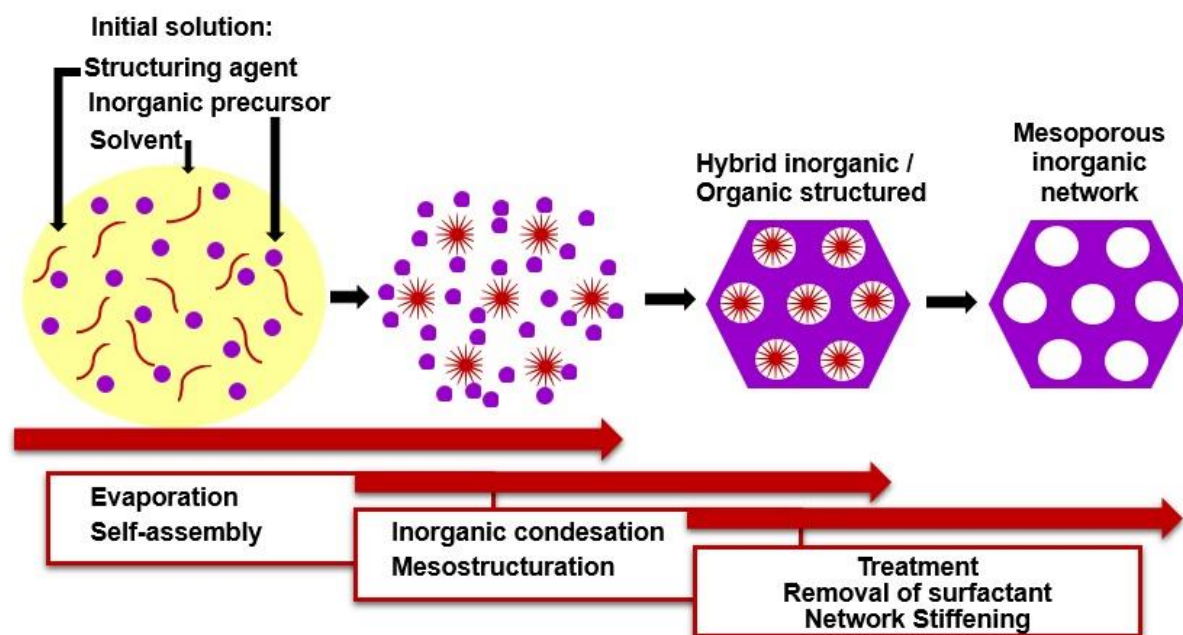
The small size of the nanoparticle is beneficial for the modification of the chemical composition of TiO_2 due to the higher tolerance of the structural distortion than that of bulk materials induced by the inherent lattice strain in nanomaterials (Burda et al. 2003) and this led to dope the titanium dioxide with almost all the elements from metals to non-metals.

Dopants are largely used to shift the adsorption band of the photocatalyst, that is originally in a UV region, into the visible light region and this is usually possible replacing a ti^{+4} with a non-metal material (so called third generation of TiO_2) (Chen and Mao 2007) to use the catalyst with the solar light (Chen and Mao 2007) and take advantages from its free energies.

Metal-doped TiO_2 (second generation of TiO_2) is studied over the past decades for its capacity of improving the performance on the degradation of organic compounds: the presence of metal ion dopants in the TiO_2 matrix significantly influence the charge carrier recombination rates and interfacial electron-transfer rates (Chen and Mao 2007) without necessarily change its adsorption band. The photo reactivity of doped TiO_2 is affected by many variables for examples the dopant concentration, the energy level of dopants within the TiO_2 lattice, their

_____

electronic configurations, the distribution of dopants or the electron donor concentrations and the light intensity (Chen and Mao 2007).

In this work the catalyst is irradiated with UV light so it does not need to absorb light in the visible region or change the adsorbed band so, in this investigation silica is chosen as a dopant for its capacity to improve the surface texture and enhance its physical characteristics (Sun et al. 2012) and not because of the usual property of the non-metal element. The absorption of the photocatalyst remains in the same range if the atoms of silica does not enter into the crystalline lattice of anatase (Katsunori and Puyam 1999). The surface area is improved greatly for the contribution of the high surface area of SiO2 (1600 m^2/g) and also the elevated thermal stability that consent a very high calcination temperature that reduces the concentrations of defects without the grown of crystals and finally silica act blocking the crystal transition from anatase to rutile phase (Chen and Mao 2007).

It is tested also a catalyst doped with cerium because of its capacity of charges imbalance, vacancies and unsaturated chemical bonds on the catalyst surface that led to increase the absorption of oxygen on the surface of the catalyst. Compared to the other metals, Ce is a very good electron trap in the reaction because of its varied valences and its special 4f level. For Ce^{3+}- TiO$_2$, the Ce 4f level plays also an important role in interfacial charge transfer and elimination of electron-hole recombination. So, doping with cerium can enhance the electron-hole separation and increases the formation of active radicals (Liang, Li, and He 2012).

1.3.3 Surface modifications

The surface modifications are another methodology to modify titanium monoxide, the process is called sensitization of the surface. This process is used when the band gap of the semiconductors is too high compared to the energy of the incident radiation so it reduces the required energy for creating the electron-holes. This process is also used for improving the absorption of a particular reagent that otherwise it will not be attracted from the surface: it make the surface sensible to a specific chemicals (Chen and Mao 2007).

The sensitize surfaces are therefore used with particular reactions (antibacterial purpose for example) or to use a photocatalyst with solar light instead of a dopant.

For these reasons in this work the surfaces modifications are not investigated because it is used a UV radiation with a final application of a mixture of VOCs.

1.3.4 Interlayer

One of the problem of this analysis is the stability and the durability of the photocatalyst immobilized into the support over the time. The previous investigation (Persson 2015), in fact, reveals a real problem of attachment of the catalyst during the test that is not acceptable.

_____

From the figure 1.6 it is possible to deduce that the test with an exfoliated layer does not give a consistent result due to difference of the surface and the thickness of the deposited photocatalyst.
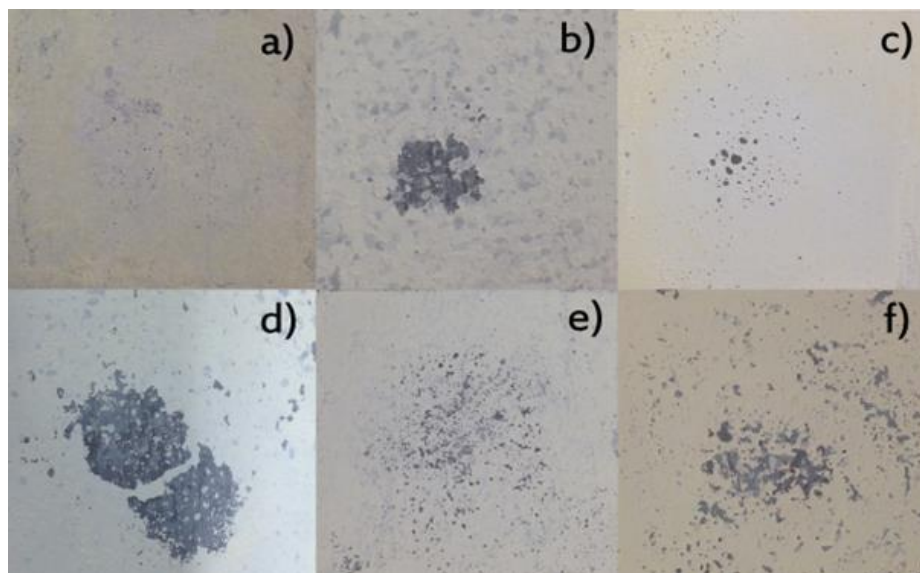

Figure 1.6. Supports of different samples used in the previous investigation after the test. They show the problem of the attachment of the photocatalytic layer.

To improve and to avoid as much as possible the problem it is introduced a sublayer: between the support and the film of photocatalytic powders that confer a good adhesion of the catalyst that is enough for the applications (Yuan et al. 2008).
This layer decrease also the deactivation and the photoactivity of the catalyst as it is reported in the work of Yuan (Yuan et al. 2008) because of the inertial properties of this layer that does not transfer the photoexited electrons into the support (Yuan et al. 2008).

1.3.5 Safety data

Titanium dioxide (TiO_2) is considered as an inert and safe material and has been used in many applications. However, TiO_2 nanoparticles, with numerous novel and useful properties, are increasingly manufactured and used with an increasing of human and environmental exposure which has put TiO_2 nanoparticles under toxicological scrutiny. Mechanistic toxicological studies show that TiO_2 nanoparticles predominantly cause adverse effects via induction of oxidative stress resulting in cell damage, genotoxicity, inflammation and immune response (Skocaj et al. 2011) and it has been classified by the International Agency for Research on Cancer (IARC) as an IARC Group 2B carcinogen, meaning it is possibly carcinogenic to humans (IARC Working Group on the Evaluation of Carcinogenic Risks to Humans 2010).

_____

1.4 Relative activity

The relative activity (R) is a parameter created to evaluate the performances of the catalysts among the vastness of solutions that are available in literature.

It is nearly impossible to compare different systems because of numerous different factors for examples the reactor, the reagents or the conditions of the reaction from one source to another. It is possible to note, however, that most of the analysed works compare their own sample to evaluate with the photocatalyst Degussa® P-25, a famous commercial photocatalyst. It is immediate, then, that there is a connection between different solutions and thanks to this catalyst that act as a reference.

The normalized parameter R tries, in fact, to get round of this problem and it gives us a number about the activity of a catalyst respect the activity of the P25 in the same conditions and the same system. This deduction allows to correlate different systems with different catalyst because both of them are correlate to the activity of the P25. It is defined as the ratio between the reaction rate constant of a tested catalyst over the reaction rate constant of the P25 expressed in equation (1.1)

$$R = \frac{k_{sample}}{k_{P25}}$$
(1.1)

It is possible to assume the reaction as a pseudo first-order reaction for a low concentration of VOC (Herz 2004); the model of the reactor, instead, is developed by Puddu (Puddu et al. 2010) because the two reactors are similar in both investigations and their mathematical expression are (1.2) and (1.3):

$$r = k[C_{VOC}]$$
(1.2)

$$r = \frac{F * C_0 * X}{A}$$
(1.3)

Where A is the surface exposed to the UV radiation (the surface of the plate irradiated), F is the total volumetric flow, C_0 is the inlet concentration of VOCs and X is the conversion of the reactor.

If the equation (1.2) is combined with (1.3) to give equation (1.4):

$$R = \frac{k_1}{k_2} = \frac{r_1}{C_{OUT1}} \frac{C_{OUT2}}{r_2} = \frac{F * C_0 * X_1}{A} \frac{A}{F * C_0 * X_2} \left(\frac{C_{OUT2}}{C_{OUT1}}\right) = \frac{X_1 C_{OUT2}}{X_2 C_{OUT1}} =$$
$$= \frac{X_1(1 - X_2)}{X_2(1 - X_1)}$$
(1.4)

When the two catalysts have the same exposed surface and inlet conditions.

_____

1.4.1 Photocatalysts selection

Considering the methodology and the dopants discussed in the sections §1.3.1 and §1.3.2, six different catalysts are selected and then reproduced in this investigations considering the relative activities and, therefore, the improvements to the P25. All the methodologies that are taken into consideration are studied of removal of VOCs from an air stream with lamps that emit in the UV-range like our system.

- The first photocatalyst is the one produced and tested by Puddu (Puddu et al. 2010). It is a simple sol gel without any dopants but with optimized types and quantity of regents to give the best results in terms on photo activities and physical properties. The figure 1.7 represents the rate constant of the different catalysts used in his work. It is possible to extract the best one: the catalyst is calcined at 600°C (purple line); the relative activity is given by the ratio between the constant rate at this temperature and the reference P25 at 10 watt/m2 that is the power of our system, and is R=1.75.
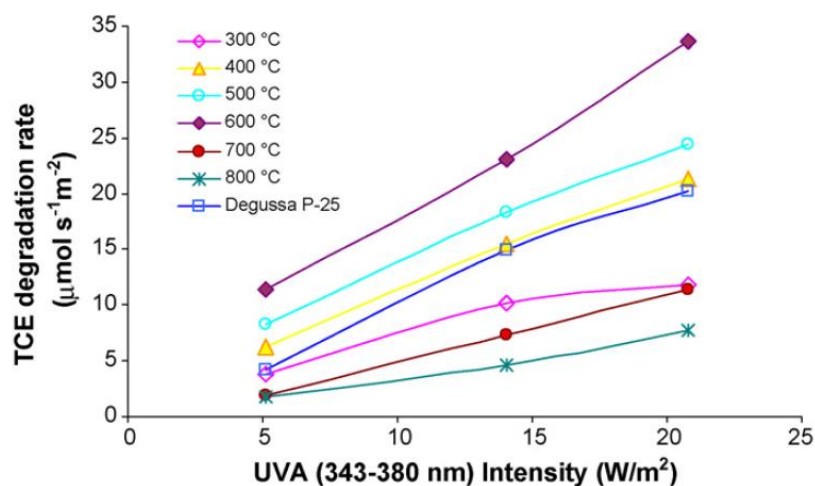

Figure 1.7. Degradation rate constant of the different catalyst produced in Puddu's investigation. (Puddu et al. 2010)

In the same paper it also shows that it is possible to expect a better activities respect all the other samples at temperature of 600°C after the physical analysis. From the XRD and the TEM images (see figure 1.8) it is clearly visible that over 600°C the rutile phase become predominant and this drastically reduce the potentialities of the photo material.

From the TEM images, under 400°C the sample are mostly amorphous and the good properties (high surface area and small pores) are cancelled by the presence of defects and amorphous phase; also at 500°C there are agglomerations of crystals but also amorphous phase. At 600°C, instead, the structure is highly crystalline and it is also the

_____

reason why it is the most active one even if its properties are worse than the samples calcined at lower temperature.
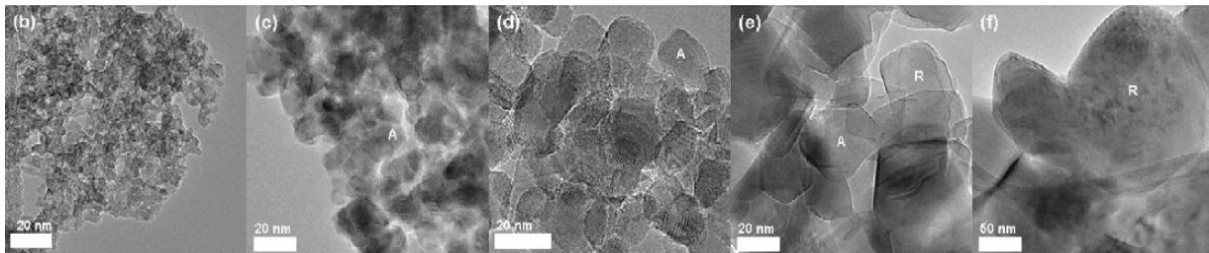

Figure 1.8. TEM image of Puddu's photocatalyst at different calcination temperatures: (b) 300°C, (c) 400°C, (d) 500°C, (e) 600°C, (f) 700°C. (Puddu et al. 2010)

- The second photocatalyst chosen is reported in the work done by Ismail (Ismail et al. 2004). It does not have any comparison with the P25 but instead it is a complete study that maximize the activity of the photocatalyst doped with silica that gives all the benefits that are reported in the paragraph §1.3.2. It is a classical procedure of production with the sol gel techniques where the quantity of the solvents, of the dopant and the gelation time are changed to improve the photoactivity. The suggested conditions that maximize the activity are follow reported:
  - C_2H_5OH:TEOS molar ratio of 10;
  - Si:Ti: molar ratio of 1:6;
  - H_2O:TEOS molar ratio of 8;
  - HNO_3 (1 M):Si $(OC_2H_5)_4$ molar ratio is 0.25

The product is very promising because it has very good physical quality where the sol gel without any solvents will never arrive.

- The catalyst of Liang (Liang, Li, and He 2012) is another sample made with the sol gel method and doped with cerium.

In the following graph is shown the progression of the reaction for a photodegradation of acetaldehyde for 3 different samples in a batch system.

Silver studies are very common in literature and it is quoted as one of the best metal dopant for this catalyst without changing the band gap of the titanium dioxide (Kumar and Devi 2011) but in this investigation it is proven that the cerium has also better potentiality and the reasons are already discussed.

The rate constant reported are respectively 0.1871 0.2302 and 0.2724 with a relative activity of the cerium sample respect the P25 is R=1.46

_____
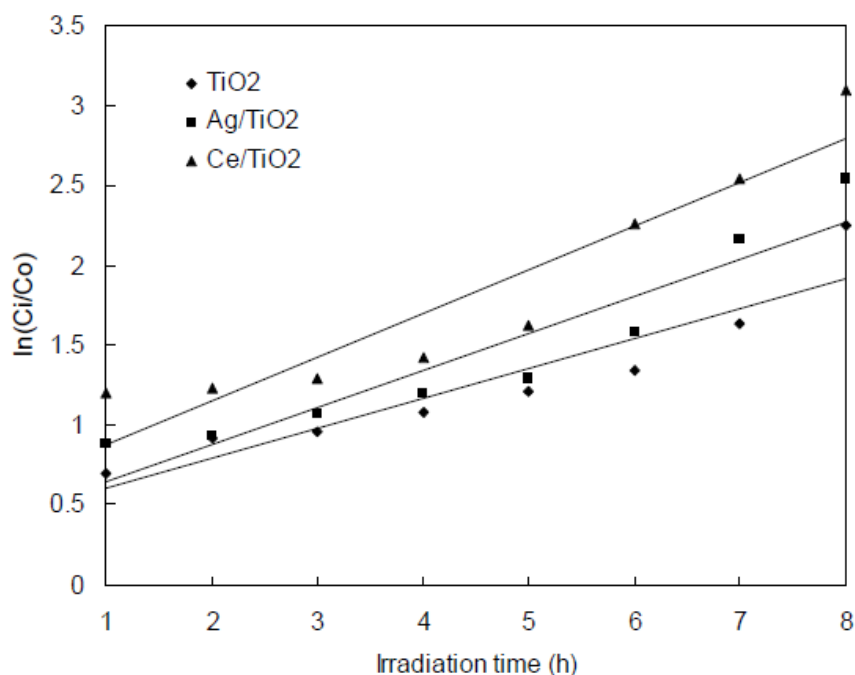
Figure 1.9. Relationship between ln(Ci/Co) and reaction time of the photocatalyst investigated by Liang. (Liang, Li, and He 2012)

- Fan (Fan et al. 2007) continues the studies of Yang; he proposes a standard method to produce mesoporous nanostructured materials, Fan applies the methodology and improves the techniques for the titanium dioxide and it create a very active catalyst. The results are shown in the figure 1.10 and the it represents the activities of his catalysts.

Figure 1.10. The degradation rates of acetaldehyde in close system with MT400, MT500, MT600 and Degussa® P25. (Fan et al. 2007)

_____

From the SEM and the XRD analysis reported in this paper it is clear that all the samples are composed by crystals of anatase and the performance are getting worse increasing the temperature because the properties of the material collapses: the pores and the surface area diminish and the crystal size grows. The relative activity declared is 2,47.
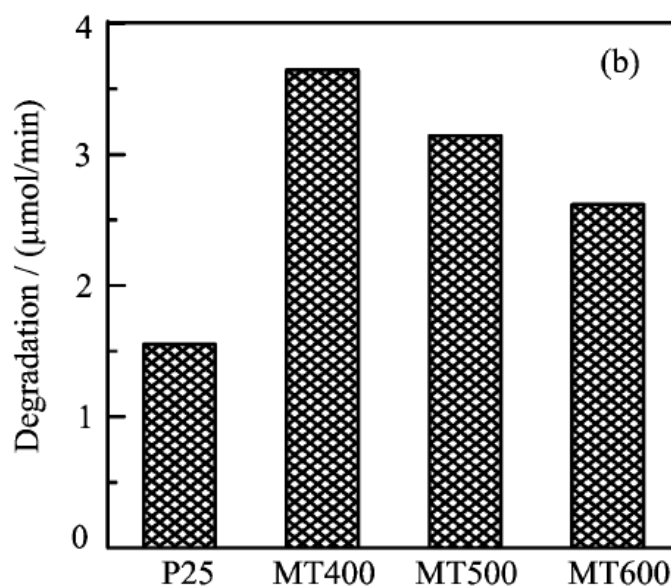
- The last selected catalyst is produced by Kosuge (Katsunori and Puyam 1999). This synthesis provide a mesoporous material mostly composed by silica oxide and from 2% molar of titanium oxide.

The figure 1.11 shows the results of the catalyst over the most active commercial catalyst that it is supposed P25.
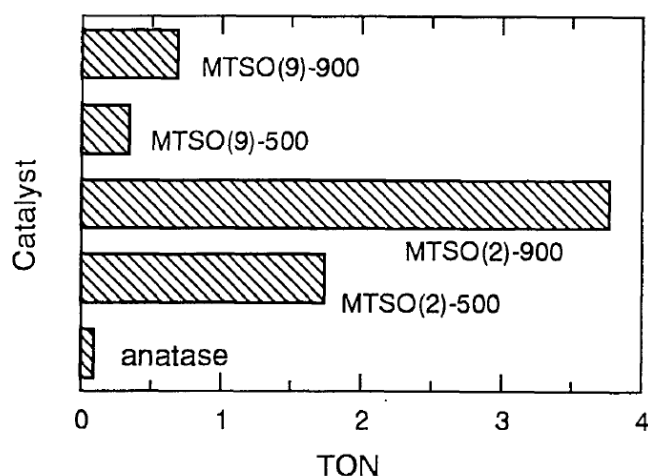
Figure 1.11. photocatalytic activity on different catalysts of Kosuge. TON means the numbers of reagents converted per one mole of Ti. (Katsunori and Puyam 1999)

The first consideration is the very high calcination temperature (up to 900°C) permitted by the high amount of silica. The physical properties, like the surface area are also prohibitive for an un-doped sample.

The promised result of the MTSO(2)-900 are declared as 39 time more active than the P25 in terms of number of molecules converted per second that a single catalytic site.

1.5 Dip coating

Dip coating is used as a technique to transfer and fix the micro-powders synthetized to a ceramic plate with a function of support for the catalyst; it is preferred over the other methods, like spin or spray coating, because of its versatility with batch and continuous process, its ability to coat large area, complex shapes and double sided tape so it could be easily scaled up for an industrial application (Amit 2005).

_____

The powders are dispersed in ethanol because it is the best convenient medium co prepare colloidal TiO_2 (P V Kamat, Bedja, and Hotchandani 1994) and a sonicator is used to achieve a good dispersion.

Sonication is a process in which sound waves are used to agitate particles in solution so it can divide the agglomerated particles that are stacked together and it is commonly used in nanotechnology for evenly dispersing nanoparticles in liquids (Jiang, Oberdörster, and Biswas 2009).

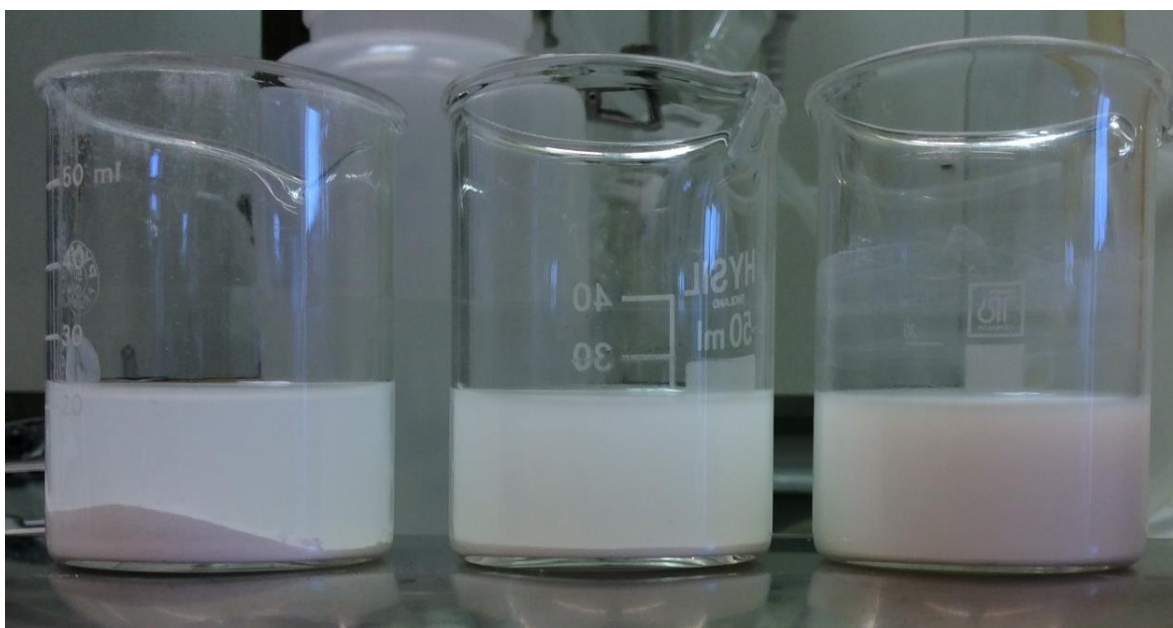A difference in dispersion of the TiO_2 powders is shown in figure 1.12.

Figure 1.12. Three different mixing solution results. From left to right the powders are stirred, ball-milled and sonicated.

In this investigation a ceramic place is used as support instead of a metallic plate because of its more affinity with titanium dioxide. The deposition of a layer in a Metallic plate are more challenging: there are problems of the stability of the layer with problem of cracks and the photocatalyst does not have the mechanical strength (see figure 1.6) to resist into the reactor when is performed the test; all these problems are solved changing the support.

The purpose of this work is the evaluation of the activity and the screening of different catalysts so we took the most suitable support and leave the challenge of coating TiO_2 on metal for future works.

1.5.1 loading

The dip coating process is very suitable techniques to create thin films over substrates; usually, when it is projected in a large scale production the velocity and all the other implied variables are specific designed to have a perfect layer of the desired thickness. This procedure is, unfortunately, not possible in a laboratory scale when there are various solutions that, in

_____

contact with the surface of the support, leaves a layer of different thickness that is dependant of various factor: the viscosity of the solution, the affinity between the solution and the support or dependant on the procedure of the dip coating itself.

Another aspect to take into consideration is the reaction because, since it is a superficial reaction, it is activated by the light and the amount of catalyst that is not irradiated does not participate to the reaction. This mean that if there is a layer of titanium dioxide too much thick, the crystals in contact with the support are not activated and viceversa if the layer is too thin, the absorption of the photocatalyst is not maximised and the reaction depends on the thickness of the film.

The investigation made by Krysa (Krysa et al. 2005) over a layer of titanium dioxide reveals that a layer of 2 μm absorb about 80% of the incident radiation and a thick of 10 μm is enough to have a complete absorption and in his article proves that also the reactor does not improve the performance above a certain load of titanium.

In this investigation is chosen to create a stratum of photocatalyst of 50g/m2 that correspond, without the pores, to a 13,23 μm. This value is being chosen to be consistent with the previous investigations (Persson 2015).

The loading of this amount is not possible in one dip of the support so the operation is repeated till the desired amount that increases each dip.

1.6 Characterization

The characterization of the synthetized titanium dioxide is fundamental because the activity is strictly related to the physical propriety and it is also good tools for comparing the characteristics with the catalyst of the references to evaluate how the synthetize samples differ to their references.

The catalysts were characterized by X-ray powder diffraction (XRPD) that from now on for simplicity will be called XRD. The result of this analysis gives a diagram where the intensity is in function of the angle (diffraction pattern) and from the position of the picks is possible to detect a particular phase of the element presents in the powder. This technique gives also information about the dimension of the crystals because it is related to the broadening of a peak in a diffraction pattern. The Bragg law describes this relation and it can be written as:

$$\tau = \frac{K\lambda}{\beta \cos\theta} \qquad (1.5)$$

Where τ is the mean size of the ordered (crystalline) domains, K is a dimensionless shape factor, with a value close to unity, λ is the X-ray wavelength, β is the line broadening at half the maximum intensity (FWHM), θ is the Bragg angle (Li et al. 2005).

_____

The Brunauer–Emmett–Teller (BET) analysis is an important technique for the measurement of the specific surface area of a material by physical adsorption of gas molecules. It provides also information about the average pore size and the porosity of the material (Puddu et al. 2010).

A scanning electron microscope (SEM) is used to produce images of a sample by scanning it with a focused beam of electrons. The pictures taken give a clear and unequivocal view of the micro and meso structure of the particles and it can also be a confirmation of properties like crystal size or the size of the pores (Takeshi et al. 2010).

1.7 Acetaldehyde

The molecule of acetaldehyde (CH3CO) with the structure in figure 1.13 is colourless, soluble in water.
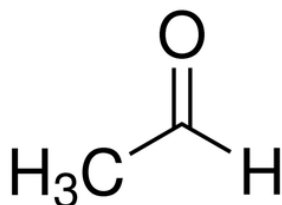

Figure 1.13. Chemical structure of acetaldehyde.[9]

This compound is used as a model compound for the photocatalytic abatement of this investigation instead of a mixture of different VOCs that are usually presents in an industrial process because they are difficult to control and analyse. Aldehydes are also detected in a large amount in a flue gas in a food industry that is one of the fields where the investigation is directed and acetaldehyde in particular is well known to be odour active (Nagata 2003) and the fact that it is used as an intermediate in industrial chemical synthesis such as polyester, dyes and perfumes make it a low price chemical.

These reasons, in addiction of its low price and low toxicity (legal limits of exposure is 200 ppm [3] if compared with other VOCs make it perfect for this investigation and in general representative for indoor VOCs to determine the effectiveness and capacity of gas-phase air filtration equipment for indoor air applications (Fan et al. 2007).

The hydroxyl radicals carry a complete decomposition of acetaldehyde (Fan et al. 2007; Ismail et al. 2004) with the reaction (1.6):

$$CH3CHO + 2.5\,O2 \rightarrow 2CO2 + 2H2O \tag{1.6}$$

_____
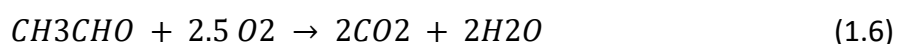
1.7.1 Safety data

Acetaldehyde is irritant in case of eye contact, of ingestion, of inhalation. It is slightly hazardous in case of skin contact. It is classified 2B for carcinogenic effects (Possible for human.) by IARC and mutagenic for mammalian somatic cells. Teratogenic effects are possible for human[3].

Chapter 2

Experimental part

This part will start from the synthesis and the deposition of the catalysts, and it continues with the explanation of the testing rig and all the experimental part of the investigation.

2.1 Catalysts synthesis

The preparation of a catalyst is always a critical part because every single step could deeply change the final result of the property and the performance of the catalyst. For this work, as reported in the introduction, six different methods are selected and carefully reproduced following the procedure found in each article.

To coat the catalyst on the support, 4 g of TiO_2 sample are needed but we produced 12 g in total because it is expected that 2g are lost in the making process, 2g are used for the characterization and 8g are used for 2 tests.

2.1.1 Sol gel

This synthesis is made following the procedure described by Puddu (Puddu et al. 2010).

Nanocrystalline TiO_2 is prepared through a simple sol–gel process. This paper shows that pure anatase exhibit higher activity than commercial TiO_2 (P25) under UV radiation; conversely, pure rutile and mixed phase TiO_2 materials showed significantly lower activity and the increasing in the crystallinity of anatase TiO_2 upon calcination overcame the depreciation in its structural properties (decrease in surface area and porosity) for the decomposition of VOCs and for these reasons it is decided the temperature of calcination at 600°C.

The procedure to obtain the photocatalyst is the following.

Titanium tetraisopropoxide (TTIP) is mixed in isopropanol with a ratio of 30 moles of i-PrOH each mole of TTIP and vigorous stirred. The stirred solution is added into deionized water dropwise at a H2O/TTIP molar ratio of 100:1 and stirred for 1 hour for completing the reaction and create a suspension. The particles are recovered with a vacuum filtration (a büchner flask and the vacuum system are needed for this operation), washed with water and dried in a ventilated oven for 2 hours at 50°C, this temperature is below the boiling point of the isopropanol but enough for a good evaporation. The powder is immersed in acetonitrile

overnight to extract the entrapped solvent and finally calcined one hour at 100°C to remove most the remain solvent and then another one hour at 600°C with a ramp rate of 3°C/min.

To produce 12g of catalyst are used (calculations are in appendix §A.1.1):

- 44.41 ml of TTIP
- 344 ml of i-PrOH
- 270 ml of H2O

2.1.2 Sol gel Si

This synthesis is made following the procedure described by Ismail (Ismail et al. 2004).

In the paper, the authors have interested in preparation and optimization of TiO_2–SiO_2 sample as a photocatalyst to volatile compounds. The TiO_2–SiO2 mixed oxides has been prepared via sol–gel approach. The conditions that could be used to obtain aerogel material that can be used efficiently for photocatalytic degradation of cyanide may be listed as:

- Si:Ti: molar ratio of 1:6;
- C_2H_5OH:TEOS molar ratio of 10;
- H_2O:TEOS molar ratio of 8;
- HNO_3 (1 M):$Si(OC_2H_5)_4$ molar ratio is 0.25

It is used the following procedure.

Two solution are prepared: the solution one contains titanium tetraisopropoxide (TTIP) and water, the solution 2 is a mixture of etraethyl orthosilicate (TEOS), water, ethylic alcohol and nitric acid with a molar ratio of 1:1:10:0.25 respectively. The first solution is added dropwise into the solution two to obtain a mixture with a final ratio between the reagents of 6 moles of TTIP and 8 moles of water every mole of TEOS. The final mixture is left gelling overnight and putted in an oven at 100°C for 2 hours to evaporate the solvent and then calcined at 500 degrees for 5 h.

To produce 12g of catalyst (calculations are in appendix §A.1.2):

First solution

- 44.4 ml of TTIP
- 3.15 ml of H_2O

Second solution

- 5.21 ml of TEOS
- 0.19 ml of H_2O
- 11.5 ml of Et-OH
- 0.66 ml of HNO_3 60%

There is a critical difference from this catalyst and the description followed of the paper: it requires an autoclave that is not available in our laboratory. Pressure decrease the temperature that is required to the crystallization and permits a slow growth of the crystals

_____

without any stress derived by high temperature and uneven thermal expansion (Lu and Wu 2004). In this investigation it is replaced by a calcination oven with possible lower physical properties that will reflect to the performance of the catalyst.

2.1.3 Sol gel Ce

This synthesis is made following the procedure described by Liang (Liang, Li, and He 2012)

The TiO_2 photocatalyst was prepared with 100 % anatase using the sol gel method, and immobilized as a film, a precursor of cerium is also used to modify the sample with the following procedure.

Titanium butoxide (TNBT) is mixed with ethanol, then diethanolamine (DEA) and the solution is left stirred for 2 hours. Another solution of ethanol, deionized water and Ce(NO3)3 were added dropwise to the first solution and stirred for 15 minutes; N,N-dimethylformamide(DMFA) is added. Finally, a third solution of ethanol and polyethylene glycol (PEG) is dropwise after 24 hours to form a stable gel.

To obtain powder, the gel is dried at 100°C for 5 hours and then calcined at 500°C for 2 hours.

To produce 12g of catalyst (calculations are in appendix §A.1.3):

First solution
- 51 ml TNBT
- 122.4 ml of Et-OH
- 8.81 ml of DEA

Second solution
- 15.3 ml of Et-OH
- 3.24 of water
- 0.16 g of $Ce(NO_3)_3$

Third solution
- 15.3 ml of Et-OH
- 0.55 g of PEG

The sample presents a pale yellow powders that are typical of the cerium oxide. The catalyst presents a difference in preparation: the procedure described by Liang involves to use the stable solution for coating a glass support but in this investigation a ceramic support is used instead of a glass support. The coating over this material is not possible because the viscous solution creates a very thick film with a lot of bubbles that explode and boil when the support is heated up (see figure 2.1). It is decided so to calcine the film to form the powders and then create the film; this procedure is also preferred also because it is coherent with all the prepared film made with the other photocatalysts.

_____

Figure 2.1. Sample of Sol gel Ce before (left) and after (right) the calcination process

2.1.4 Mesoporous

Fan (Fan et al. 2007) produce mesoporous TiO_2 powder with worm-like channels by an evaporation-induced self-assembly approach that exhibit higher photocatalytic activities than Degussa® P25. It is used block copolymers as structuring agent and $TiCl_4$ as the precursor with the following procedure.

Titanium chloride is added in a solution of pluronic P123 dissolved in ethanol and stirred for half an hour. The solution is left gelled for four days ay 40°C and then calcined at 400°C for an hour in a calcination oven.

To produce 12g of catalyst (calculations are in appendix §A.1.4):

- 16.4 ml $TiCl_4$
- 150 ml of Et-OH
- 15 g of P123

2.1.5 Mesoporous Si

This particular photocatalyst is produced by Kosuge (Katsunori and Puyam 1999) and consists in a mesoporous material mostly composed by silica with just 1,57% molar of titanium dioxide. The titanium is dispersed into the silicate framework. Thanks to the silica the calcination temperature is decided at 900°C. the simple procedure is described below.

A solution of TEOS and TEOT (the precursors of titanium the silica) is stirred for 15 minutes and then mixed with octylamine (the structuring agent) and finally hydrocloridric acid is added dropwise. The solution is left gelled for four days ay 70°C and then calcined at 900°C for an hour in a calcination oven.

To produce 12g of catalyst (calculations are in appendix §A.1.5):

_____

- 0.63 ml of TEOT
- 43.7 ml of TEOT
- 19 ml of octylamine
- 3.73 ml of HCl

The procedure is not clearly described in the paper and it is open to various interpretations. Different attempts are made covering all the alternatives and to finally choose the only one that create a solid powder structure after calcination.

2.1.6 Interlayer

Yuan (Yuan et al. 2008) creates a stable sol that is used to coat the ceramic support, this layer isolate the photocatalyst and improves the efficiency and the stability of the titanium. The procedure is following described.

Aluminium chloride hexahydrate and ethyl silicate (TEOS) are added to ethanol into a flask connected with a reflex condenser. The solution is stirred, it is kept boiling at 60°C and refluxing until the aluminium chloride hexahydrate is dissolved and no more visible as a salt. The solution is made with

- 24.145 g of precursor of aluminium
- 7.467 ml of TEOS
- 116.6 ml of ethanol

The resultant mixture is then a uniform, stable, and transparent sol of Al_2O_3–SiO_2 and ready for the dip coating of the support.

2.2 Commercial samples

Beside the synthetized sample in this investigation it is also tested the performance of four different commercial photocatalysts.

Commercial sample of three companies with high experience in production of titanium dioxide are evaluate besides the synthesized sample.

- AEROXIDE® TiO_2 P25 (Degussa®) is the most famous photocatalyst, it has the perfect combination between rutile and anatase to maximise the activity with the weight ratio of approximately 80 / 20.

  It is a fine white powder that consists of aggregated primary particles with crystals of several hundred nm in size and the primary particles have a mean diameter of approx. 21 nm. Particle size and density of ca. 4 g/cm³ lead to a specific surface of approx. 50 m²/g. Due to the formation of aggregates and agglomerates, the tamped density of AEROXIDE® TiO_2 P25 is only about 130 g/l. Both crystal forms are tetragonal[4].

_____

- AEROXIDE® TiO$_2$ P90 (Degussa®) is a development of P25 by variation of the production and another depuration in order to increase the photocatalytic properties: The result is a product with an average primary particle size of 14 nm[4].

- HOMBIKAT® TiO$_2$ M211[5] consists of densely packed particles. TiO$_2$ are produced using a unique production process and it is part of the new generation of catalytic TiO$_2$ performance materials. Particles consist of TiO$_2$ aggregates, which make up highly porous secondary particles. This material has a much larger mesopore size (D50 are from 20 to 30 nm) combined with high pore volume (0.8 cm^3/g) and a large surface area (~320 m^2/g), a combination unique among the commercially available TiO$_2$ catalyst. These typical features can be retained even under extreme conditions, including high temperature, a suitable characteristic when this material is used as support for other applications.

- CristalACTiV® TiO$_2$ PC105(Catalizador TiO$_2$ n.d.)[6] is a high surface area and high purity ultrafine TiO$_2$ powder that are recommended for evaluations in photocatalytic applications.

The properties of the three catalysts are summarized in table 2.1

Table 2.1. Physical main characteristics of the commercial samples.

	Crystal Size [nm]	Porosity	BET (m^2/g)
P25	17.69	0,343	53.95
PC105	16.56	0,413	86.42
P90	12.1	0,722	108.10
M211	4	0,3	320

2.3 Characterization

The evaluation of the physical proprieties is evaluated with XRD, BET and SEM and following the general procedure of the instruments.

The XRD analysis is performed on a Siemens D5000 diffractometer with Cu-Kα radiation (2θ= 10–90°, step size = 0.02°) shown in figure 2.2.
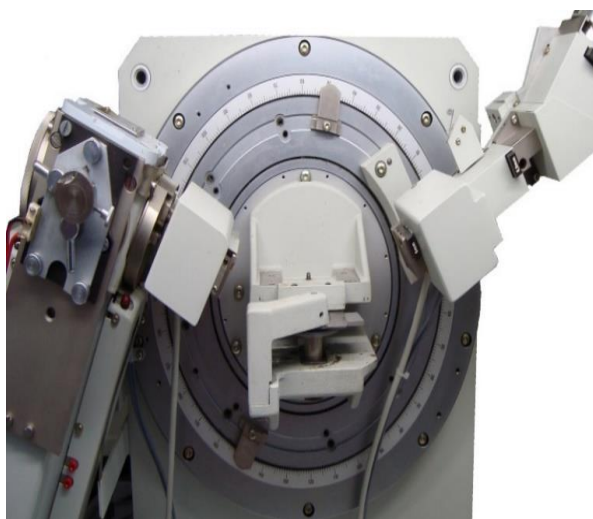
_____

Figure 2.2. The XRD machine.

The Brunauer–Emmett–Teller (BET) shown in figure 2.3. The surface area, pore volume and pore diameter were measured with a Micromeritics ASAP 2000 unit. The BET surface area was estimated by N_2 adsorption at liquid nitrogen temperature at relative pressures between 0.06 and 0.2. The pore size distribution of the catalysts was obtained with the same equipment using the Barrett-Joyner-Halenda (BJH) method, considering a pore size between 17 Å and 3000 Å.

Figure 2.3. The BET machine.

For the SEM analysis INCA PentaFET-x3 is used (figure 2.4).

Figure 2.4. The SEM machine.

2.4 Dip coating

After the synthesis, the catalysts are created and they all are in form of granular powders. Each photocatalyst is conceived to maximise its potential activities according to the best sample found in its respective paper; the following step is to fix the powders on a support to create an active layer and avoid the problem of having powders into the reactor.

The supports are dip coated with a suspension of titanium dioxide and the procedure has been standardized to minimize the difference from one sample to another: the screening work required that the only differences between different tests are only the catalyst and nothing else.

The dip-coating process can be separated into six stages (Rahaman and Rahaman 2006).

The first step is the preparation of the slurry, the synthetized powder or the industrial samples are mixed in ethanol used as a solvent in a mass ratio of 1:20 and then sonicated for an hour to create a colloidal suspension.

The second stage is called start up: the support is immersed into the solution and left there for about 5 seconds; the support in not completely immersed into the solution but only the bottom surface is in contact with it: the catalyst is deposited just in the irradiated surface so

_____

the other face of the plate is completely inert. Without this expedient it is necessary to remove the catalyst from the other surface of the support by scratching it away that is an undesired operation (some crystals of titanium could be remain and it is difficult to evaluate the exact amount of catalyst loaded).

The deposition happens while the substrate is pulled up. The withdrawing is carried out at a constant speed to avoid any jitters and the drainage is made tilting the dish and letting it drip for a few seconds from an angle of the support.

The operations from the start up to the drainage are repeated for each angles of the support to have a very uniform layer. In the end the evaporation of the solvent starts in the fumehood for 10-15 minutes and proceed into an oven at 70° C (below the boiling point of the ethanol) and weigh.

This procedure is repeated until the support is loaded the minimum amount of calculated catalyst

To prevent any traces of adsorbed solvent from the catalyst the plate is finally heated up at 200°C for 2 hours and it is ready to test.

2.4.1 Catalyst to load

It is decided a quantity of 50g/m^2 for all the samples and imaging a titanium dioxide material without pores and compact. The anatase density is 3.78 g/cm^2.

$$\frac{3.78\ g}{cm^3} = 3.8 * 10^8 g/m^3 \tag{2.1}$$

$$S = \frac{50\ g/m^2}{3.78 * 10^8\ g/m^3} = 13.2 * 10^{-8}\ m = 13.2\ um \tag{2.2}$$

S is the thickness of the deposited layer and it is enough to lose the dependence on the thickness.

The dimension of the support is 78 mm length and 80 mm width so the quantity of catalyst (Q) is:

$$Q = 50\ g/m^2 * 78 * 10^{-3}\ m * 80 * 10^{-3}\ m = 0.312\ g \tag{2.3}$$

The dip coating process is repeated till the support reach an increasing of weight of 0.312 g.

2.5 Experimental set-up

The layout of the testing system consists in four different parts: gas supplying &stabilization, humidifying and mixing, the reactor and the analyser (figure 2.5).
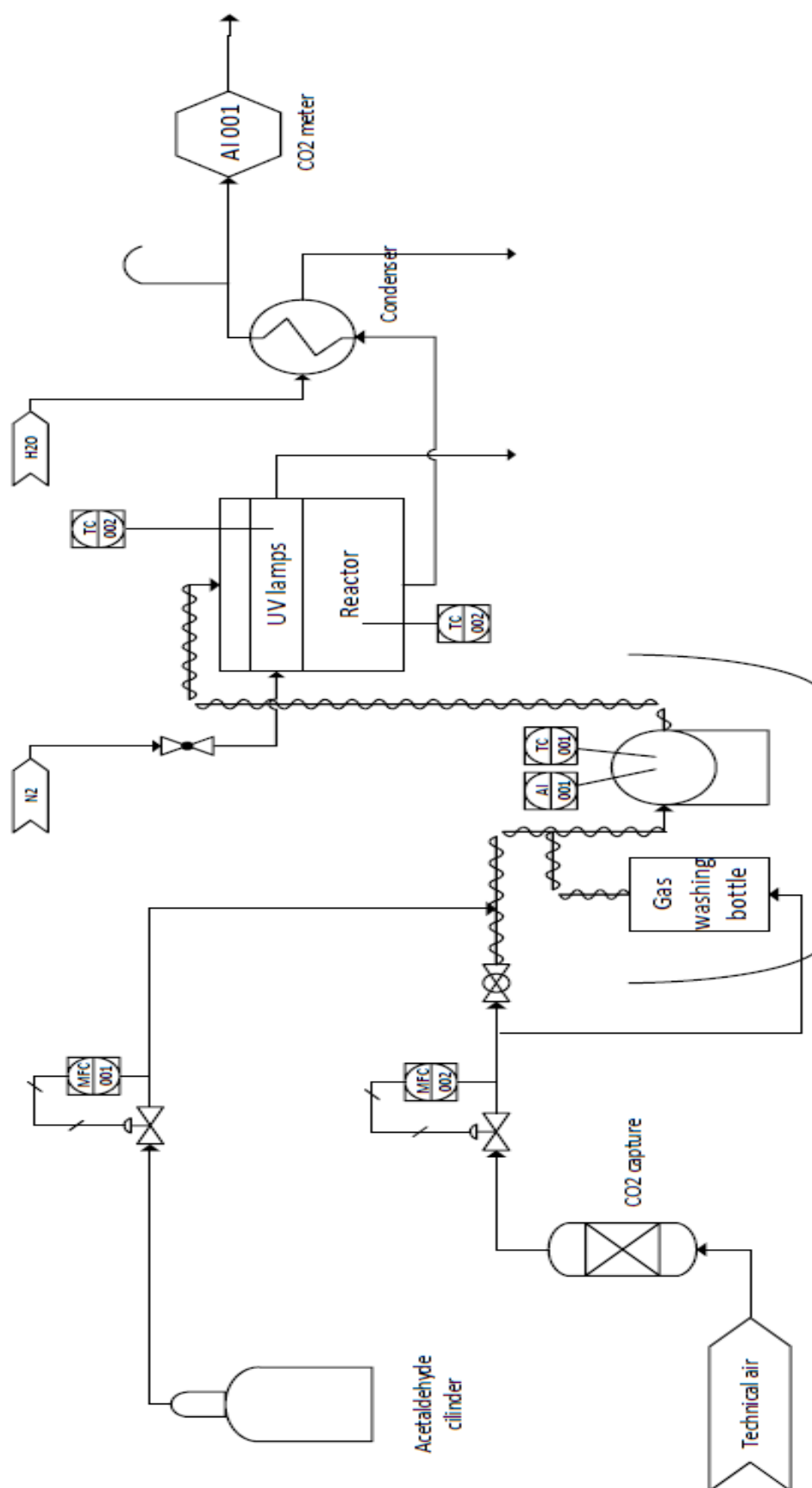
Figure 2.5. Scheme of the experimental setup.
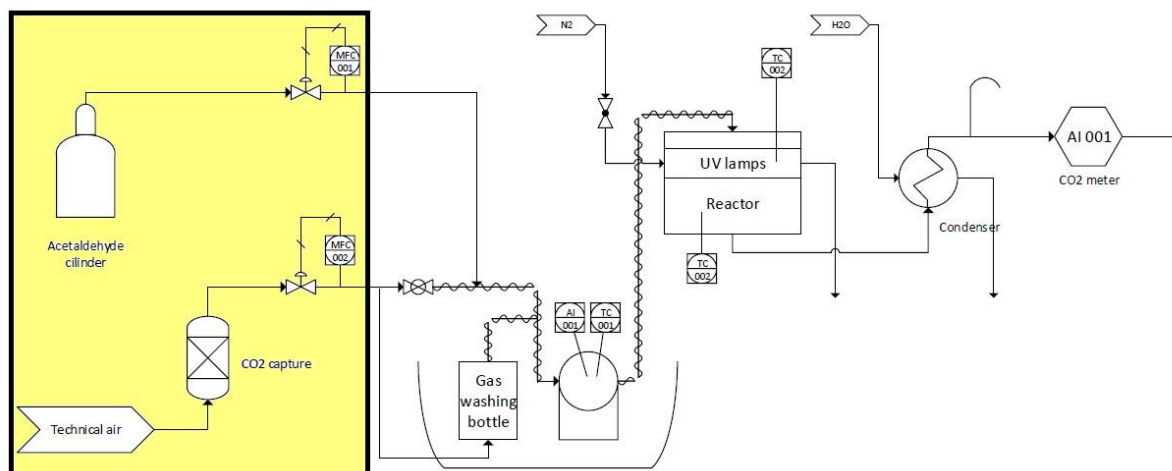
2.5.1 Gas supply & stabilization

Figure 2.6. Scheme of the experimental setup with the gas supply & stabilization part highlighted.

Technical air and acetaldehyde are the two inlet streams of the process (figure 2.6).

- Acetaldehyde is the pollutant to remove from our stream, it represents the VOCs and it is supplied to the system from a gas cylinder of 1 % acetaldehyde in nitrogen. The flow of gas from the cylinder is controlled by a pressure regulator that stabilize the pressure after the bottle and a mass flow controller (Brooks 5850E series, max 2 L/min of nitrogen) to flow exactly the calculated amount of gas.
- Technical air is available by the gas service of the laboratory. It is a stream of compressed air depurated firstly by a catalytic convertor to remove hydrocarbons and then a PSA (pressure swing adsorption) remove moisture and CO_2 (appendix §A.2). The air flow is controlled with another mass flow controller (Brooks 5850E series, max 25 L/min of air).

Purity of the carrier gas is fundamental in a system where the pollutants are in concentrations of just hundreds of ppm, furthermore, a presence of hydrocarbons that might be converted into carbon dioxide or fluctuations of CO_2 itself are detected from the detector making impossible the evaluation of the real conversion of the catalyst. These reasons explain why it is used a stream of technical air with all its limitations instead of the more typical compressed air that are not purified; the problematic is investigated in the previous analysis with the result of the impossibility of utilization of compressed atmospheric air (Persson 2015).

The characteristics of the carrier gas after depuration are:

- Air (same gas composition of the atmosphere) without dust or other solid particulates
- No hydrocarbons (less than 0.1 ppm)
- About 2 ppm of CO_2
- $6g/m^3$ of humidity
- 4 bar of pressure

- Flowrate up to 10 L/min (technical limitation of the depuration system)

The problem of the detection of carbon dioxide observed with compressed air (Persson 2015) is almost overcame with technical air but there are still some oscillations of its concentration of about 2 ppm (Persson 2015). To get round the problem is inserted a packed bed (CO_2 capture in the figure 2.5) made of commercial zeolites with molecular sieve function for the removal of CO_2. The carbon dioxide capture is in equilibrium and it does not act as an absorber, it stabilizes the system from the fluctuations of CO_2 (appendix §A.3). technical air is fluxed in a washing bottle filled with the zeolite instead of water (figure 2.7).

Figure 2.7. Photo of the washing bottle filled with zeolites with function of CO_2 captured.
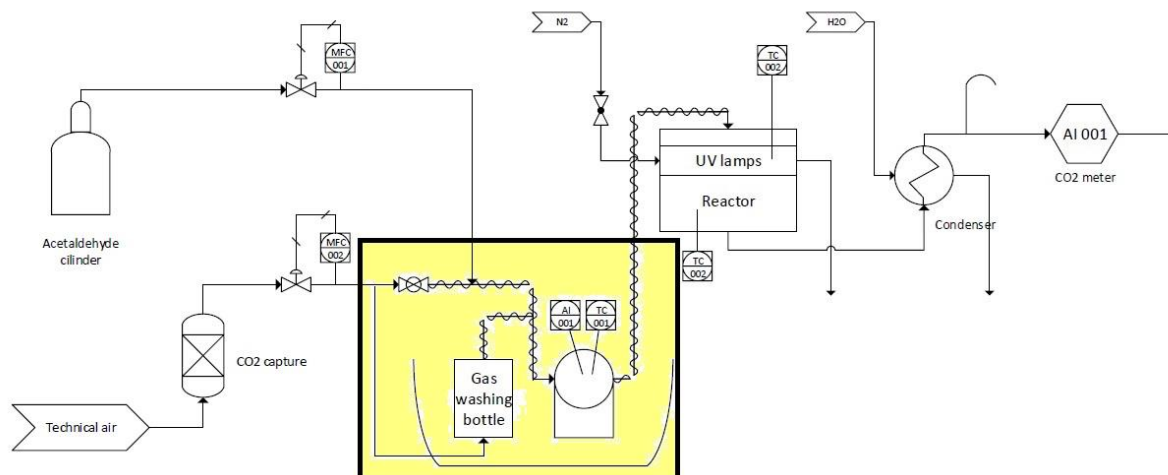
_____

2.5.2 Humidifying system & mixing

Figura 2.8. Scheme of the experimental setup with the humidifying system & mixing part highlighted.

Carrier gas is almost dry after the purification: it contains 16% of relative humidity at 37°C and to add moist and reach the set point It is installed a humidification system. It works splitting the stream of air and part of it is bubbled throw a washing bottle (Saveen Werner 1000 ml Porosity 2) filled with water.

The flux throw the humidification system is modulated by a ball valve inserted in the by-pass of the system (see figure 2.8); this specific type of valve is chosen instead of the classical globe valve normally used as a regulating flow because it has no relevant pressure drops or limitations of its operative conditions: properties of this type of valves are fundamentals in this rig without critical elements that create difference in pressure and this cause that every globe valve tried does not allow any regulations of the flow.

Acetaldehyde stream is connected after this valve and it does not flow into the humidifying system because of water, otherwise it would be trap in the washing bottle for its high solubility.

Another important aspect in order to reach the desired amount of humidity and operate in the best condition for the reactor is the temperature control. The system is heated up at controlled temperature from the washing bottle to the reactor with both a thermostatic bath (Grant JB1) at 50 degrees where it is immersed the humidifier and the glass sphere with the hygrometer, and heating tapes rolled up the pipes thermally insulated with glass wool.

The humidity is measured just before the reactor (Wood's SS-7002), it shows the temperature and the relative humidity (RH) with an accuracy respectively of 0.1°C and 1% HR at that point. As said before, the probe is inserted in a glass sphere in order to have a better mixing of the three streams and since it is a place with less gas velocity if some condense on the pipes (due

_____

to some cold spots) or a droplet came out from the washing bottle, it is not dragged by the gas stream to the reactor but it is trapped in the sphere.

Another advantage is provided by the thermostatic bath because it keeps at fixed temperature the hygrometer so the humidity data taken refers all to the same absolute humidity.

2.5.3 Reactor

The reactor is designed for a photocatalysts screening, it is show in figure 2.9 and 2.10.
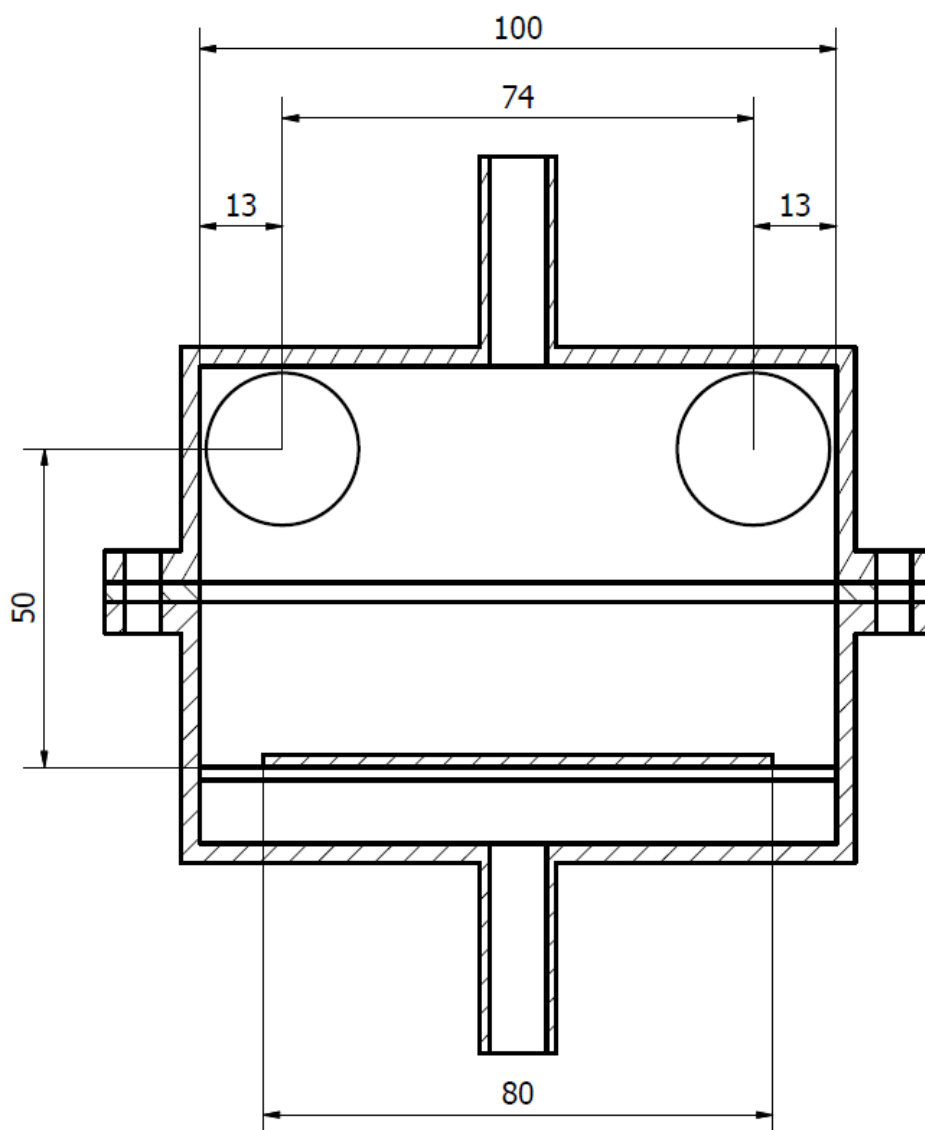

Figure 2.9. CAD drawing of the UV reactor with the dimensions of the distances between the elements in the UV reactor.
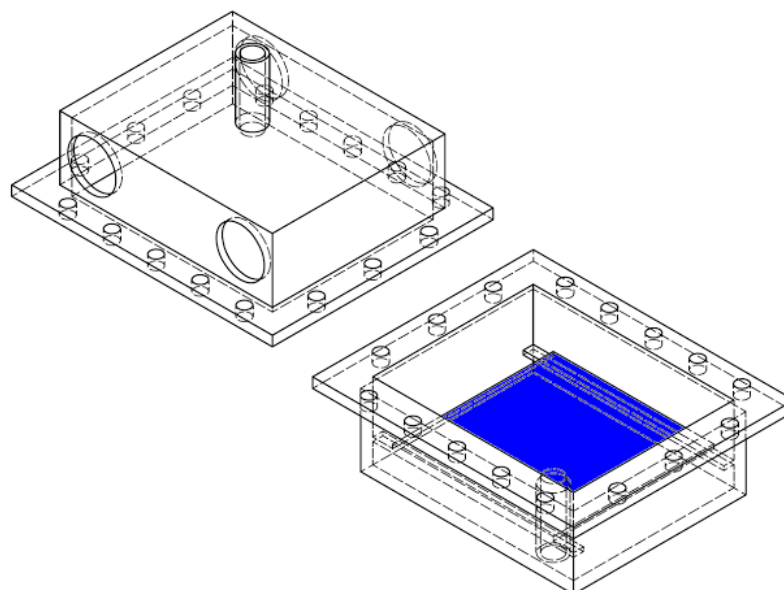
_____

Figure 2.10. CAD drawing of the UV reactor for the tests of photocatalysts.

The reactor is made of stainless steel (316) with a volume of 0.615 dm3 with an inner width of 10 cm, height of 7.5 cm and depth of 8 cm. There are two tubes of quartz glass in the upper part of the reactor sealed on the reactor with silicon for the insertion of the UV lamps.

A gasket is made of EPDM and together with screws are used for keeping the reactor closed and it can be opened easily and quickly to replace the catalyst. A thermocouple is inserted without losing the sealing thanks to the gasket.

The catalyst plate (size 7.8*8 cm^2) is inserted and lean against its metallic guides inside the bottom part of the reactor (the blue surface in figure 2.10 indicates the catalyst).

The inlet comes inside the reactor from the top and orthogonally with the plate and it goes out from the bottom to minimize the mass transfer limitations from the bulk and the surface and to have a gas velocity predictable, useful in a future model.

Fluid dynamics of the reactor

The reactor is studied to detect the difference in terms of activity among various samples of titanium dioxide and a fluid dynamics simulation has been made with the software COMSOL (Montecchio et al. 2016). It is shown in figure 2.11.

The calculation is performed under the assumption that the reaction is much faster than the diffusion, in others words the reactor works in mass transfer regime. With this hypothesis it is considered the best possible catalyst in order to see the upper limit of the performances of the reactor.
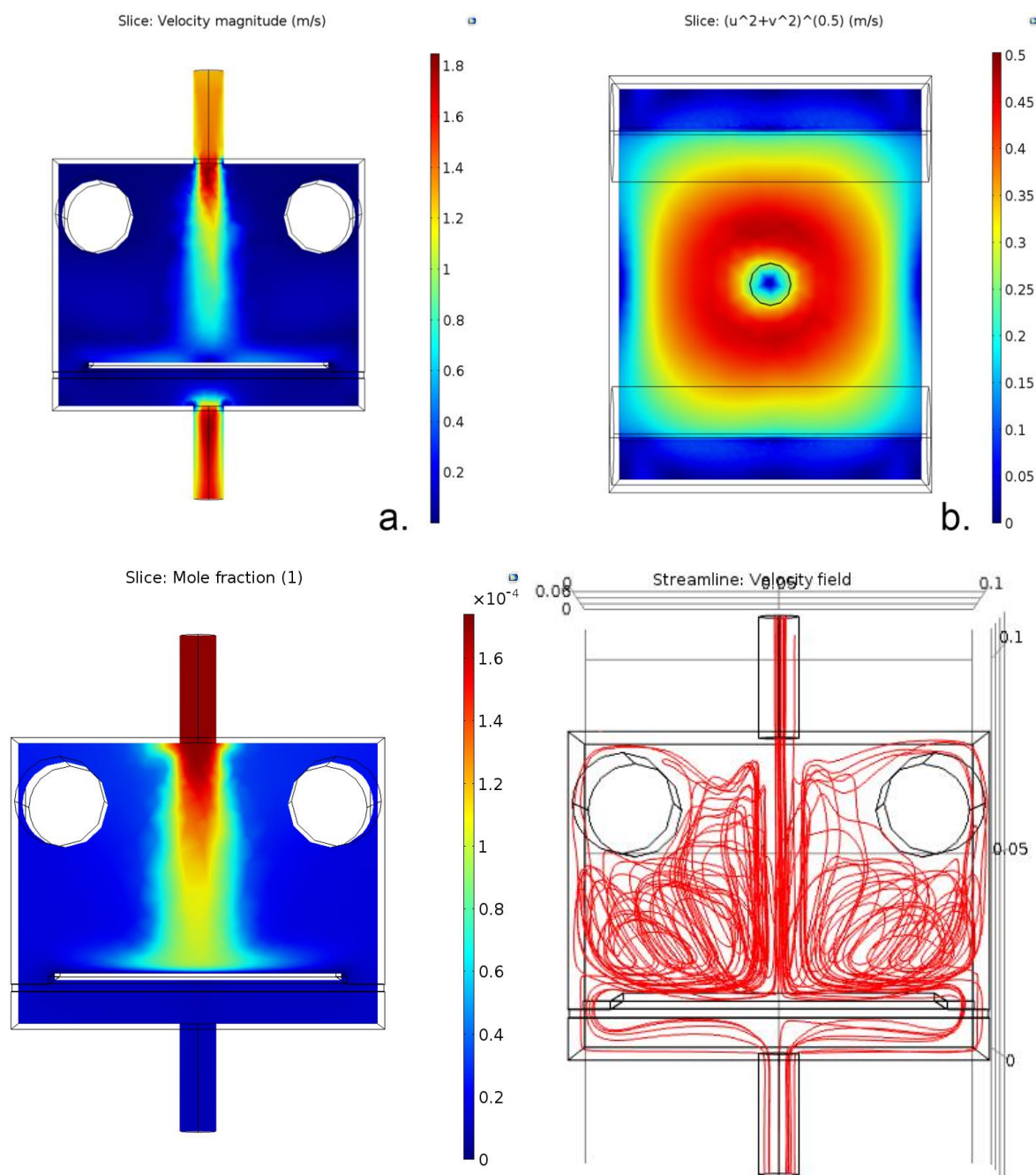
Figure 2.11. Velocity profile of the gas inside the UV reactor in a vertical slice at the centre of the reactor (a), on the catalyst surface (b), molar fraction inside the UV reactor in a vertical slice at the centre of the reactor (c) and the path of the gas inside the reactor (d).

The figure 2.12a is a representation of the velocity of the process stream inside the reactor, it is possible to note that most of the fluid of the inlet goes directly to hit the surface of the catalyst and it is propagated radially along the surface (figure 2.12b). The figure 2.12d shows also a recirculation of the fluid inside the reactor to arrive at the conclusion that almost all the gas gets in contact to the catalytic surface before the exit and this is confirmed from the figure 2.11c that represents the concentration in each point inside the reactor and a calculation about the total conversion reveals the conversion of acetaldehyde X=94%.

_____

UV lamps

The UV-lamps used for the investigation of photocatalytic oxidation were Heraeus GPH135T5L/4 with an arc length of 5.5 cm. The lamps use 5W each to emit 1.2 W light at 254 nm. The UV intensity according to the data sheet is 10 µW/cm^2 at 1 m distance from the lamp [Ultraviolet, 2015 #45].

The reactor was designed using a 2D simulation with the software MATLAB (Persson 2015), the final solution is shown in figure 2.12. The position of the lamps into the reactor are funded with the simulation minimizing the difference of the UV radiation over the surface of the catalyst using the Inverse-square law (the intensity of the radiation E in each points is inversely proportional to the square of the distance r from the source of that physical quantity), equation (2.4).

$$E = \frac{I}{r^2} \qquad\qquad (2.4)$$

From the figure 2.12 is it possible to note that the intensity of the radiation for both of the lamps and the sum of them. The total irradiation is quite homogeneous over the catalyst plate and this is very important in our system because it is fundamental to get uniform reaction and use the entire surface at the same conditions. The best configuration is funded with the lamps placed 3.7 cm from the centre and 4.76 cm above the photocatalyst plate.
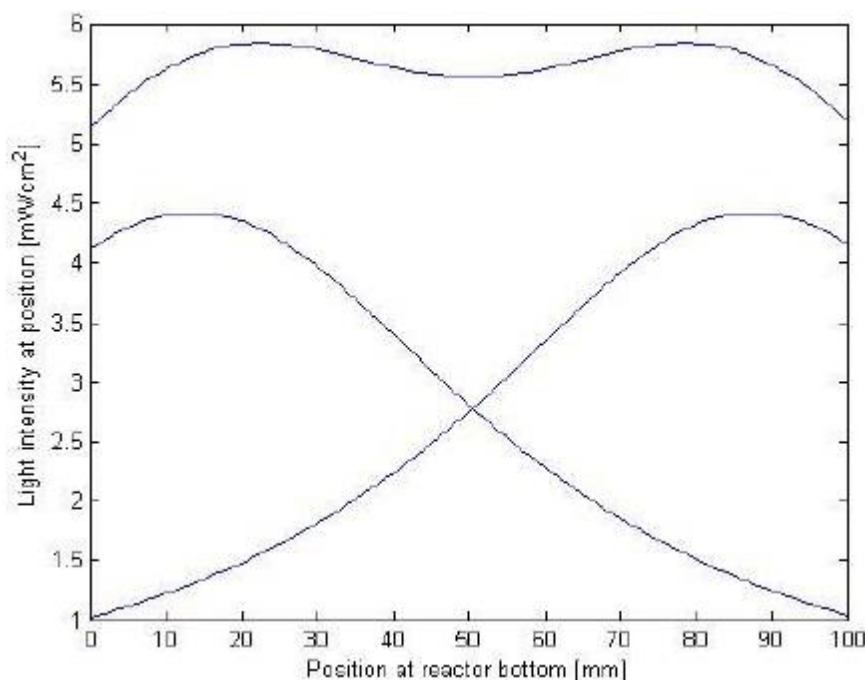

Figure 2.12. 2D results simulation of the UV radiation on the catalytic surface. The figure shows the contribution of each lamps and the total irradiation.

Homogenous irradiation is required but physically impossible due to the shape of the lamps and the geometry of the reactor.

To have a better estimate of the incident radiation it is developed a more accurate 3D model; it works with the same assumptions of the previous 2D simulation and the data are then validated experimentally with a UV sensor: they are amended taking in consideration the real power of the two lamps used, that are slightly less than the value reported in the data sheets probably due to the wear of the lamps figure 2.13 (appendix §A.4).
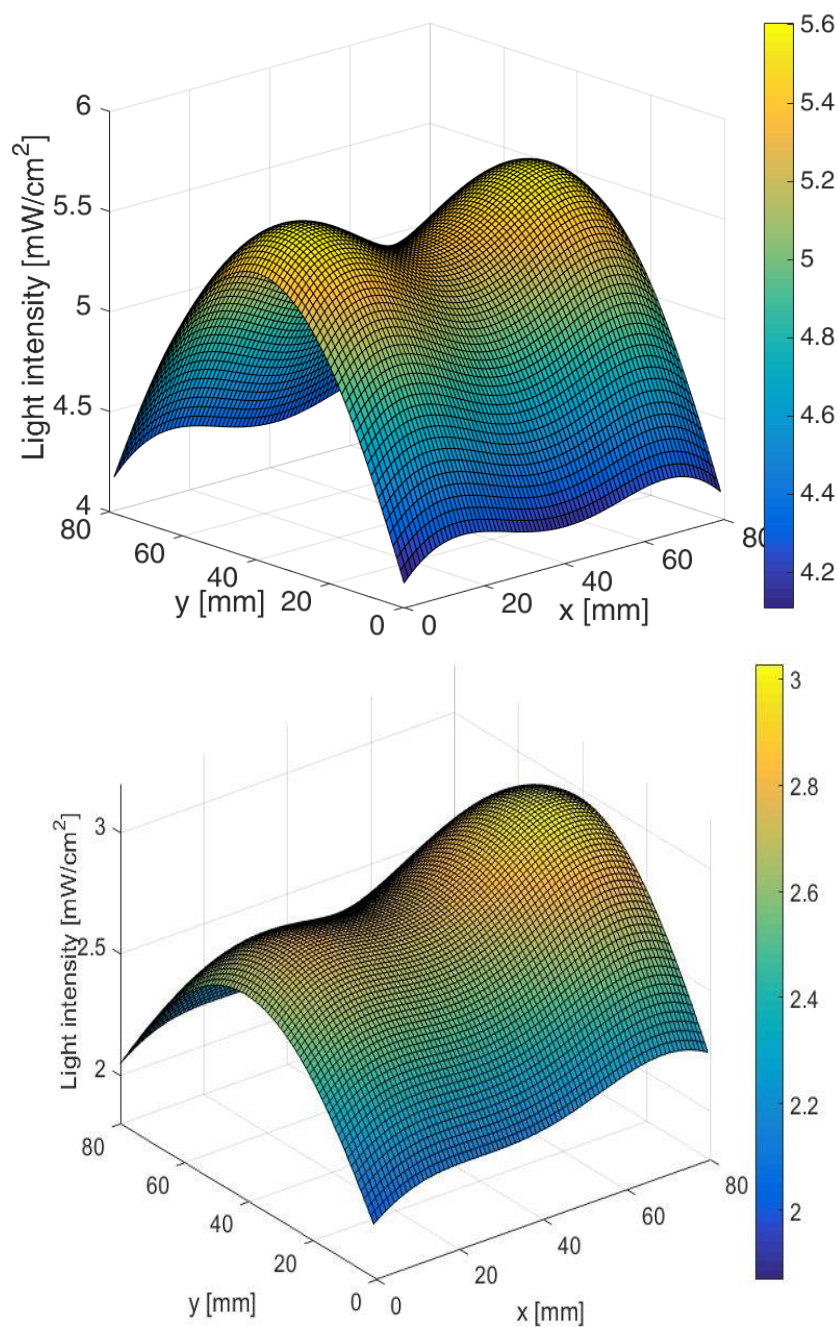

Figure 2.13. 3D MATLAB simulation's result of the UV radiation on the catalytic surface. The figure above is the theoretical irradiation the second one is a fitting of the experimental data.

_____

Overall the radiation is satisfactory homogeneous, the MATLAB calculation permits to calculate the irradiation in every position of the catalyst (Montecchio et al. 2016) and it will be very useful for further studies.

The UV low-pressure lamps work well at temperature of 40°C[7] but they maintain the same performance up to 50°C (above this temperature the efficiency of the lamps are getting low) and, in order to maintain this temperature, a stream of nitrogen is flowed between the lamps and the tube of quartz of the reactor to cool them down. The nitrogen permits also the reactor to maintain at temperature set point.
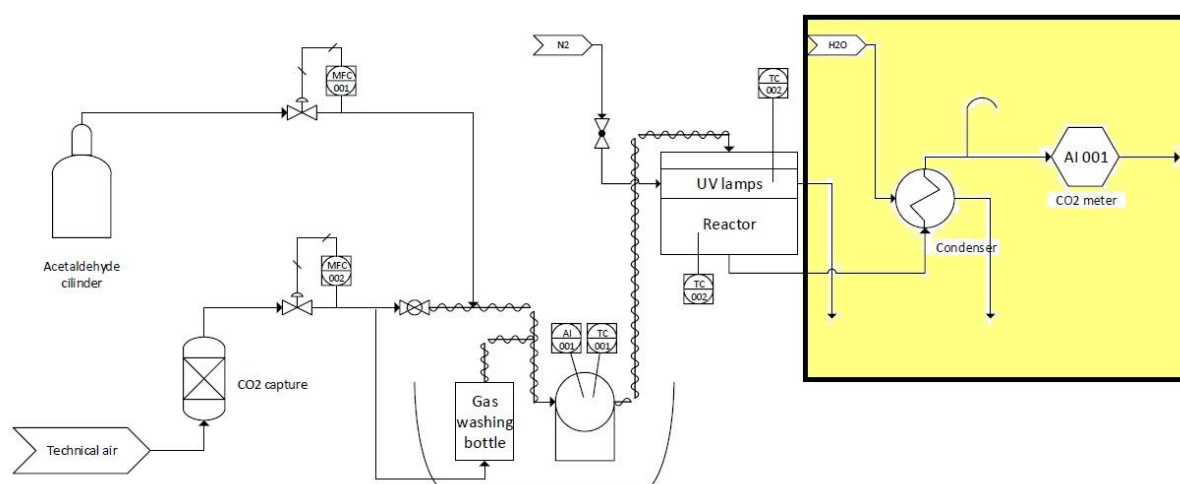
2.5.4 Dehumidification and analysis

Figure 2.14. Scheme of the experimental setup with the dehumidification and analysis part highlighted.

After the reactor the stream is dehumidified in a condenser with cool water in counter current to remove all the water because the detector is very sensible to moisture (Hodgkinson et al. 2013). A condenser trap cools down the gas stream below the saturation point so it is able to remove most of the humidity from the process stream and, in the unlikely case, some water droplets to avoid the instrument from damages.

The dehumidification system removes also some acetaldehyde because of its solubility in water so it makes impossible to detect directly the conversion. The catalyst activity is evaluated from the data of CO_2 quantity in the dried stream after the humidity trap (see figure 2.14).

Carbon dioxide is measured with a nondispersive infrared sensor (NDIR) (FLS Airloq rosemound 2000) with a display that shows the instantaneous concentration of the CO_2, CO and CH_4 (figure 2.15).

_____

Figure 2.15. photo of the IR analyser

The IR analyser works with a constant flow of 1.5 L/min and it has its own pomp to take the needed amount of gas so the process stream is divided and purged right before the inlet of the analyser. The purge puts the system at atmospheric pressure.

2.6 Set-point of the system

The purpose of the study is to evaluate the performances of different catalysts in order to select the most active one and this analysis is possible only if the system works always in the same conditions and the only difference among the tests are the samples of different photocatalysts.

It is crucial to find the best conditions for reproducing as much as possible the plants conditions: it is chosen a fried plant of removing the VOCs from the exhausted gas that has high temperature and humidity but very short residence time to maximize the production. On the other hand, working with laboratory equipment is very different: it has limits and different problems.

The first aspects to consider is the flow of air, it has a maximum flow of 10 L/min because of the technical limits of its purification system. Another important limit is the working temperature of the lamps that are imposed by the producing company to maximize the efficiency of the lamps at 45°C. Lamps in the commercial application are different than the lamps used in this investigation and their works in another range of temperature avoiding this problem but it is impossible to used them because it is required lamps less powerful and another fundamental difference is that the lamps commercially used create ozone from the air. Ozone is another good agent that is create with another band of the light and it oxidize the VOCs but for the purpose of this investigation is not usable, otherwise it will cover the activity of the catalyst and its correlate results.

The working conditions of the reactor after these considerations are kept at 40°C that is a perfect temperature because the nitrogen flow that cools down the lamps influences also the temperature inside the reactor and, in a steady state, reaches this temperature so it is in equilibrium with the process fluid and does not create thermal instabilities; a total flow of 6 L/min that is also the flow chosen for performing the fluid dynamic simulation of the reactor, with a content of relative humidity of 20% for avoid all the problems with condensation and with the CO_2 analyser and a concentration of 150 ppm of VOC to oxidize.

 All the inlet informations are in table 2.2

Table 2.2. Inlet conditions at the reactor.

	N2	O2	VOC	H2O
volumetric flow (L/min)	4,69	1,22	9,00E-04	8,64E-02
molar flow (mol/min)	0,21	5,46E-02	4,02E-05	3,86E-03
massive flow (g/min)	5,86	1,75	1,77E-03	6,95E-02

 The table above shows the inlet condition into the reactor; humidity content, the volumetric flow and the other values are calculated considering the process stream an ideal mixture of

_____

ideal gases that is reasonable for a flow mostly composed by air with a temperature of 40°C and at atmospheric pressure.

The system has a stabilization time that requires about one hour and a half after the starting up where three operations are performed to conduct the setup in a steady state:

- Adjust the flowrate between the humidification system and the bypass with the globe valve
- Control the inlet temperature at the reactor changing the power given to the heating tape
- Adjust the flow of nitrogen to cool down the lamps at the set-point

Once the system is in a steady state the performances are evaluated for 3 hours taking the value of the converted CO_2 every thirty minutes to be sure that the system and the result are really stable.

2.6.1 Calculations

The streams with all their parameters to control in the setup change with the temperature and they need to be estimated.

The first important parameter to fix is the pressure: the purge of excess gas before the analysis system keeps the pressure fixed at 1 atm and, with a good approximation, this value is assumed for the entire rig.

Another reasonable simplification, since the streams are considered ideal solution of ideal gasses, is to consider the volumetric fraction and molar fractions the same value.

Streams are provided in the lab at 22°C that is also the working temperature of the two mass flow controllers; the hygrometer instead operates at 37°C because it is immersed in the thermostatic bath.

The conditions inside the reactor are 40°C of a flux of 6L/min, 20% HR and 150 ppm of VOC

- Acetaldehyde

  Volumetric flow rate of acetaldehyde in the reactor:

$$V_{VOC} = PPM * 10^{-6} * flux = 150 * 10^{-6} * 6 = 9 * 10^{-4} L/min \tag{4}$$

  Volumetric flow rate from the gas bottle:

$$V_{BOT} = \frac{VVOC}{1\%} = \frac{9 * 10^{-4}}{10^{-2}} = 9 * 10^{-2} \ L/min \tag{4}$$

- Water

  Quantity of water is calculated from the equilibrium vacuum pressure to obtain the partial pressure of water or simply from experimental data[8].
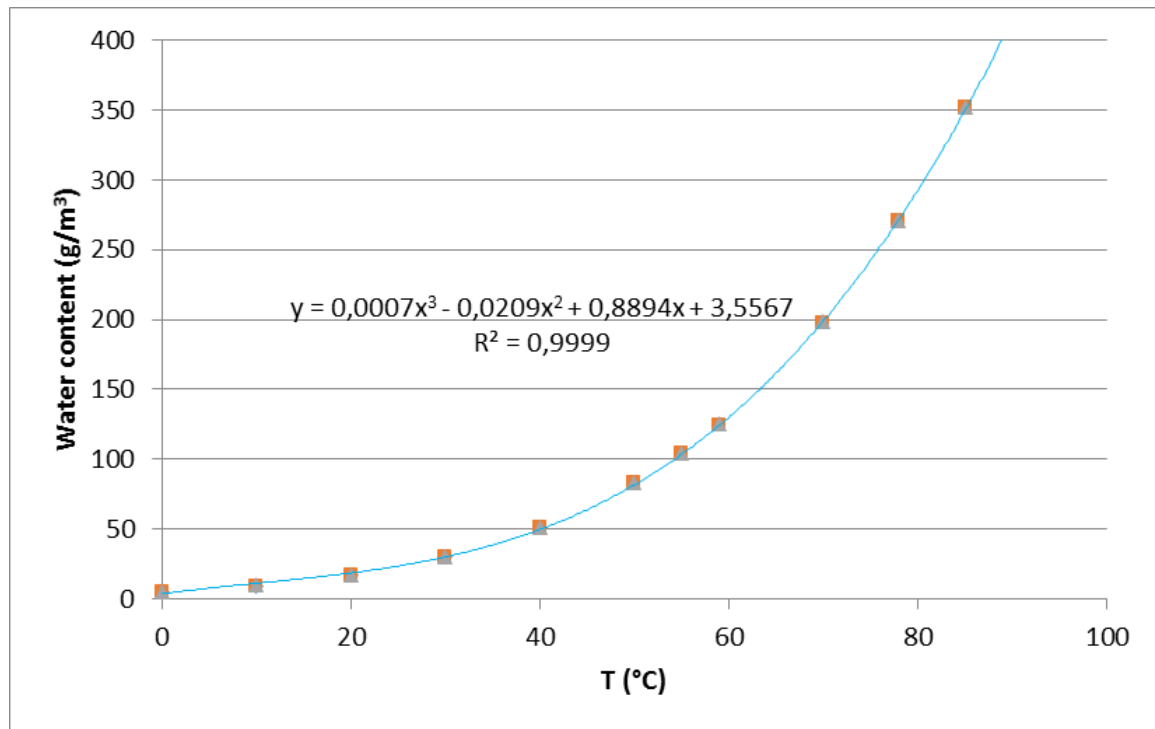
Figure 2.16. Amount of water in air at 100% of relative humidity across the range of temperature.

The saturation point (50.5 g/m3) is extracted from the graph.

$$AH = SP * RH = 50.5 * 0.2 = \frac{10.1\ g}{m3} = 0.0101\ g/l \tag{2.5}$$

$$H2O\ mass\ flow = AH * totflow = 0.0101 * 6 = 0.0606 g/min \tag{2.6}$$

$$H2O\ volumetric\ flow = \frac{mass\ flow}{molecular\ weight}\frac{R*T}{P} =$$
$$= \frac{0.0606 * 0.082 * (40 + 273)}{18 * 1} = 0.0864\ l/min \tag{2.7}$$

AH is the quantity of water that is required into the total flow to have 20% of humidity at 40°C
And both of them are balanced with technical air.

$$air = 6 - 0.0864 - 0.09 = 5.82\ l/min \tag{2.8}$$

These calculation regards the reactor.
All the flows are then corrected with the working temperature of the flow controllers with the Charles's law:

$$V(22°C) = \frac{V(50°C) * T(22°C)}{T(40°C)} \tag{2.9}$$

_____

$$air = \frac{5.82 * 295}{313} = 5.49 \ l/min \tag{2.10}$$

$$VOC = \frac{0.09 * 295}{313} = 0.0848 \ l/min \tag{2.11}$$

The calibration of the flow controllers gives us the values, in percentage, to set them and have to have these flows.

The figure 2.16 gives us also the saturation point at the temperature of the humidity sensor (37°C): 43.31g/m3, so the target humidity to visualize at the sensor is:

$$HR = \frac{10.1}{43.3} * 100 = 23\% \tag{2.12}$$

2.7 validation of the results

The validation of the results is performed after a week with the same test. In this part of the investigation there is an implementation of the system resulting from the difficulties of the humidity control in the process stream: the globe valve does not an accurate control and it is installed a tip on the valve over a goniometer to be more precise (see figure 2.17).
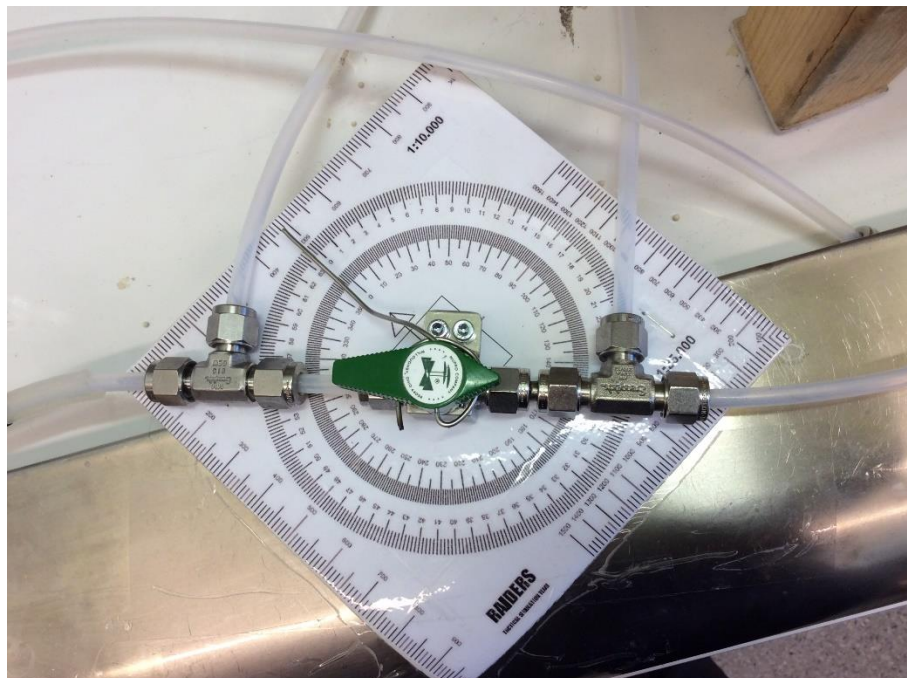

Figure 2.17. Photo of a goniometer made to have a better control on the valve.

With this improvement the humidity is more easily controllable, to the benefit of possible future experiments testing various humidity conditions.

Chapter 3

Results and discussion

In this section the results of the experimental work are shown and discussed; the Chapter starts with the physical analysis of the various photocatalyst synthetized and it proceeds with the results of the test.

3.1 Photocatalysts characterization

There is a tight correlation between the photoactivity of the photocatalysts and their physical proprieties (see paragraph §1.3.1) so the characterization of the synthetized TiO_2 gives the first estimation about the activity of the catalyst.

The figures 3.1, 3.2 and 3.3 shows the important parameters derived from the characterization of the samples: porosity and surface area that are calculated by the BET whereas the values of crystal size are extracted from the analysis made with XRD (appendix §A.5). The results of the synthetized samples obtained are shown on the blue columns and each result presents also its respective value reported in the literature (orange columns).
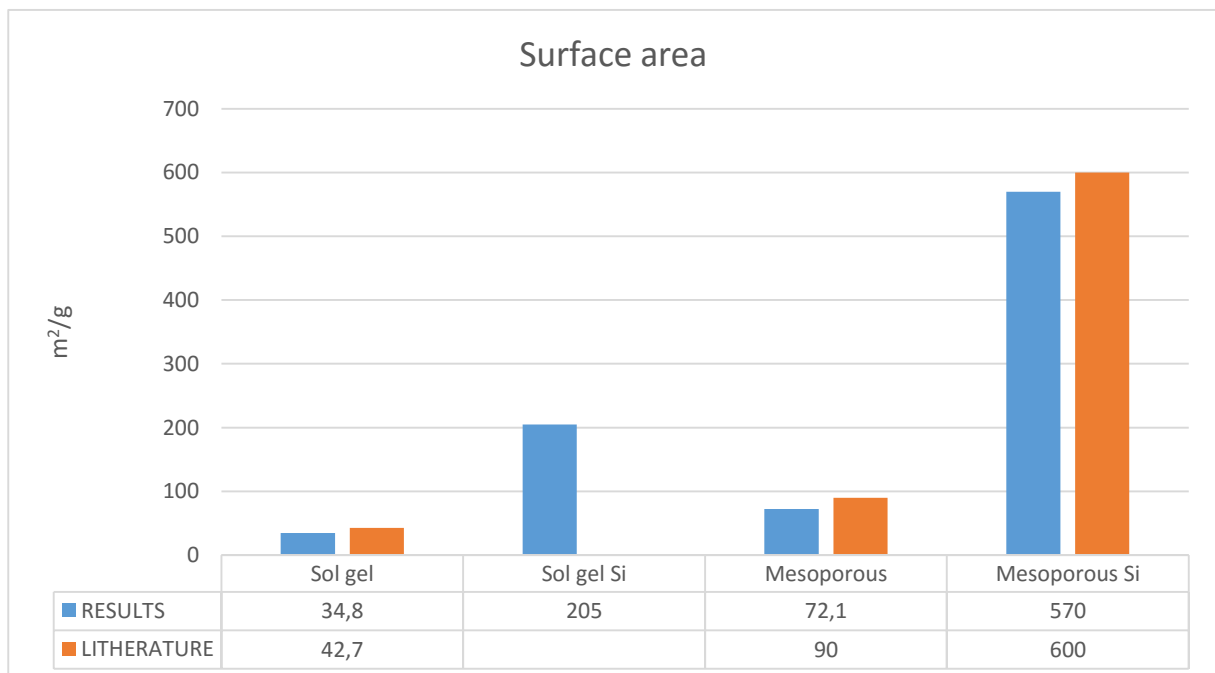
Surface area

	Sol gel	Sol gel Si	Mesoporous	Mesoporous Si
RESULTS	34,8	205	72,1	570
LITHERATURE	42,7		90	600

Figure 3.1. Surface area of the synthetized samples

_____

Porosity

	Sol gel	Sol gel Si	Mesoporous	Mesoporous Si
RESULTS	0,182	0,231	0,207	0,4
LITHERATURE	0,23		0,2	0,33
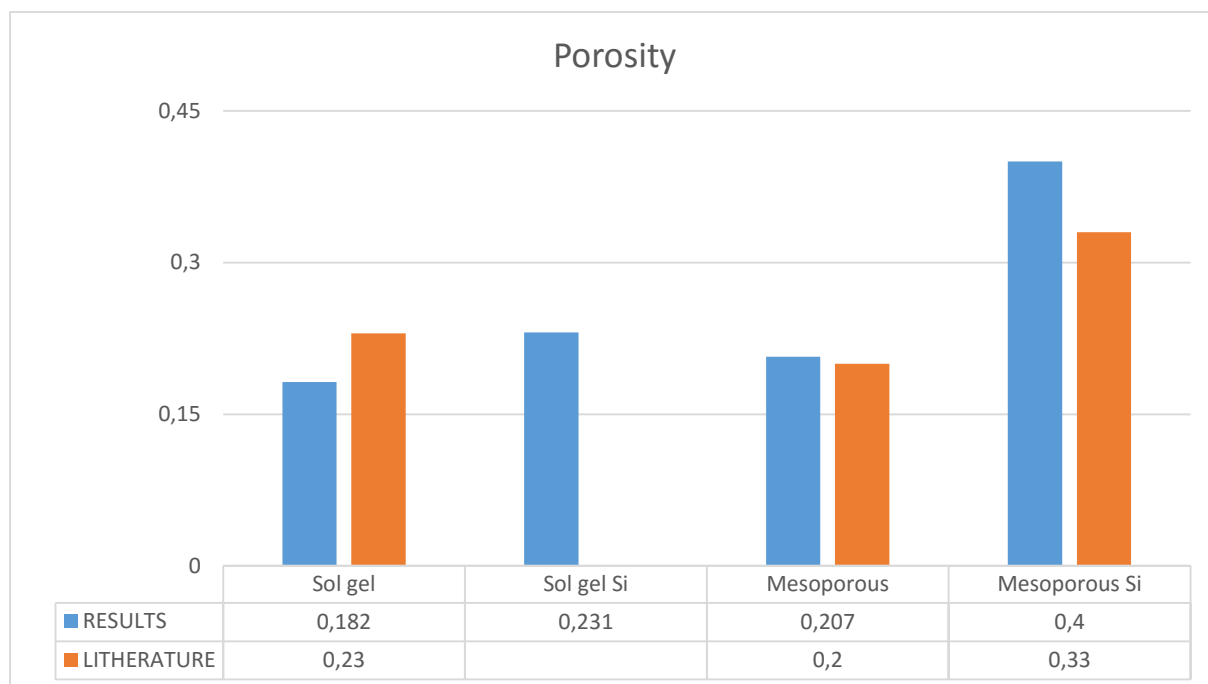
Figure 3.2. Porosity of the synthetized samples

Crystal size

nm

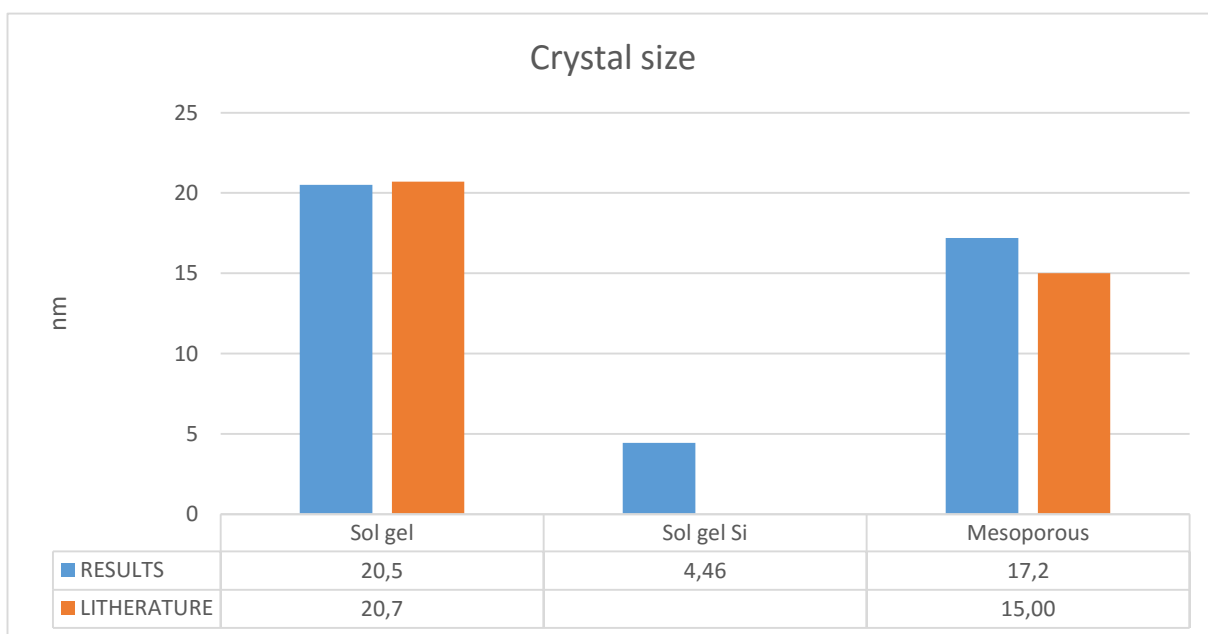|	Sol gel	Sol gel Si	Mesoporous
RESULTS	20,5	4,46	17,2
LITHERATURE	20,7		15,00

Figure 3.3. Crystal size of the synthetized samples

The first observation possible is a general trend about all the 3 properties represented: from the Sol gel witch has low physical characteristics, the Mesoporous improves them to arrive finally with the doped samples that presents optimal traits; so it is expected, as a first impression, a trend also in the activity results.

Sol gel characterization confirms the same expected values that are reported in literature (Puddu et al. 2010), a slightly less surface area but the two photocatalysts seem to be very

_____

similar and this confirms that the sol gel technique is a very simple and it is a repeatable way to produce titanium dioxide. From the results of the test of this catalyst is attended a similar relative activity that is calculated in the article of Puddu (Puddu et al. 2010).

The Mesoporous sample presents some differences with the photocatalyst presented in the paper of Fan (Fan et al. 2007), it has lower surface area and porosity but larger crystal size: exactly the opposite of the good prerequisites required of the sample and for this reason it is expected a less photocatalytic activity than the one reported in the reference.

The Mesoporous sample doped silica is produced after many attempts to find the correct procedure but the final result does not differ from the values that Kosuge (Katsunori and Puyam 1999) reports in his article: it presents the same surface area and even higher porosity. About the crystal size of the Mesoporous with silica, the sample does not have crystals of titanium dioxide due to the very high quantity of dopant and the atoms of titanium are dispersed into the silica framework: it is possible to note this in figure 3.2 where no picks of titanium dioxide appear from the XRD patterns (all the XRD diffractograms are in appendix §A.5).
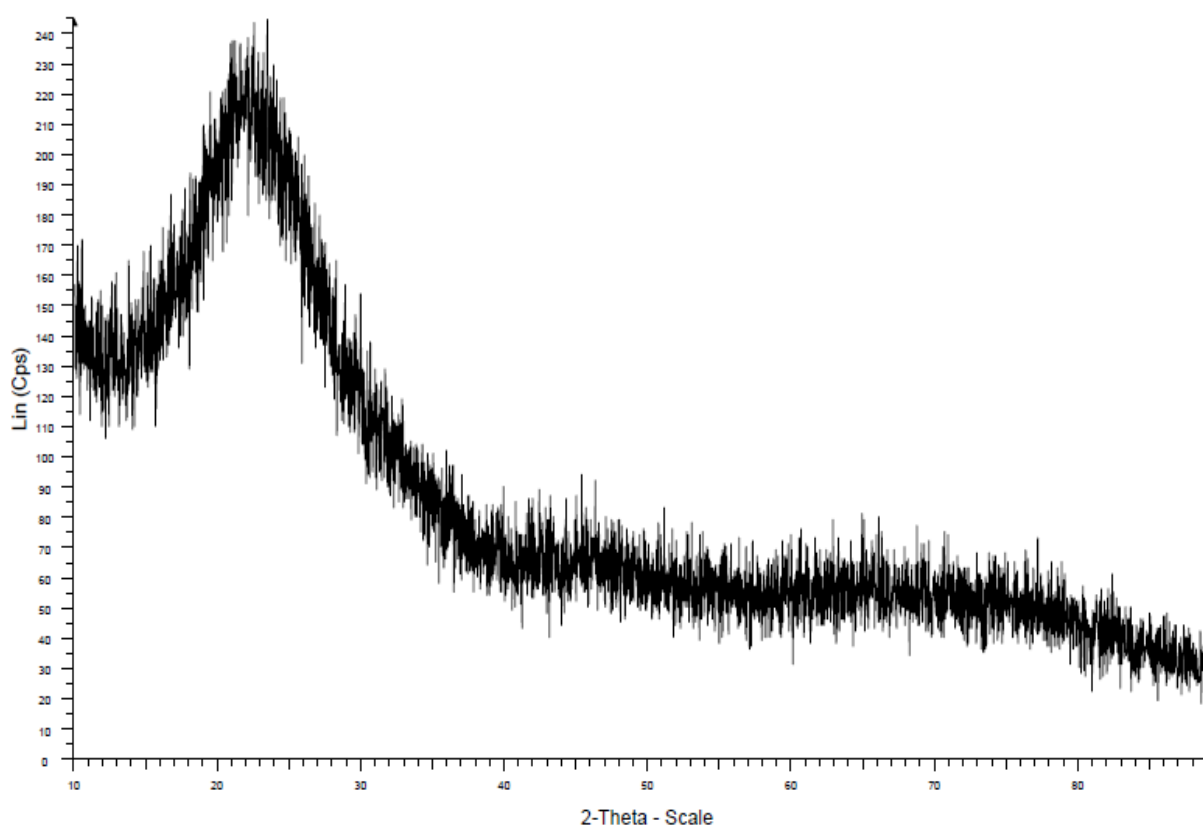

Figure 3.4. The XRD result of the Mesoporous Si sample.

Ismail (Ismail et al. 2004) in his article of the Sol gel with silica does not report any characterization results of his work; there is just the value of his surface area that are very

_____

different from the value of our synthetized catalyst. This difference came up because the synthesis procedure has being changed in this investigation (see paragraph §2.1.2): the step of the process when the solvents need to be evaporated is controlled perfectly in the article because it is used an autoclave; this machine permits, since the pressure and temperature are regulated, the crystallization process could be optimized because it changes the boiling temperature of the solvent and it promotes the crystallization with the increasing of pressure. In this work it is substituted with a calcination oven losing all the advantages of the catalyst described un the paper.

There is another synthetized sample that it is not exhibited in the figures 3.1, 3,2 and 3.3 above: the Sol gel sample doped with cerium. The XRD diffractogram is in figure 3.5.
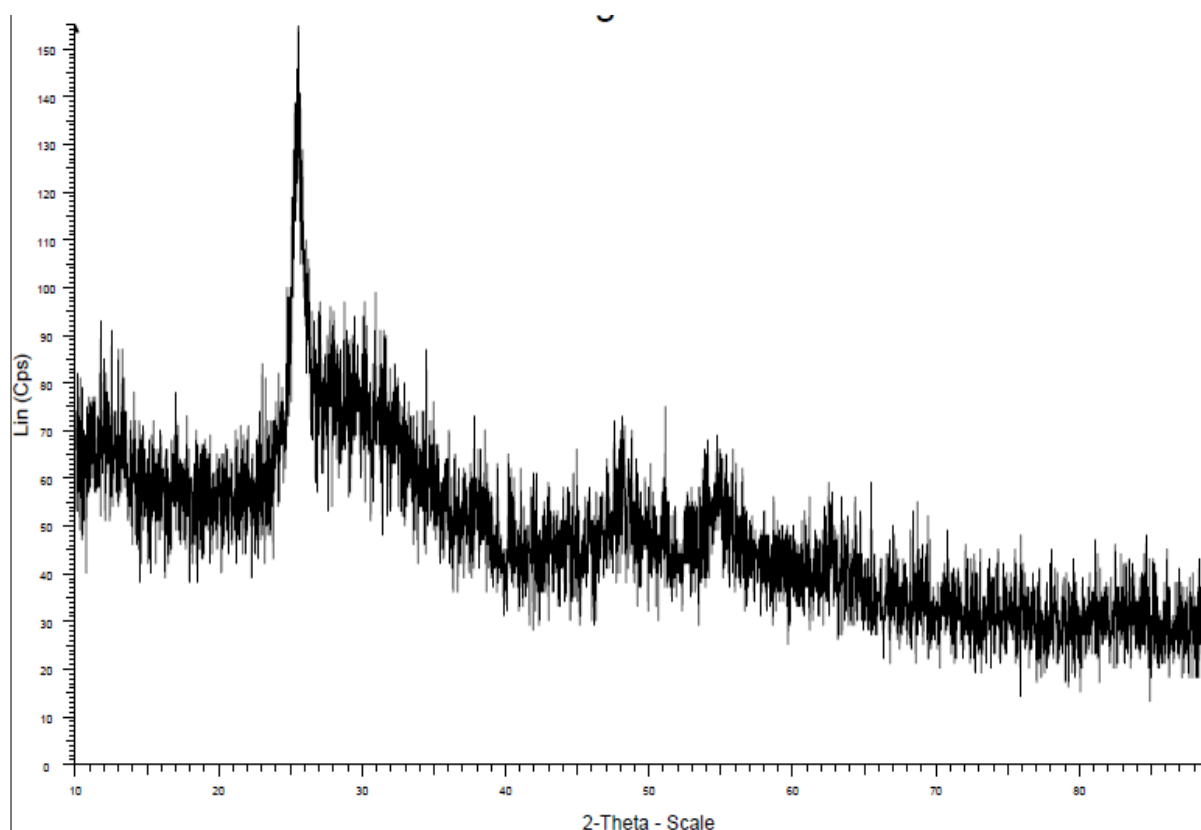

Figure 3.5. The XRD result of the Sol gel Ce sample.

The analysis shows a result very different than the others with a peak in the position of the titanium dioxide, but its intensity is not comparable to the other samples and it presents a typical amorphous shape (all the XRD patterns are shown in appendix §A.5); it suggests that in this sample, beside the crystals of anatase, there is also an amorphous phase that can play an important role in the recombination of the charges. It is expected a low activity from this sample.

3.1.1 SEM analysis

The analysis with the scanning electron microscope has been performed to see the surface of the Sol gel and the Mesoporous catalyst to investigate deeper the differences of the structures derived from the two different methodologies of synthesis. It is also proved the dimension of the crystals and the pores diameter found with the other characterization methods.
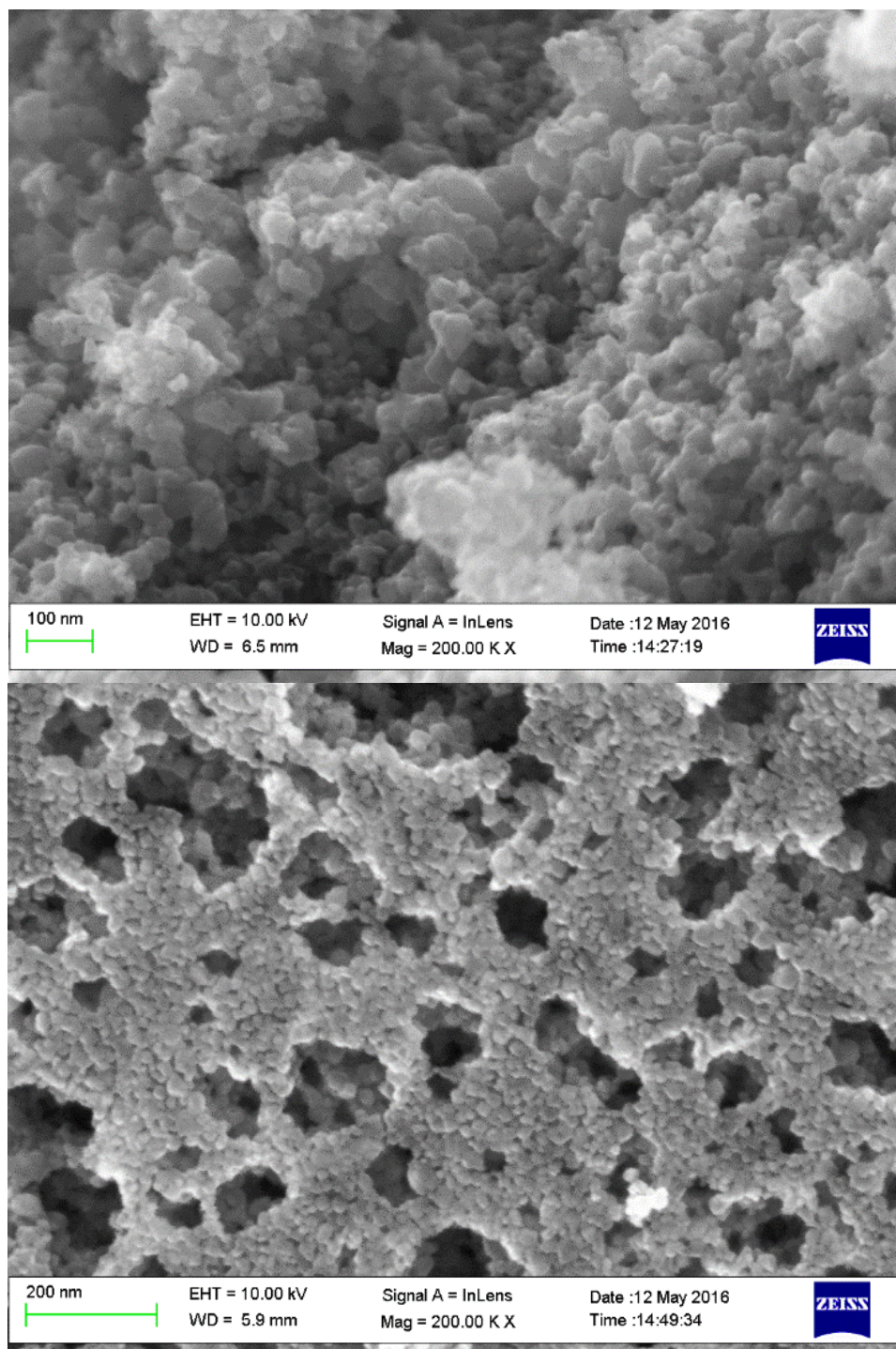

Figure 3.6. SEM images of the Sol gel sample (above), and of the Mesoporous sample(below).

The figure 3.6 shows the microstructure of the two samples and it is clear the difference of the surfaces between them. The Mesoporous sample has actually pores due the evaporation of the polymer that leaves many long hole on the surface of the powder. The Sol gel structure is, instead, less compact and it presents a complex 3D surface structure. It is also visible that the crystals of the Mesoporous samples are smaller but they are all squeezed in the structure and the Sol gel crystals are dispersed.

The microstructure is useful to understand the differences in the performances of the catalysts.

3.2 Photocatalysts coating

The dip coating process is also an important step of this investigation, the procedure has to be equal for all the photocatalyst in order to avoid difference on the attachment of the powder or other uncertainties.

In the figure 3.7 it is reported the loading throw the various dips that leads to the minimum amount of catalyst discussed in paragraph §2.4.1 (represented as 100%) on the support.
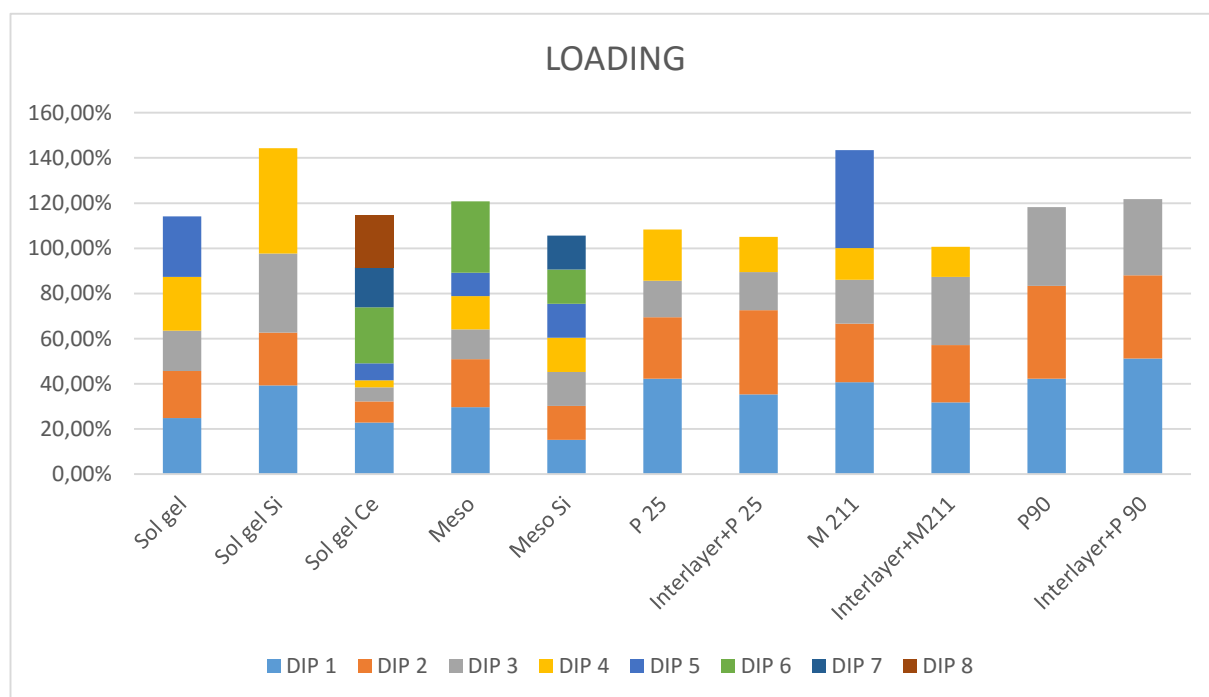

Figure 3.7. Amount of loaded catalyst every dip for all the samples.

The colloidal solution of the powder and ethanol presents a very good stability for all the samples and also the coating of the support is very stable and uniform (figure 3.8).

_____
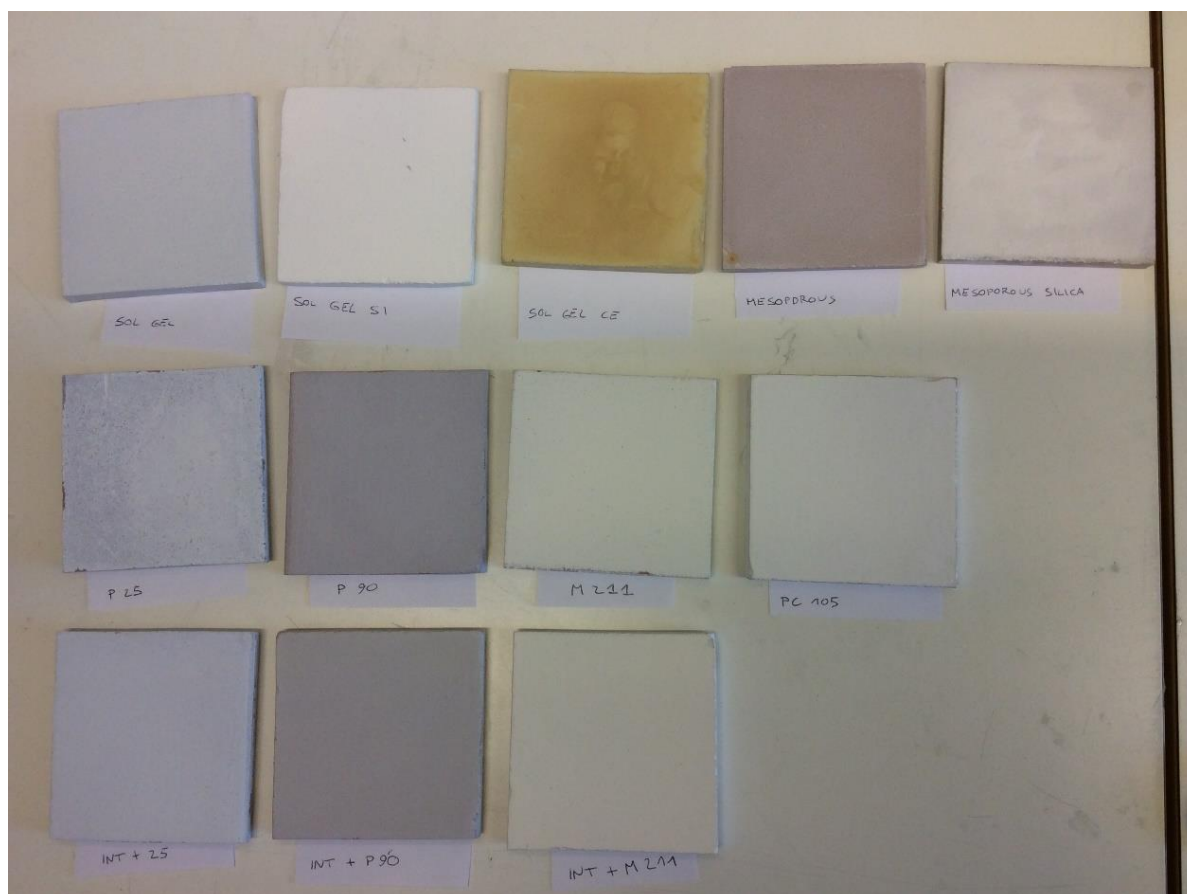
Figure 3.8. Supports coated with the photocatalyst after the test.

The difference in the quantity loaded each dip derives from the difference in the process that is made manually with inevitable differences each time, and also because each powder sample interacts differently with the ceramic support.

Another aspect is, differently from the previous investigation (Persson 2015) and the fig 1.6, no differences are detected between before and after the test about the catalytic layer. This is checked controlling the difference of weigh of the support and no optical modification are revealed.

_____

The figure 3.9 focus the attention on the layers without (the three samples above) and with (the three samples below) sublayer. It is possible to note that the P25 is improved by the intermediate layer but the other two do not present any differences. This consideration will probably effect also the performances of this samples.
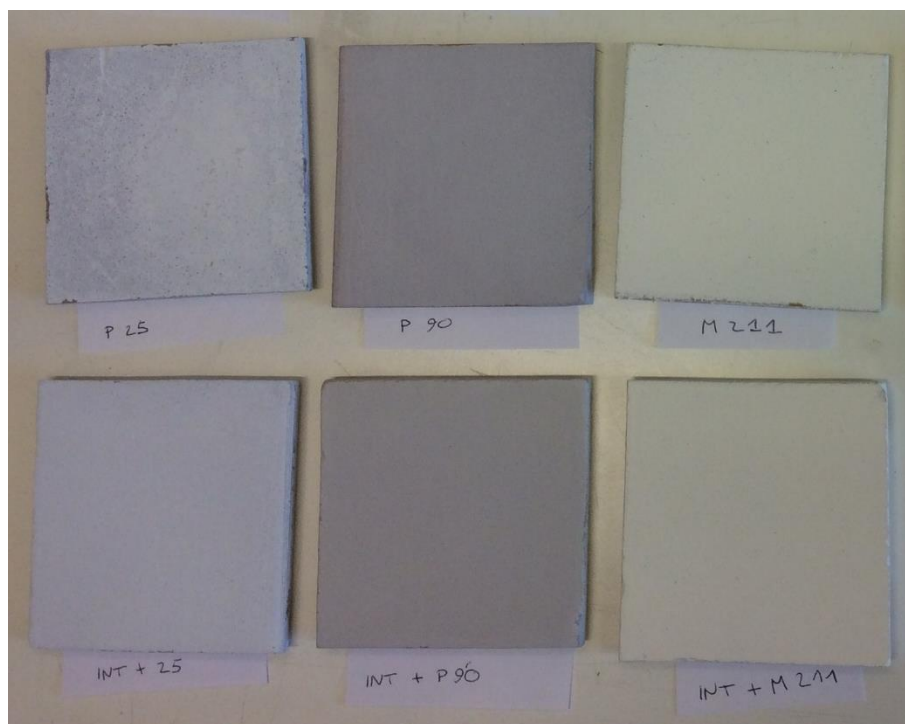

Figure 3.9. Supports coated with catalysts without sublayer (above) and with sublayer (below).

3.3 Activity

The tests, like in the previous section §3.2 about the dip coating step, are performed always in the same conditions to have an accurate comparison between different samples and the conditions are described in paragraph §2.6.

During the test, the values of the CO_2 from the analyser are collected every 30 minutes (6 times) and the system is very stable because the fluctuations of the values of CO_2 during all the performed analysis are about 1.00 ppm (±0.50 ppm).

The calibration of the analyser (reported in appendix §A.6) is performed zeroing the system with technical air in order to remove the about 13 ppm of CO_2 that are present in the technical air to the values taken from the instrument. This deviation of the calibration is taken in consideration also for the other point of the calibration of the instrument. The reported data from now on about the quantity of CO_2 in the outlet stream from the reactor are rounded to units of ppm and has the error of 1 ppm instead of the error of the analyser (±0.01 ppm).

3.3.1 Blank test

The blank test consists in an analysis with the same condition of the activity test (concentration, flows and temperature), with the catalyst inside the reactor but the lamps are off. It is performed before every test of every sample. A blank test is used to evaluate the integrity of the system.

As expected the value detected from the analyser during the blank test is 0 ppm of CO_2 because without irradiation on the catalyst there is no reaction; it is also a good procedure to find out possible problems of the system that can affect the results: for examples a leak can contaminate the system with atmospheric CO_2 or the instrument that needs a recalibration are possible scenarios where the test is essential to detect the anomaly. This procedure makes the results more reliable.

3.3.2 Photocatalytic oxidation results

The analyser gives us data about the quantity of carbon dioxide, carbon monoxide and methane but for all the analysis the values of CO and CH_4 do not change: it is proven that the photodecomposition of acetaldehyde does not give any intermediates that contain this two compounds (Liu et al. 2008).

The results of the test consist in a value of the concentration of CO_2 in the output of the stabilized system. The stabilized system means that the 6 values taken from the analyser are
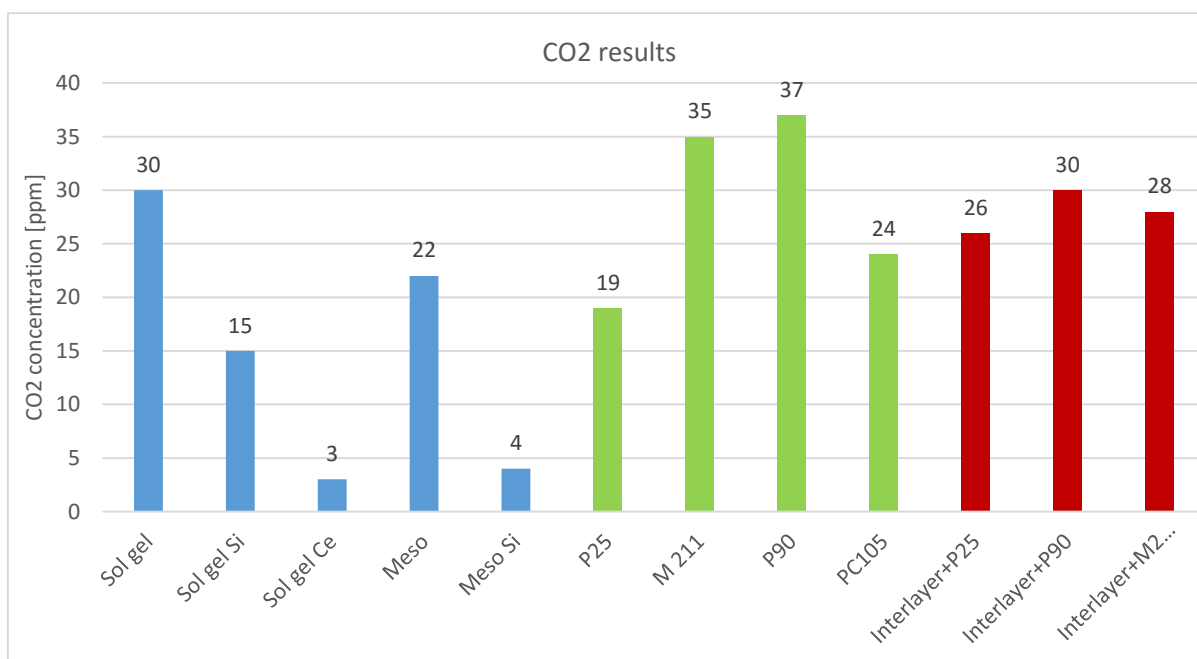

Figure 3.10. Results of CO_2 concentration detected by the analyser for all the samples.

all the same. This procedure is done for each analysis each sample for both synthetized (blue columns) and commercial (green columns) photocatalyst, results are shown in the figure 3.10.

In the figure 3.10 are presented also the results for the samples with the interlayer (red columns).

The results are then transformed into conversion for the chemical reaction (1.6) and the general formula of the conversion (calculations are in appendix §A.5)
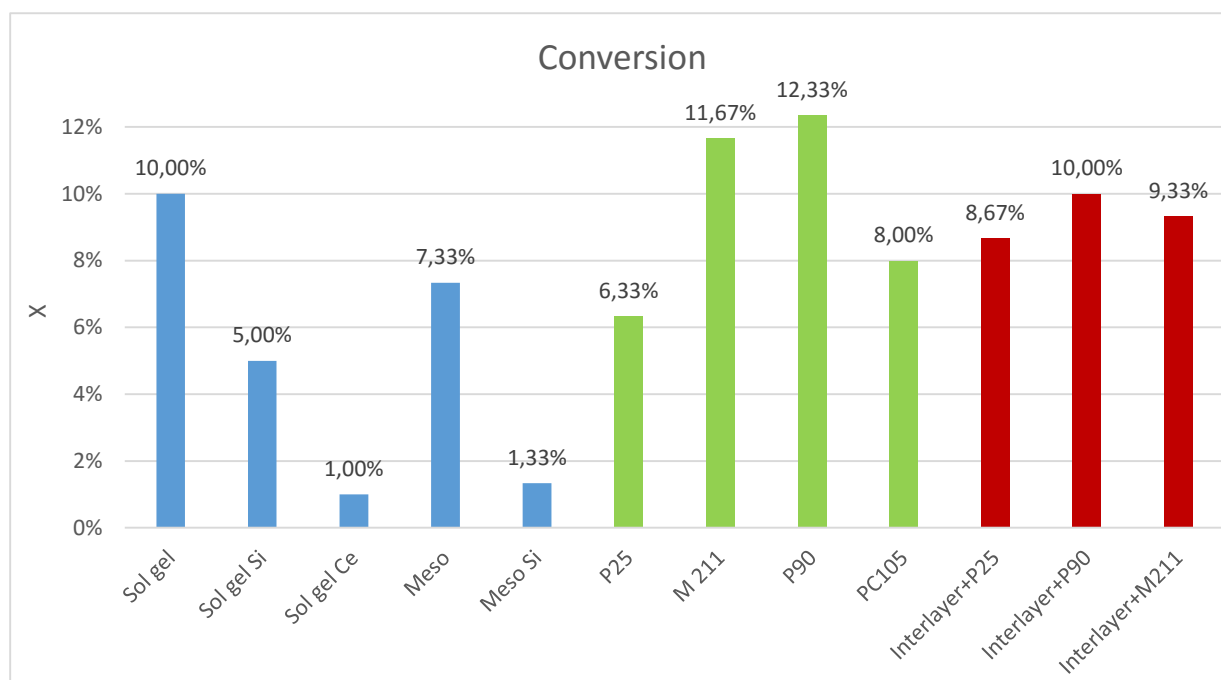

Figure 3.11. Conversion of the tested samples.

The graph of the conversion (figure 3.11) presents the same trends of the previous figure that shows the CO_2 concentrations values after the reactor (figure 3.10) since the inlet conditions are the same. From these values it is possible to evaluate the situation inside the reactor: the highest conversion reached is about 12% that is very far from the maximum conversion reached in the same reactor in mass transfer regime (see the fluid dynamic simulation on paragraph §2.5.3) and this mean that the reactor works completely in kinetic regime.

A very little conversion is desired and it is achieved using weak lamps, a small surface area of the catalyst and using a very stable compound to oxidize (acetaldehyde). This low conversion ensures that the difference among catalysts, in terms of activities, is derived just from itself and it is not influenced by the diffusion.

To correlate and compare the results of this investigation with the activities of the references and also from the previous work (Persson 2015) because he used the same reactor but different working conditions so the results of conversion are not comparable; it is necessary

_____

to convert the results from conversion to relative activities: the topic is treated in paragraph §1.4 and the calculations are in appendix §A.5.

Synthetized photocatalysts

The figure 3.12 shown the relative activities for all the five catalyst synthesized (blue columns) with their own comparisons of the literature (orange columns).

	Sol gel	Sol gel Si	Sol gel Ce	Mesoporous
RESULTS	1,64	0,78	0,15	1,17
LITHERATURE	1,75		1,46	2,43
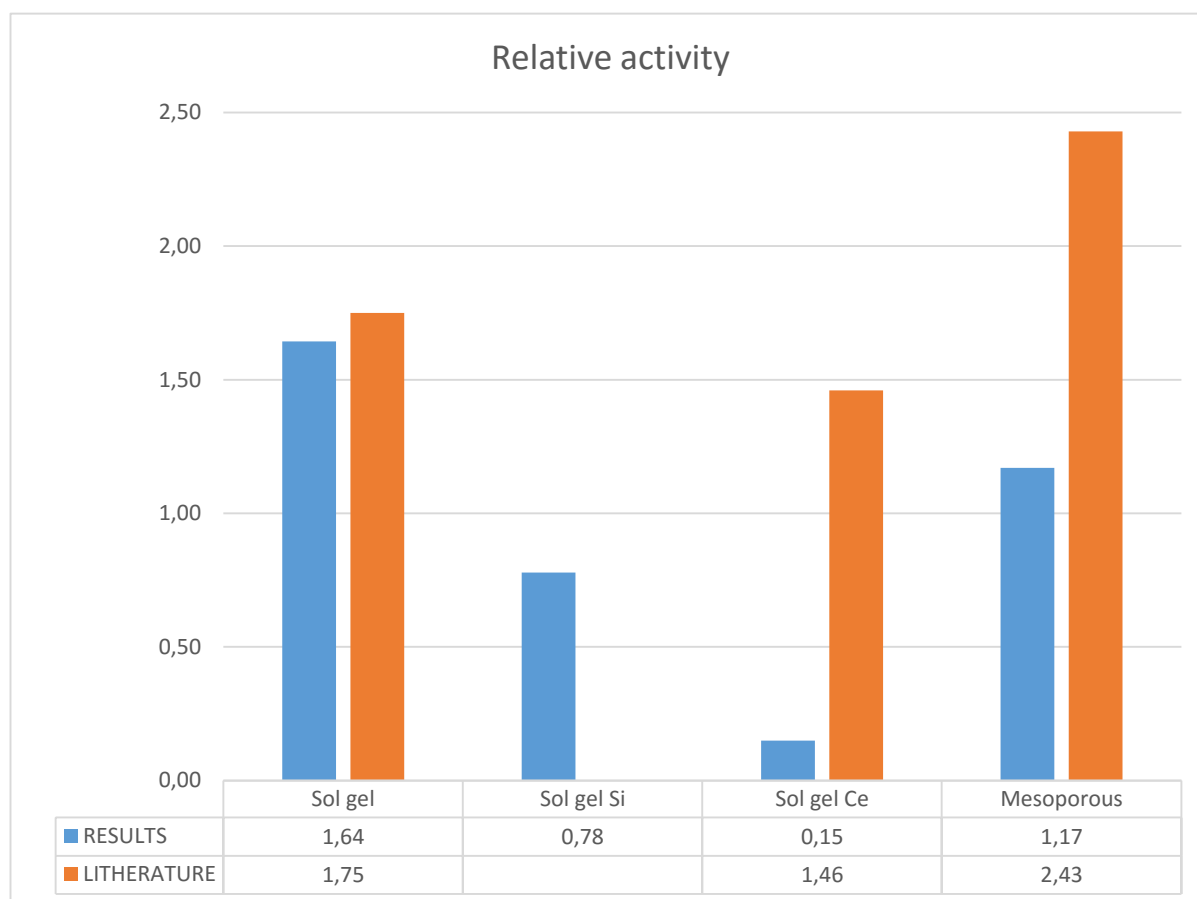
Figure 3.12. Comparison between the relative activity of this investigation and the results of the literature for the synthetized samples.

Sol gel sample has the highest conversion, it is more than 60% more active than the P25, also the Mesoporous sample gives a good result (17% more active than Degussa® P25). Samples with dopants, on the other hand, have a low photoactivity.

The same graph contains also the comparisons with their references (orange columns).

It is immediate the comparison of the Sol gel sample with its reference: it presents a similar relative activity and this confirms that the catalyst synthetized is equal to the one produced by Puddu (Puddu et al. 2010) since it has both the same relative activities and the same physical characteristics.

_____

Silica is chosen for its characteristics to improve the key parameters of the titanium dioxide as it is discussed in paragraph §1.3.1; the Sol gel sample doped silica, that actually has this physical improvements, does not enhance the performance of P25 but instead it has a lower activity of 22%. This unexpected result is explained because of the utilization of the oven instead than the autoclave (it is discussed in paragraph §2.1.2). It leaves the crystallization incomplete with a lot of defects that decrease the efficiency of the catalyst due to recombinations of the electron-holes.

The Sol gel doped with cerium presents a limited crystalline phase with an amorphous phase that is also fundamental for the charge recombination. Its low activities could be expected after the XRD characterization and the test verifies it.

 The Mesoporous sample does not have the same performance of its reference (Fan et al. 2007) and these results are explained because of the differences in physical key parameters shown before in figure 3.1, 3.2 and 3.3. There is also the SEM analysis of the microstructure of this sample in the paragraph §3.1.1. It shows the micro pores on the surface of the catalysts and the diffusion inside them need to be investigated to understand better why its physical improvements from the Sol gel are not reflected to its activity (it was expected an R less than the reference, but higher than the Sol gel).

Mesoporous with silica require a special discussion; its relative activity is 0.20 that is extremely low, on the other hand, this sample contains just 2% molar of titanium dioxide so it is valuated the performance normalizing the conversion for grams of titanium (red column) and also, since the reaction takes place on the surface of the catalytic plate, it is normalized for the volumetric fraction of titanium presents on the surface of the plate (blue column) with the calculation in the appendix §A.8. The results are shown in figure 3.13.
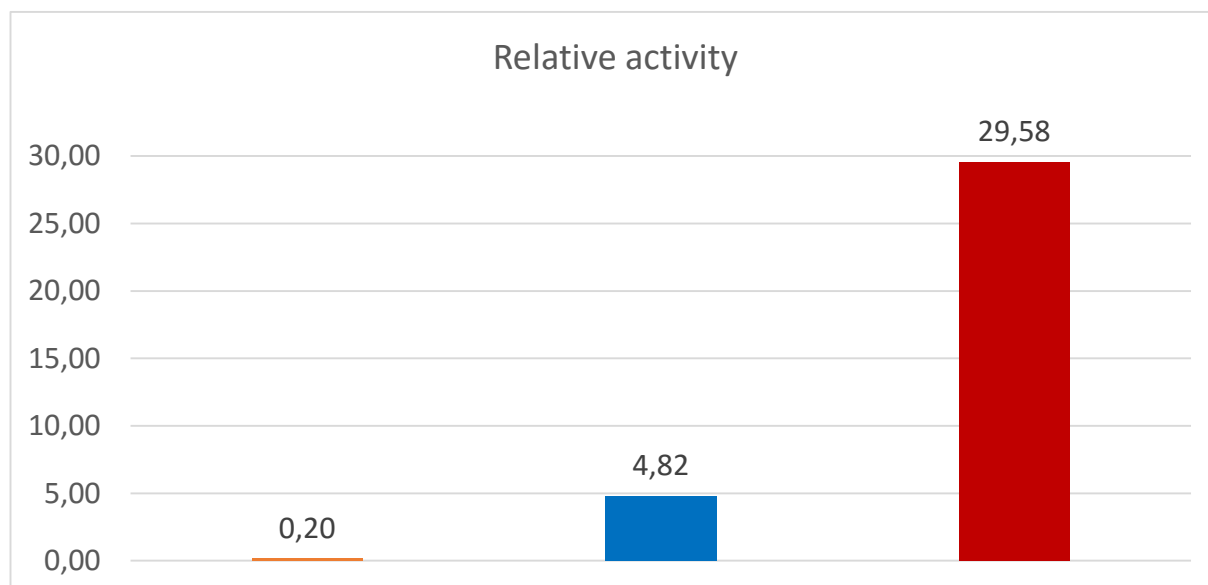

Figure 3.13.

_____

 The first figure 3.13a is referred to a gram of titanium and the result of this investigation is comparable to the result in the paper (Katsunori and Puyam 1999). The second image takes in consideration the fraction of titanium dioxide on the surface and from this calculation it is possible to find the relative activity. this result is shown in figure 3.13b and it says that the absolute activity of the catalyst is improved: material has been improved, it is used in a better way.

<u>*Commercial samples*</u>

The results of commercial samples of the green column in the figure 3.14 are also converted into relative activity.
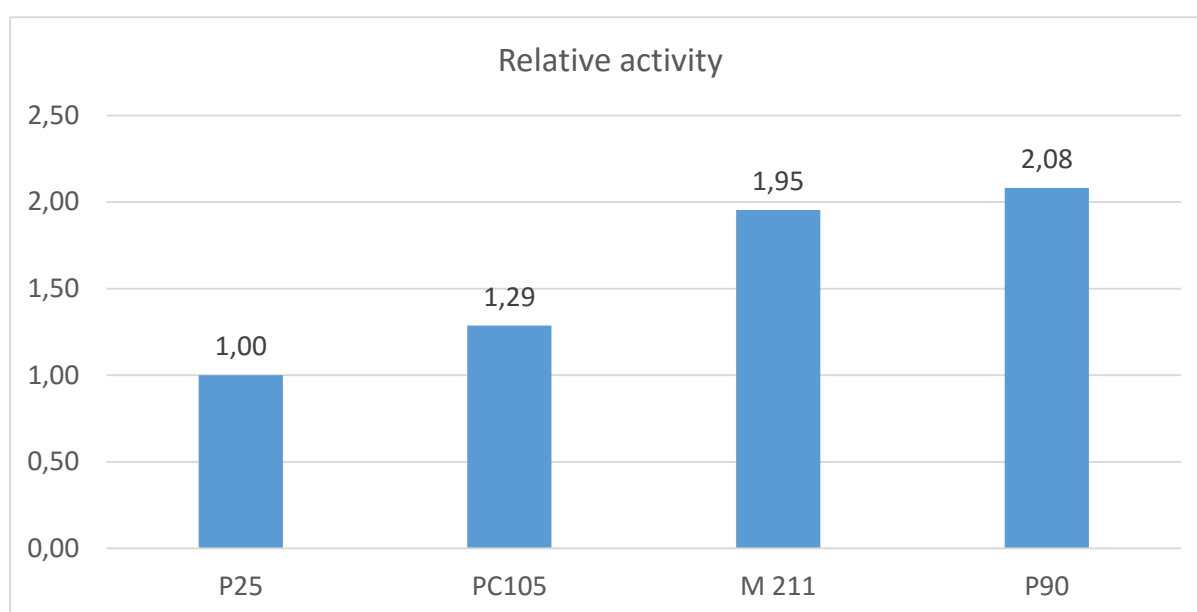

Figure 3.14. Relative activity of the commercial samples.

P25 has unitary activity because it is the reference whereas all the other commercial photocatalysts show better performances. PC105 improves the performance of 29%, M211 of 95% and the P90 is even more than 2 times better: the activity is 208% higher respect the P25 and this is the best catalyst tested in this investigation.

It is, however, impossible to find a correlation between the physical properties reported in table 2.1 with the photoactivity results because it is unknown the synthesis process and all the characteristics of these samples (for examples if there are dopants or which surface structure these catalysts have).

<u>*Interlayer*</u>

The last part of this investigation is the implementation of the interlayer. This solution is tested with the reference P25 and with the two most active samples; as reported in paragraph §2.2.6, the ceramic support is firstly dip coated to create an intermediate layer (called interlayer) and

subsequently it is formed a photocatalytic film with the classic dip coating techniques used without any interlayer. The results are reported in figure 3.15.
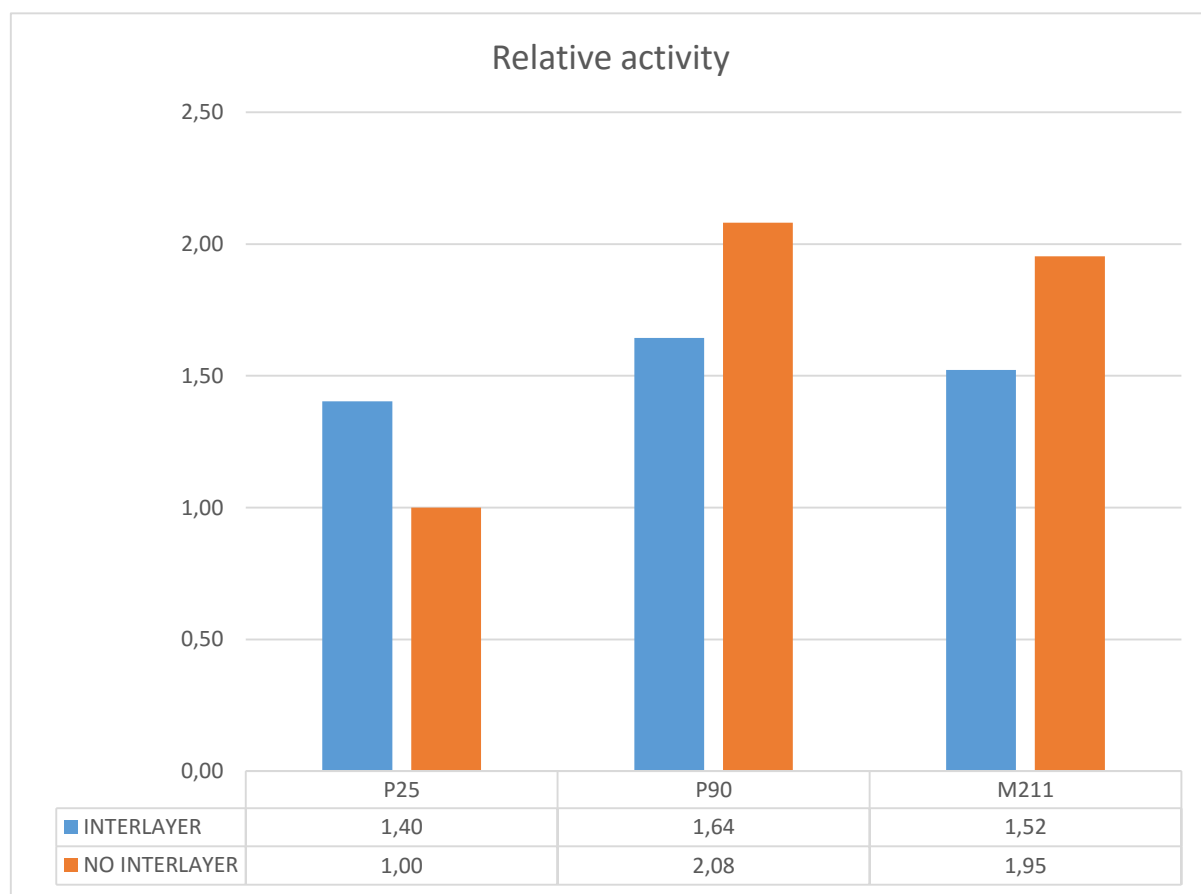

Relative activity

	P25	P90	M211
INTERLAYER	1,40	1,64	1,52
NO INTERLAYER	1,00	2,08	1,95

Figure 3.15. Comparison between samples with sublayer and without sublayer.

From this graph is it possible to underline that the interlayer improves the photoactivity of the P25 of 40% more that is exactly what is expected from the result of the work of Yuan (Yuan et al. 2008) that is used as a reference; on the other hand, it decreases the photo activities of the other 2 catalysts.

The results can be explained with the figure 3.9. for the sample P25, the difference of the coating with the sublayer is much uniform than without any intermediate films and this is probably the main reason of its improvement of activity. The other two catalysts, whereas, do not present big differences. The investigation of Yuan, moreover, it is made with the P25 and this could be another reason why that sample is the only one improved: the sublayer is probably well designed for the P25 and the enhancement of the charge imbalances does not work on the other types of photocatalysts.

_____

Previous results

The results are also compared to the results derived from the previous investigation (Persson 2015). His analysis includes the evaluation of a Sol gel without any dopants and it is prepared following the synthesis proposed by Zhang (Zhang and Liu 2008): he uses the same sol gel techniques but a different precursor of titanium, a different concentration and solvents; the investigation also reports the activity of the commercial samples P25, P90 and the PC105. It is important to underline that he uses the same reactor but with a different system rig and also
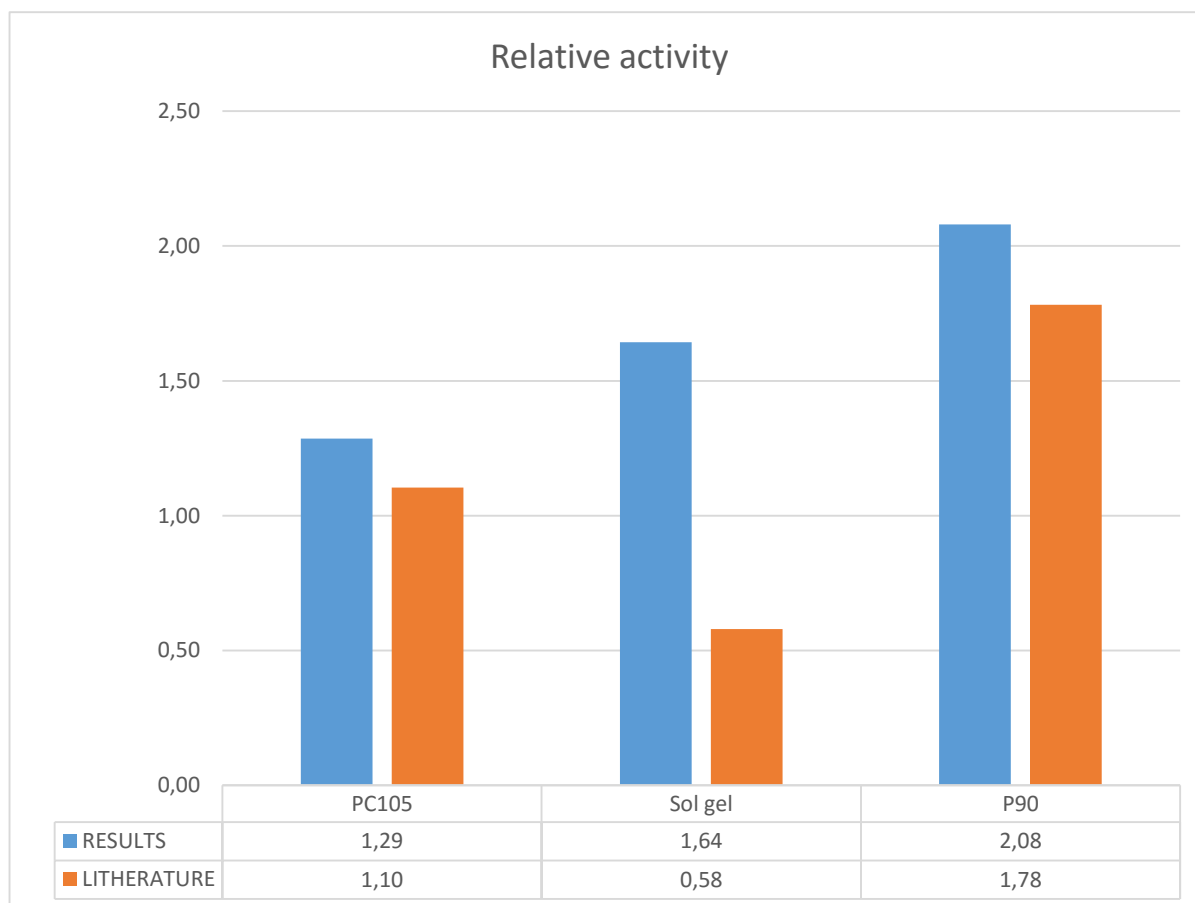
Figure 3.16. Comparison of relative activity between the results of this investigation (blue columns) and from the previous analysis (orange columns).

a different working conditions so the conversion results of his work are not comparable to the results of this work. The values of conversion are transformed to relative activities (calculation are in appendix §A.5), shown (orange bars) and compared with the results of this investigation (blue bars) in the figure 3.16.

From the figure, the sol gel synthesis is without any doubt more active. The two commercial samples, instead, present a similar activity.

In the table 3.1 there are the characteristics of two Sol gel samples.

_____

Table 3.1. Main characteristics of the Sol gel sample produced in this and in the previous investigation (Persson 2015)*.*

	Crystal Size [nm]	Porosity	BET (m2/g)
Persson's Sol gel	18,8	0,331	37
Previous investigation's Sol gel	20,5	0,182	34,8

From the table 3.1, the Sol gel synthetized in the previous work should be more active so the problems are the defects of the sample or a different superficial structure.

The two commercial sample present similar relative activities, the reason of the differences in the results could stay in the improvements of the system and the better attachment of the catalyst on the support.

Conclusions

The aim of this investigation was screening different photocatalysts in order to reduce odours in commercial plants for possible future uses. We need to get an overall idea about the possibility and the profitability of synthetizing a catalyst compared to adopting a commercial one.

A number of interesting results are obtained. At the beginning, the analysis of the state of the art provides the required knowledge about the correlation of properties such as porosity, surface area and crystal size with the photoactivity of the catalysts. These characteristics are then sought though two different synthesis methods, sol gel end mesoporous because of their good flexibility that permits a fine tuning of the final product.

Doping the titanium is another option to improve the catalyst's activity. The two best candidates are Ce as metal dopant and Si as non-metal dopant, included in the synthesis.

The produced samples and some established commercial photocatalysts were then tested in a set-up specifically designed to detect the minimal differences in terms of conversion. The reactor has been designed with fluid dynamics simulations and a model that maps the distribution of UV radiation on the catalytic surface.

The results of the oxidation test together with the characterization of the different materials reveals the difficulties of the reproducibility of the samples since it is has being used a batch process.

The defects inside the crystalline matrix of the material or the presence of an amorphous phase derived from the synthesis play an important role in the recombination of the created electron-holes. These imperfections are found in the Sol gel Si and Sol gel Ce and they represent the parameter that most influence the photoactivity, more than any other physical characteristics.

The catalysts activity has been compared through the relative activity, a parameter that allows to correlate and compare different systems with diverse reactor or conditions. It compares the kinetic constant, that is peculiar of just the activity of catalyst, and it is referred to the fixed activity of a reference catalyst removing the dependences of the system.

Activity has always been compared to P 25, a commercial photocatalyst from Degussa®, that make a compromise among different useful features and it is a reference compound.

The catalyst produced by sol gel method exhibits a relative activity of 164% compared to the P25. A similar Sol gel catalyst produced in previous investigation reveals a relative activity of 58%, less active than the P25 and 64% less performant than the one produced.

_____

Commercial samples syntheses have been optimized so they have no crystalline defects, for this reason they are all more active than the reference sample. Among the commercial, the sample P 90 is the best one tested and it improves the activity of the reference P 25 by 208%. The mesoporous sample doped silica presents a relative activity of 4.82, but based on the volumetric fraction of just titanium, and not the catalyst volume. It is much higher than the most active sample P 90. This result is not useful for an industrial application because the titanium dioxide is an inexpensive material and a good conversion is required without increasing dramatically the catalytic surface.

A sublayer has been tested on the reference and on the 2 more active commercial samples to obtain a more stable coating of the catalyst on the structural support. With the reference catalyst (P25), the sublayer improves the activity (by 40%) and the uniformity of the active layer, but it slightly degrades the performance of the other photocatalysts. In this work it is adopted a ceramic plate as a support and no relevant problem of attachment are detected with it. The sublayer then, will be a good option for other materials with less affinity with the titanium dioxide.

Future analysis

This work presents a good starting point to study the critical issue of the catalyst aging. Another interesting research extension could be the investigation of the entire range of working conditions (temperature, humidity concentration of VOCs) to understand and set the best configuration and possible limits conditions of the final VOC abatement device.

A final suggestion is to investigate the titanium dioxide as nanotubes, a new technology that are not investigated in this work but with a good potentiality.

References

Almquist, Catherine B., and Pratim Biswas. 2002. "Role of Synthesis Method and Particle Size of Nanostructured TiO2 on Its Photoactivity." *Journal of Catalysis* 212(2): 145–56. http://linkinghub.elsevier.com/retrieve/pii/S0021951702937838.

Amit, Goyal. 2005. *SECOND-GENERATION HTS CONDUCTORS*.

Burda, Clemens et al. 2003. "Enhanced Nitrogen Doping in TiO 2 Nanoparticles." *Nano Letters* 3: 1049–51. http://pubs.acs.org/doi/abs/10.1021/nl034332o.

Busuioc, Alina Maria et al. 2006. "Structural Features and Photocatalytic Behaviour of Titania Deposited within the Pores of SBA-15." *Applied Catalysis A: General* 312(1-2): 153–64.

"Catalizador TiO2." : 105. 21 http://www.cristal.com/products-and-services/ultrafine-and-specialty-tio2/ultrafine-and-specialty-tio2-products/Pages/PC105.aspx?Country=.

Chen, Xiaobo, and Samuel S. Mao. 2007. "Titanium Dioxide Nanomaterials: Synthesis, Properties, Modifications and Applications." *Chemical Reviews* 107(7): 2891–2959.

Chen, Xiaobo, and Annabella Selloni. 2014. "Introduction: Titanium Dioxide (TiO2) Nanomaterials." *Chemical Reviews* 114(19): 9281–82.

Fan, Xiao-xing et al. 2007. "Photocatalytic Degradation of Acetaldehyde on Mesoporous TiO 2 : Effects of Surface Area and Crystallinity on the Photocatalytic Activity." *Chinese Journal of Chemical Physics* 20(6): 733–38. http://scitation.aip.org/content/cps/journal/cjcp/20/6/10.1088/1674-0068/20/06/733-738.

Fenger, J. 1999. "Urban Air Quality." *Atmospheric Environment* 33(29): 4877–4900. http://www.sciencedirect.com/science/article/pii/S1352231099002903.

Fujishima, Akira, Tata N. Rao, and Donald A. Tryk. 2000. "Titanium Dioxide Photocatalysis." *Journal of Photochemistry and Photobiology C: Photochemistry Reviews* 1(1): 1–21. http://www.sciencedirect.com/science/article/pii/S1389556700000022.

Gauthier, Serge et al. 2006. "Mild Cognitive Impairment." *Lancet* 367(9518): 1262–70.

Herz, Richard K. 2004. "Intrinsic Kinetics of First-Order Reactions in Photocatalytic Membranes and Layers." *Chemical Engineering Journal* 99(3): 237–45.

Hodgkinson, Jane et al. 2013. "Non-Dispersive Infra-Red (NDIR) Measurement of Carbon Dioxide at 4.2 Mm in a Compact and Optically Efficient Sensor." *Sensors and Actuators, B: Chemical* 186(September): 580–88.

Hoffmann, M R, S T Martin, W Y Choi, and D W Bahnemann. 1995. "Environmental Applications of Semiconductor Photocatalysis." *Chemical Reviews* 95(1): 69–96. <Go to ISI>://WOS:A1995QG96000005.

IARC Working Group on the Evaluation of Carcinogenic Risks to Humans. 2010. "Carbon Black, Titanium Dioxide, and Talc." *IARC monographs on the evaluation of carcinogenic risks to*

_____

humans / World Health Organization, International Agency for Research on Cancer 93: 1–413.

Ibhadon, Alex, and Paul Fitzpatrick. 2013. "Heterogeneous Photocatalysis: Recent Advances and Applications." *Catalysts* 3(1): 189–218. http://www.mdpi.com/2073-4344/3/1/189/.

Ismail, A. A. et al. 2004. "Sol-Gel Synthesis of Titania-Silica Photocatalyst for Cyanide Photodegradation." *Journal of Photochemistry and Photobiology A: Chemistry* 163(3): 445–51.

Jackson, K. a. 1988. "A Defect Model for Ion-Induced Crystallization and Amorphization." *Journal of Materials Research* 3(06): 1218–26.

Jiang, Jingkun, Günter Oberdörster, and Pratim Biswas. 2009. "Characterization of Size, Surface Charge, and Agglomeration State of Nanoparticle Dispersions for Toxicological Studies." *Journal of Nanoparticle Research* 11(1): 77–89.

Kamat, P V, I Bedja, and S Hotchandani. 1994. "Photoinduced Charge-Transfer Between Carbon and Semiconductor Clusters - One-Electron Reduction of C-60 in Colloidal Tio2 Semiconductor Suspensions." *Journal of Physical Chemistry* 98(37): 9137–42. <Go to ISI>://WOS:A1994PH08700009.

Kamat, Prashant V. 1993. "Photochemistry on Nonreactive and Reactive (Semiconductor) Surfaces." *Chemical reviews* 93: 267–300.

Katsunori, Kosuge, and Singh Puyam. 1999. "Synthesis of Ti-Containing Portous Silica with High Photocatalytic Activity." *Chemistry letters*.

Khan, Faisal I, and Aloke Kr. Ghoshal. 2000. "Removal of Volatile Organic Compounds from Polluted Air." *Journal of Loss Prevention in the Process Industries* 13(6): 527–45.

Krysa, Josef, Martin Keppert, Georg Waldner, and Jaromyr Jirkovsky. 2005. "Immobilized Particulate TiO2 Photocatalysts for Degradation of Organic Pollutants: Effect of Layer Thickness." *Electrochimica Acta* 50(25-26 SPEC. ISS.): 5255–60.

Kumar, S. Girish, and L. Gomathi Devi. 2011. "Review on Modified TiO2 Photocatalysis under UV/visible Light: Selected Results and Related Mechanisms on Interfacial Charge Carrier Transfer Dynamics." *Journal of Physical Chemistry A* 115(46): 13211–41.

Li, Guangshe, Liping Li, Juliana Boerio-Goates, and Brian F. Woodfield. 2005. "High Purity Anatase TiO2 Nanocrystals: Near Room-Temperature Synthesis, Grain Growth Kinetics, and Surface Hydration Chemistry." *Journal of the American Chemical Society* 127(24): 8659–66.

Liang, Wenjun, Jian Li, and Hong He. 2012. "Photo-Catalytic Degradation of Volatile Organic Compounds (VOCs) over Titanium Dioxide Thin Film." *Advanced Aspects of Spectroscopy*: 341.

Liu, Zhaoyue et al. 2008. "Efficient Photocatalytic Degradation of Gaseous Acetaldehyde by Highly Ordered TiO2 Nanotube Arrays." *Environmental Science & Technology* 42(22): 8547–51. http://dx.doi.org/10.1021/es8016842.

Lu, Chung Hsin, and Wei Hong Wu. 2004. "Photocatalytic TiO2 Thin Films Prepared via a High-Pressure Crystallization Process." *Materials Science and Engineering B: Solid-State Materials for Advanced Technology* 113(1): 42–45.

Machado, Antonio E H et al. 2015. "Applications of Mesoporous Ordered Semiconductor

_____

Materials — Case Study of TiO 2." *Solar radiation applications*: 89. http://www.intechopen.com/books/solar-radiation-applications/applications-of-mesoporous-ordered-semiconductor-materials-case-study-of-tio2.

Mills, Andrew, and Soo Keun Lee. 2002. "A Web-Based Overview of Semiconductor Photochemistry-Based Current Commercial Applications." *Journal of Photochemistry and Photobiology A: Chemistry* 152(1-3): 233–47.

Montecchio, Francesco et al. 2016. "Development of a Stagnation Point Flow System to Screen and Test TiO 2 -Based Photocatalysts in Air Purification Applications.", *Chemical Engineering Journal.* Manuscript submitted for publication

Nagata, Yoshio. 2003. "Measurement of Odor Threshold by Triangle Odor Bag Method." *Odor Measurement Review*: 118–27.

Nursam, Natalita M., Xingdong Wang, and Rachel A. Caruso. 2015. "High-Throughput Synthesis and Screening of Titania-Based Photocatalysts." *ACS Combinatorial Science* 17(10): 548–69.

Persson, Henry. 2015. "PHOTOCATALYTIC OXIDATION FOR VOC ABATEMENT." *KTH Royal Institute of Technology*, master thesis.

Puddu, Valeria, Hyeok Choi, Dionysios D. Dionysiou, and Gianluca Li Puma. 2010. "TiO2 Photocatalyst for Indoor Air Remediation: Influence of Crystallinity, Crystal Phase, and UV Radiation Intensity on Trichloroethylene Degradation." *Applied Catalysis B: Environmental* 94(3-4): 211–18.

Rahaman, Mohamed, and Mohamed N. Rahaman. 2006. *Ceramic Processing*.

Richard, E et al. 2011. "(12) United States Patent." 2(12).

Skocaj, Matej, Metka Filipic, Jana Petkovic, and Sasa Novak. 2011. "Titanium Dioxide in Our Everyday Life; Is It Safe?" *Radiology and oncology* 45(4): 227–47. http://www.scopus.com/inward/record.url?eid=2-s2.0-81755171094&partnerID=tZOtx3y1.

Stocking, Andrew, Rey Rodriguez, Tom Browne, and D Ph. 2011. "3.0 Advanced Oxidation Processes." *Evaluation* 32(9-10): 1031–41. http://www.ncbi.nlm.nih.gov/pubmed/21948142.

Sun, Mingxuan et al. 2012. "Thermal Formation of Silicon-Doped TiO 2 Thin Films with Enhanced Visible Light Photoelectrochemical Response." *Electrochemistry Communications* 16(1): 26–29. http://dx.doi.org/10.1016/j.elecom.2011.12.015.

Takeshi, Mikia, Nishizawab Kaori, Eiji Watanabec, and Taodad Hiroshi. 2010. "Effect of Calcination Temperature on the Photocatalytic Activity of Porous TiO2 Film." *Materials Science* 658: 495–98. http://www.scientific.net/AMR.476-478.1882.

Wold, Aaron. 1993. "Photocatalytic Properties of Titanium Dioxide (TiO2)." *Chemistry of Materials* 02912(16): 280–83.

Yang, P.D. et al. 1998. "Generalized Syntheses of Large-Pore Mesoporous Metal Oxides with Semicrystalline Frameworks." *Nature* 396(November): 6–9. http://www.engineering.ucsb.edu/~ceweb/faculty/bradc/pdfs/10.pdf\n<Go to ISI>://000077013300047.

Yuan, Jian et al. 2008. "Promotion Effect of Al2O3-SiO2 Interlayer and Pt Loading on

_____

TiO2/nickel-Foam Photocatalyst for Degrading Gaseous Acetaldehyde." *Catalysis Today* 139(1-2): 140–45.

Zhang, Xin, and Qingquan Liu. 2008. "Visible-Light-Induced Degradation of Formaldehyde over Titania Photocatalyst Co-Doped with Nitrogen and Nickel." *Applied Surface Science* 254(15): 4780–85.

_____

Web sites

1. http://eur-lex.europa.eu/LexUriServ/LexUriServ.do?uri=OJ:L:1999:085:0001:0022:EN:PDF
2. https://scholar.google.se/scholar?q=tio2+sol-gel&hl=it&as_sdt=0%2C5&as_vis=1&as_ylo=2015&as_yhi=2005
3. https://www.acs.org/content/dam/acsorg/about/governance/committees/chemicalsafety/safetypractices/clip-acetaldehyde.pdf
4. http://oil-additives.evonik.com/sites/lists/IM/Documents/TI-1243-Titanium-Dioxide-as-Photocatalyst-EN.pdf
5. http://www.huntsman.com/pigmentsandadditives/a/Home
6. http://www.cristal.com/products-and-services/ultrafine-and-specialty-tio2/ultrafine-and-specialty-tio2-products/Pages/PC105.aspx?Country
7. https://www.heraeus.com/en/hng/products_and_solutions/uv_lamps_and_systems/uv_low_pressure_lamps.aspx
8. http://www.humidity-calculator-online.com/fileadmin/Humidity_calculator/EEHumidityCalculator.swf
9. http://aabudholiya02.blogspot.se/2014/01/China-Acetaldehyde-Industry-Global-Industry-Analysis-Size-Share-Growth-Trends-And-Forecast-2014.html

Appendix

A.1 Calculations of the synthesis ingredients

A.1.1 Sol gel

12g of TiO_2 are 0.150 moles (the molar mass is 79.866 g/mol).

According to the description above it is required:
- 0.150 moles TTIP (the molar mass is 284.215 g/mol, density 0.96 g/cm^3)
- 0.150 x 30= 4.5 moles of i-PrOH (the molar mass is 60.10 g/mol, density 0.786 g/cm^3)
- 0.150 x 100=15 moles of water (the molar mass is 18.015 g/mol, density 1 g/cm^3)

A.1.2 Sol gel Si

12g of TiO_2 are 0.150 moles (the molar mass is 79.866 g/mol). The weight of the dopant is not taken into consideration in the calculation

According to the description above it is required:
- 0.150 moles TTIP (the molar mass is 284.215 g/mol, density 0.96 g/cm^3)
- 0.150 / 6= 0.025 moles of TEOS (the molar mass is 208.33 g/mol, density 0.933 g/cm^3)
- 0.025 x 8= 0.2 moles of water (the molar mass is 18.015 g/mol, density 1 g/cm^3)
- 0.025 x 10=0.25 moles of Et-OH (the molar mass is 46.07 g/mol, density 0.789 g/cm^3)
- 0.025 / 4= 0.0625 moles of HNO3 (the molar mass is 63.01 g/mol, density 1.51 g/cm^3)

First solution
- 0.150 moles TTIP
- 0.175 moles of water

second solution
- 0.025 moles of TEOS
- 0.025 moles of water
- 0.25 moles of Et-OH
- 0.00625 moles of HNO3

- 44.4 ml of TTIP
- 3.15 ml of h2o

- 5.21 ml of TEOS
- 0.45ml of H2O
- 11.5 ml of Et-OH

- 0.394 ml of HNO3

    But nitric acid is in water solution at 60% volumetric so:
- 5.21 ml of TEOS
- 0.19 ml of H2O
- 11.5 ml of Et-OH
- 0.66 ml of HNO3 60%

A.1.3 Sol gel Ce

12g of TiO_2 are 0.150 moles (the molar mass is 79.866 g/mol). The weight of the dopant is not taken into consideration in the calculation

0.150 moles of TNBT are 51 ml (the molar mass is 340.32 g/mol, density 1 g/cm^3)

According to the description above it is required:

- 51 ml TNBT
- 153 ml of Et-OH (the molar mass is 46.07 g/mol, density 0.789 g/cm^3)
- 8.81 ml of DEA (the molar mass is 105.14 g/mol)
- 3.24 of water (the molar mass is 18.015 g/mol, density 1 g/cm^3)
- 0.16 g of $Ce(NO_3)_3$ (the molar mass is 434.22 g/mol)
- 2.14 ml of DMFA (the molar mass is 73.09 g/mol, density 0.944 g/cm^3)
- 0.55 g of PEG

A.1.4 Mesoporous

12 g of TiO_2 are 0.150 moles (the molar mass is 79.866 g/mol).

According to the description above it is required:

- 16.4 ml $TiCl_4$ (the molar mass is 189.68 g/mol, density 1.73 g/cm^3)
- 150 ml of Et-OH (the molar mass is 46.07 g/mol, density 0.789 g/cm^3)
- 15 g of P123

A.1.5 Mesoporous Si

12 g of this sample that contains 2%molar of TiO_2 and 98% of SiO_2:

- 0.24 g of TiO_2 (the molar mass is 79.866 g/mol)
- 11.76 g of SiO_2 (the molar mass is 60.08 g/mol)

According to the description above it is required:

- 0,63 ml of TEOT (the molar mass is 228,11 g/mol, density 1.088 g/cm^3)
- 43,70 ml of TEOS (the molar mass is 208.33 g/mol, density 0.933 g/cm^3)
- 19,0 ml of octilamine (the molar mass is 129,24 g/mol, density 0.782 g/cm^3)
- 2,74 ml of HCl (the molar mass is 36.46 g/mol, density 1 g/cm^3)

_____

A.2 Technical air

The technical air is a stream of compressed air that is depurated from all the hydrocarbons and also most of the CO_2 and the water present are removed.
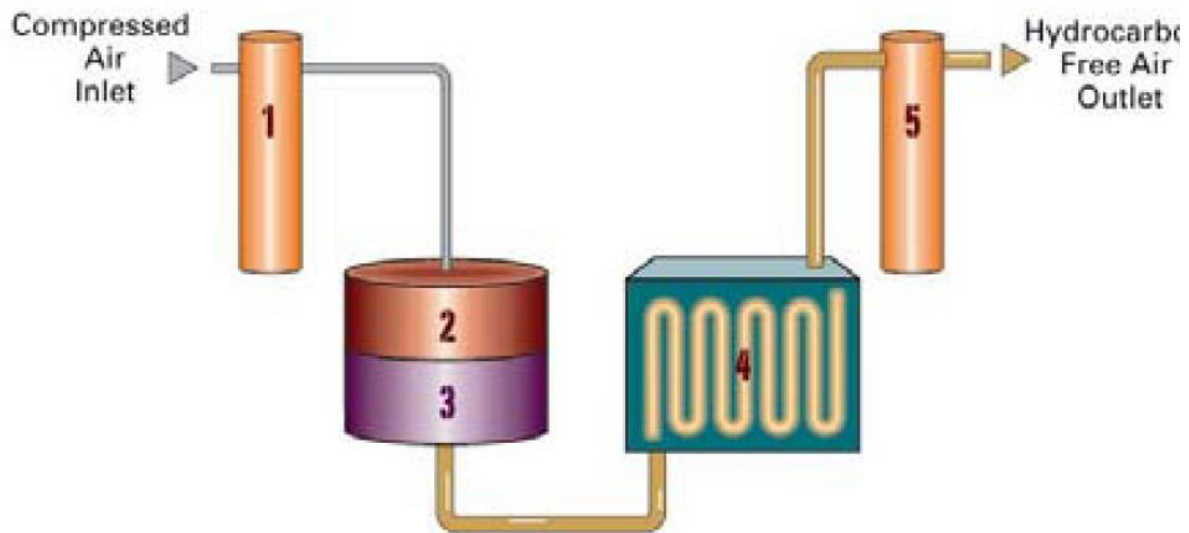The system is in figure A.1.

Figure A.1. Scheme of the Zero Air® ZA32 purification system.

The ZeroAir® generator uses catalytic conversion technology to allow the removal of hydrocarbons within a few minutes of start-up. The process is as follows: Compressed air is fed into the system through a filter [1], which removes particulates and bulk moisture via an autodrain. The air is passed over a low power heater element [2] before coming into contact with the catalytic convertor [3]. At this point any hydrocarbons are combusted into trace levels of Carbon Dioxide and moisture. The now hydrocarbon-free air is passed through a cooler [4] to return the air to ambient temperature and allow the outlet filter [5] to work efficiently.

A.3 CO_2 Fluctuations

The CO_2 concentrationis measured by the analyser to find the abatement of the VOCs that is linked to the activity of the catalyst. This is the reason why the control of the CO_2 inside the inlet stream is of primary importance.
Inside the technical air the carbon dioxide fluctuates so it a molecular sieve it is inserted to reduce them.
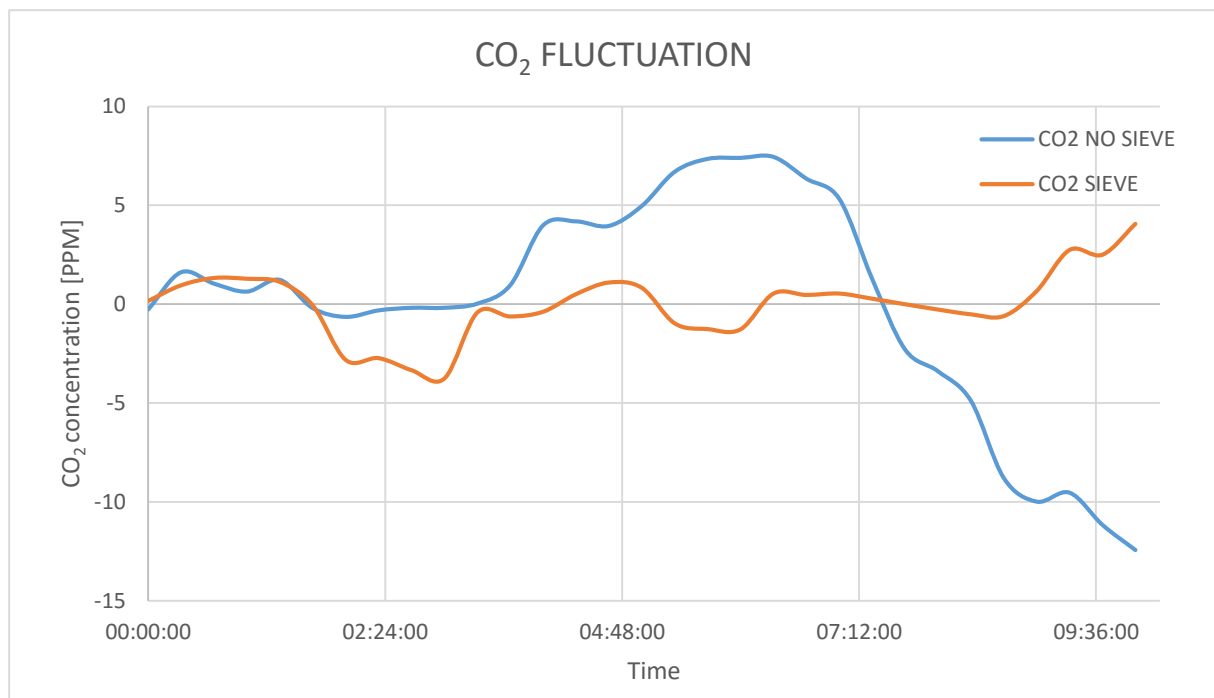The fluctuations of compressed air are studied to evaluate the improvements of the sieve (figure A.2).

_____

Figure A.2. CO2 fluctuation over time with and without the CO₂ adsorber over time.

From the figure A.2 is it possible to note the differences of fluctuations of CO_2 in a system with (blue line) and without (red line) the molecular sieve in an arch of time of 10 h. The variance, that represent how the values differs from its mean are respective 30.6 and 2,77.
The dumping effect is amplified with technical air where the content of carbon dioxide is much less.

A.4 UV radiation

The reaction is activated by the UV radiation so the value of the quantity of energy that hits the surface of the active layer is a useful information to understand if the radiation is homogeneous and it could be a good system for future investigations.
The program developed is the followed.

```
function lamppositioning


clear all
close all
clc

Lx=[0:100];                         %length of reactor [mm]
d=[0:80];                           %depth of reactor [mm]
hx=44;                              %height
dist=13;                            %lamp position
v=[];                               %multidimensional array for one lamp
L=(Lx-dist);                        %distance from the perpendicular
```

_____

```
for ii=0:(length(d)-1)                    %lamp point
    dish=[];
    for i=0:(length(d)-1)                  %row plate
        Y=i-ii;
        norobl=sqrt(hx^2+L.^2);               %x distance from lamp
        hobl=sqrt(Y^2+norobl.^2);
        dish=[dish;hobl];

    end
    v(:,:,(ii+1))=dish;
end

eff=1.00;
%lamp 1
eff1 = fminsearch(@fun,eff)


function b = fun(eff)
    I01=0.01/80*eff;                         %int scalata
    intpunt1=1000*1000*I01./v./v;
    int1=zeros(81,101);
    for i=1:(length(d))
        int1=(int1+intpunt1(:,:,i));
    end
    b=norm(1.99-max(max(int1)));
end

%lamp 2
eff2 = fminsearch(@fun2,eff)

function b = fun2(eff)
    I02=0.01/80*eff;                         %int scalata
    intpunt2=1000*1000*I02./v./v;
    int2=zeros(81,101);
    for i=1:(length(d))
        int2=(int2+intpunt2(:,:,i));
    end
    int2 = fliplr(int2);
    b=norm(2.39-max(max(int2)));
end

%int tot
int=int1+int2;

figure(1)
surf(int)
xlabel('x [mm]');
ylabel('y [mm]');
zlabel('Light intensity [mW/cm^2]');

figure(2)
surf(int1)
title('Light intensity along reactor bottom for lamp 1');
xlabel('Position at reactor bottom [mm]');
zlabel('Light intensity at position [microW/cm^2]');

figure(3)
surf(int2)
```

_____

```
title('Light intensity along reactor bottom for lamp 2');
xlabel('Position at reactor bottom [mm]');
zlabel('Light intensity at position [microW/cm^2]');
```

```
% % plot(dx,IRight)
% % hold on
% plot(dx,Itot)
% hold on
% %legend('0.1','0.2','0.3','0.4')
% P=[P d*sum(Itot(2:end))];                    %integrated power to the
surface for each positioning
% Idiff=[Idiff max(Itot)/min(Itot)];           %difference in intensity
(max/min)

end
```
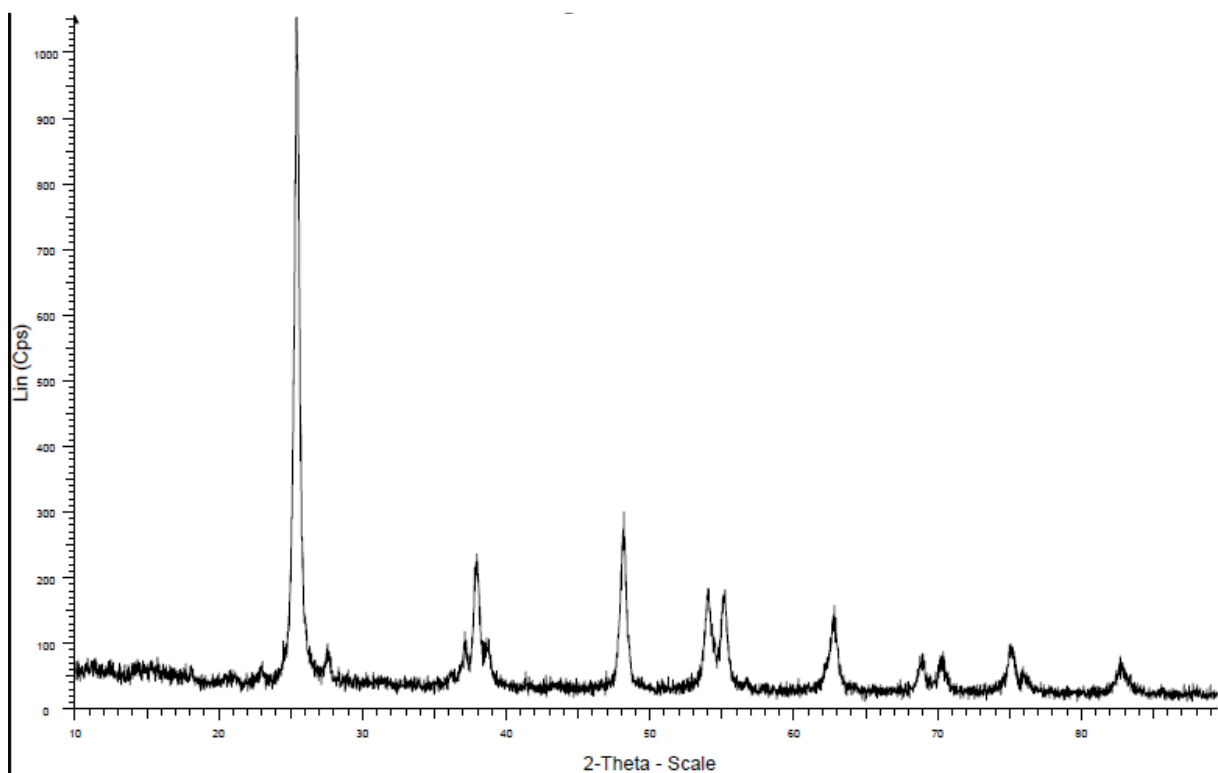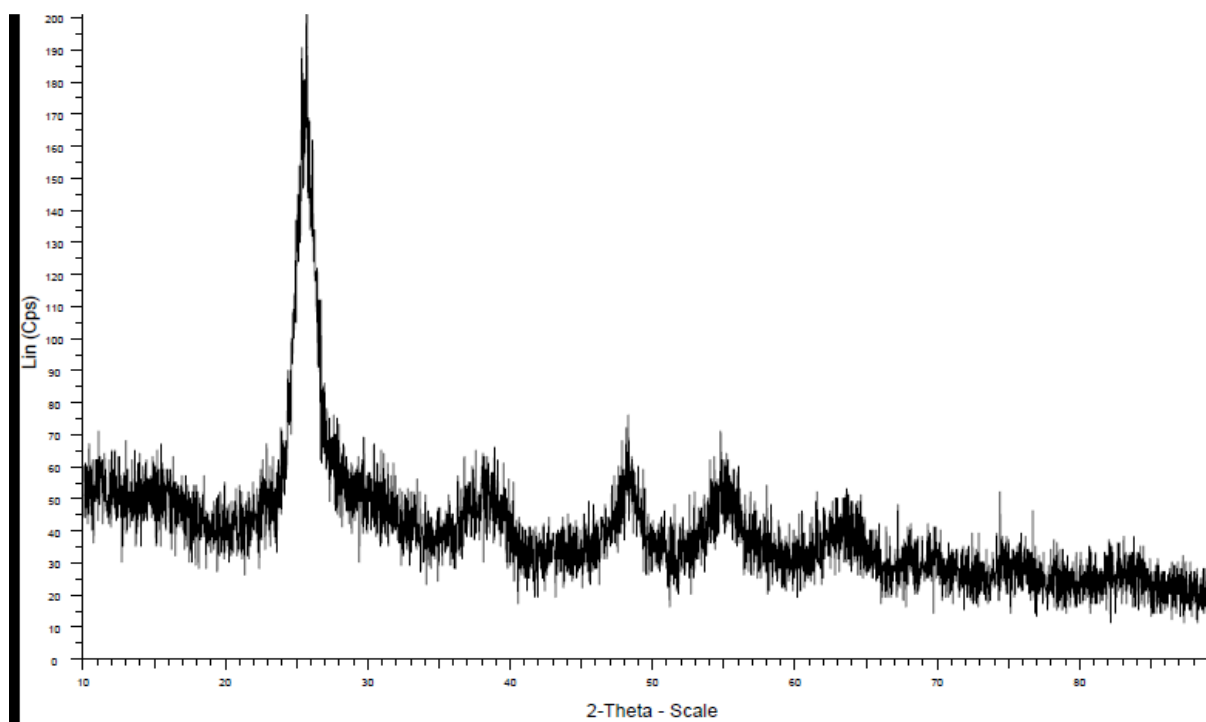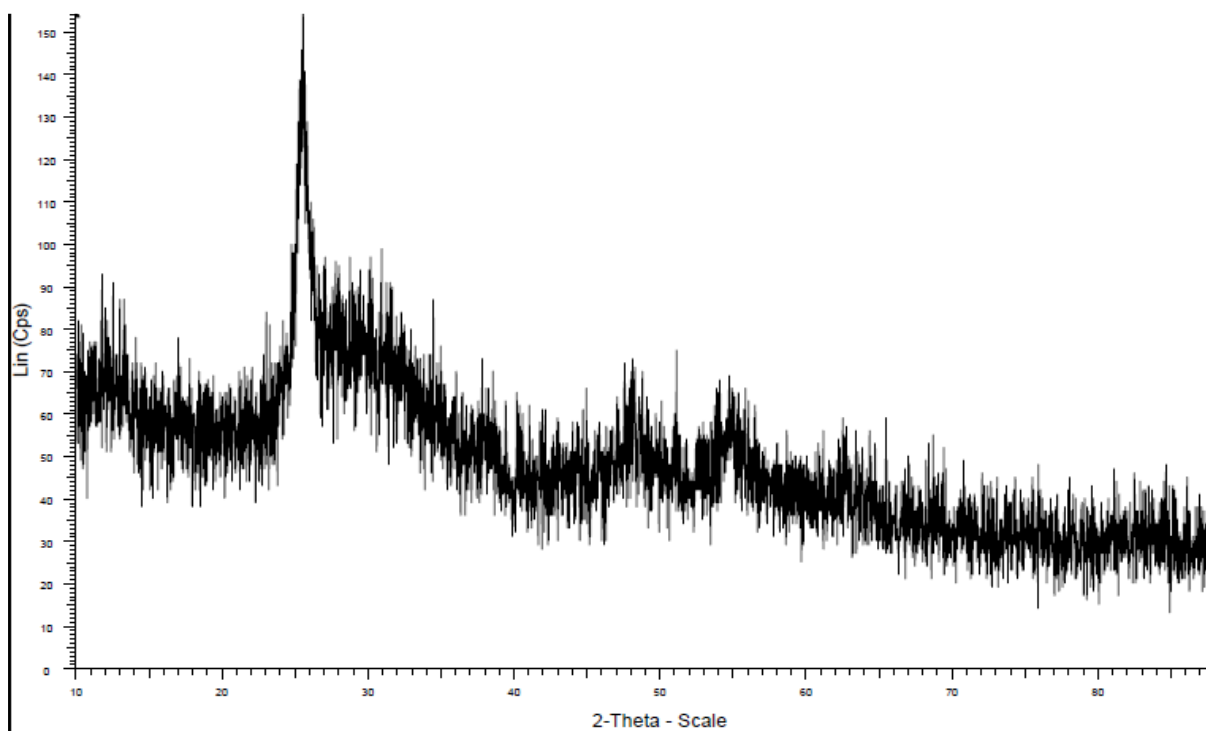
It is a matlab code that divide the lamps and the active surface, it calculates the contribution of each part of the lamp in each part of the surface and it sum all the contributes to have a final theoretical irradiation.
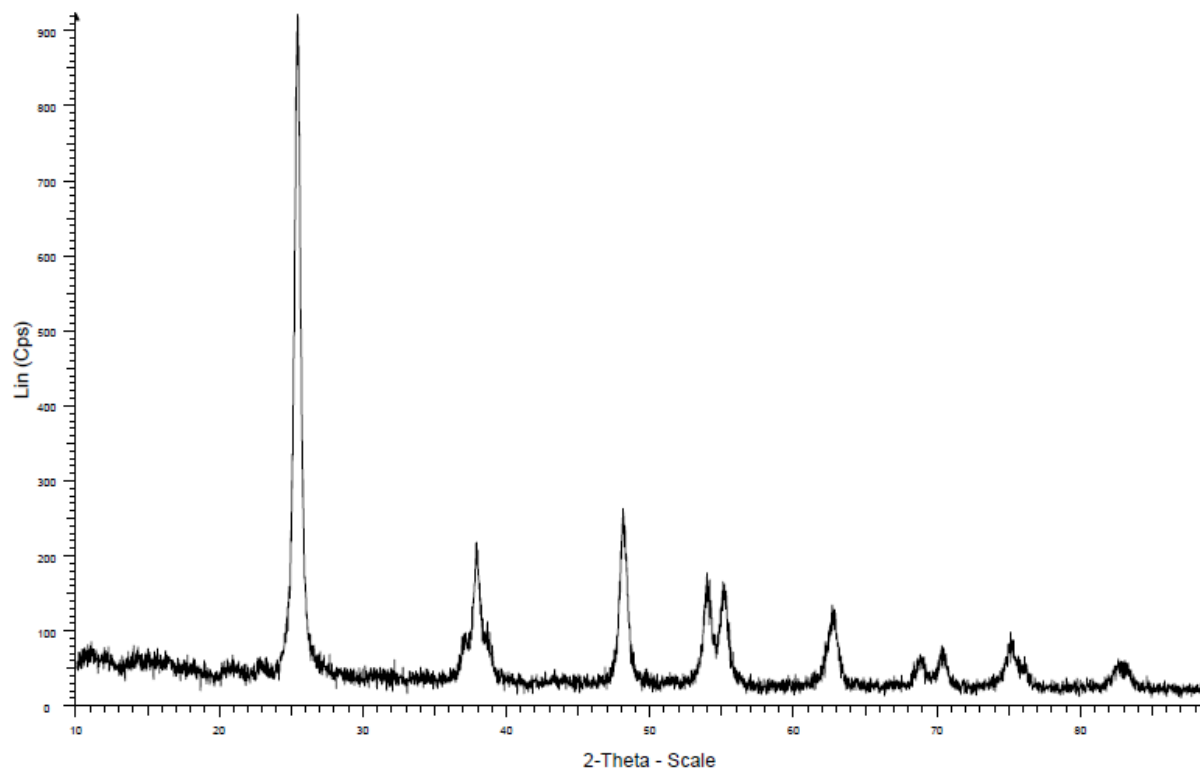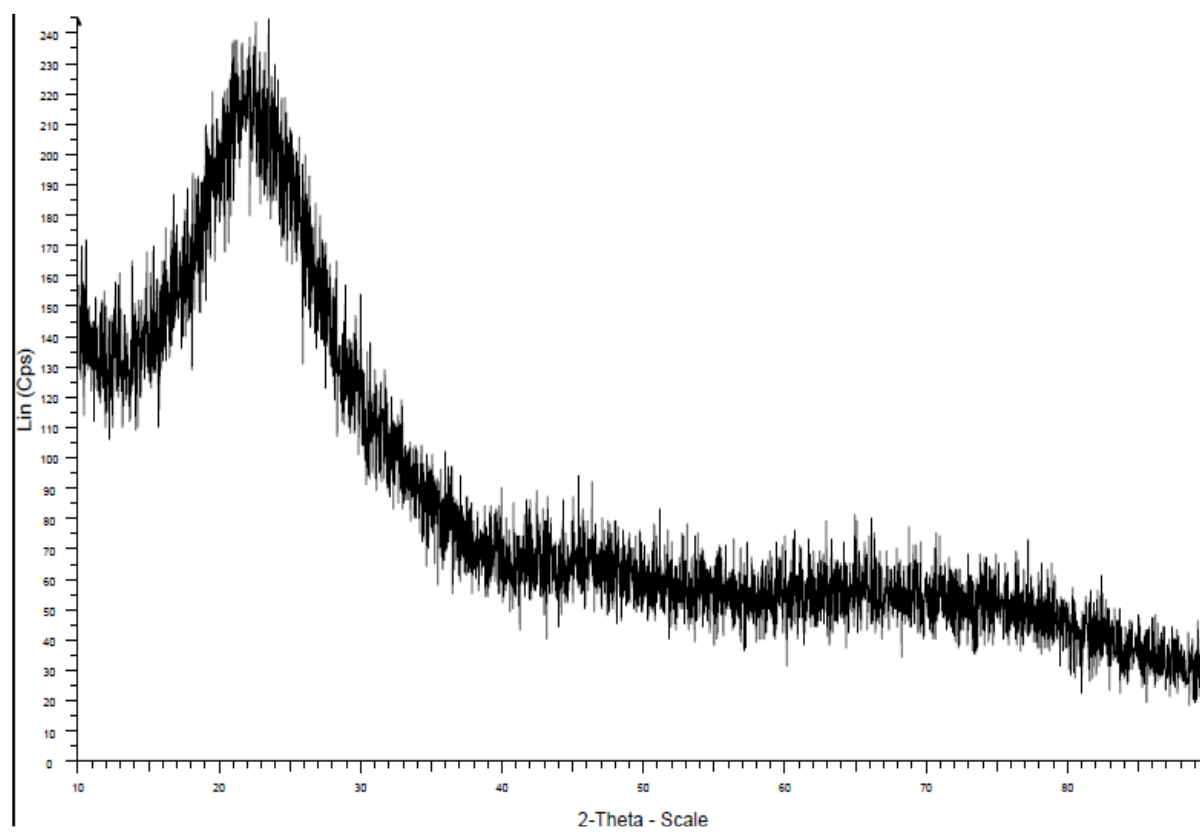
To adapt the model to a real case, the values are corrected to a real power of the lamps.

A.5 XRD diffractograms

Sol gel

_____

Sol gel Si

Sol gel Ce

_____

Meso

Meso Si

_____

A.6 Tune of the analyser

The analyser need to be tuned every time there is the suspect of errors or after a long unused period.

The tune consists on the definition of 2 point where the concentration of CO_2 is known because the answer of the instrument is linear. The 2 points are the stream of technical air after the sieve and a stream from a calibration bottle with 1000 ppm of CO_2.

The first point used does not present 0 ppm of CO_2 but, since the answer of the instrument is linear, it is set to 0 ppm so the concentration of CO_2 from this stream are cancelled from the calculations. Also the other point is deviated to have a shifted line as in figure A.2
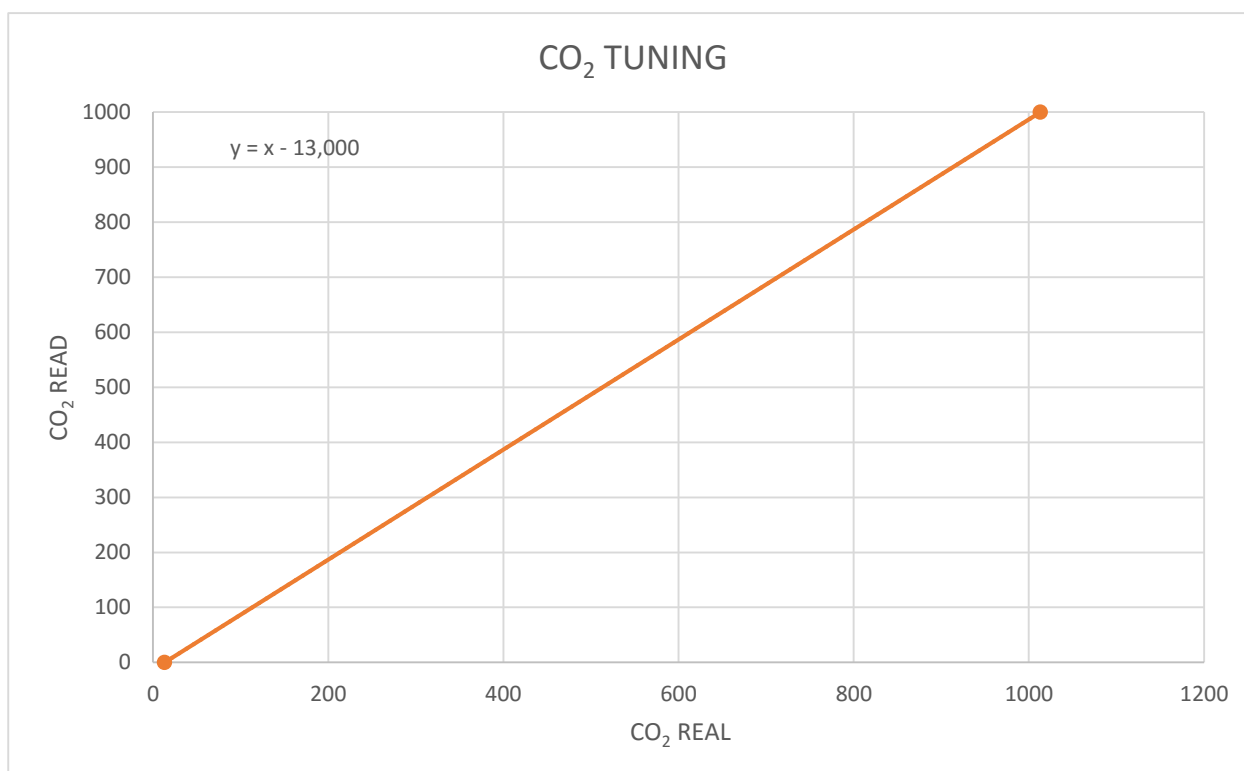

Figure A.2. Analyser calibration line for CO_2.

The figure A.2 shows the real content of CO_2 and the read value. The content into the technical air is 13 ppm of CO_2.

A.7 Conversion and relative activity calculations

The conversion is (A.1).

described as the ratio of how much of a reactant has reacted, formula (A.1).

$$X = \frac{moles\ reacted\ of\ VOC}{mole\ total\ of\ VOC}$$
(A.1)

_____

The concentration of CO_2 detected by the analyser are correlate to the VOC reacted by factor 2 (see reaction 1.6). The relative activity is calculated with the formula 1.4; table A.1 shows all the data for every samples.

Table A.1. Data and conversions for all the samples tested.

SAMPLE	CO_2 DETECTED [PPM]	VOC CONVERTED [PPM]	CONVERSION [%]	RELATIVE ACTIVITY
SOL GEL	30	15	10	1.64
SOL GEL SI	15	7.5	5	0.78
SOL GEL CE	3	1.5	1	0.15
MESO	22	11	7.33	1.17
MESO SI	4	2	1.33	0.2
P25	19	9.5	6.33	1
M211	35	17.5	11.67	1.95
P90	37	18.5	12.33	2.08
PC105	24	12	8	1.29
INTER+P25	26	13	8.67	1.40
INTER+P90	30	15	10	1.64
INTER+M211	28	14	9.33	1.52

A.8 Relative activity calculation for Mesoporous Si sample

It is possible to operate on the conversion or to the surface to find the relative activity related to the titanium dioxide and not for the entire sample.

- The superficial area of titanium is also the volumetric amount inside the sample: 4.15%

$$r = \frac{F * C_0 * X}{A_{TiO2}} = \frac{F * C_0 * X}{A * \phi} \tag{A.2}$$

$$R = \frac{k_{mesoSi}}{k_{P25}} = \frac{r_{mesoSi}}{\phi * C_{mesoSi}} \frac{C_{P25}}{r_{P25}} = \frac{X_{mesoSi}(1 - X_{P25})}{X_{P25}(1 - X_{mesoSi}) * \phi} = \frac{R * 100}{4.15} = \tag{A.3}$$

$$= \frac{0.2 * 100}{4.15} = 4.82$$

- It is also calculated the conversion for amount of titania inside the reactor.
  In this sample there are just 2% of titania so the conversion of 1,33% will be 66.67% for the same amount of material used in the other photocatalyst with the relative activity of R=29.58